

# Fe(OTf)<sub>3</sub>- and $\gamma$ -Cyclodextrin-Catalyzed Hydroamination of Alkenes with Carbazoles

En-Kai Xiao, Xian-Tao Wu, Feng Ma, Xiaohua Feng, Peng Chen,\* and Yi-Jun Jiang\*



Cite This: *Org. Lett.* 2021, 23, 449–453



Read Online

ACCESS |



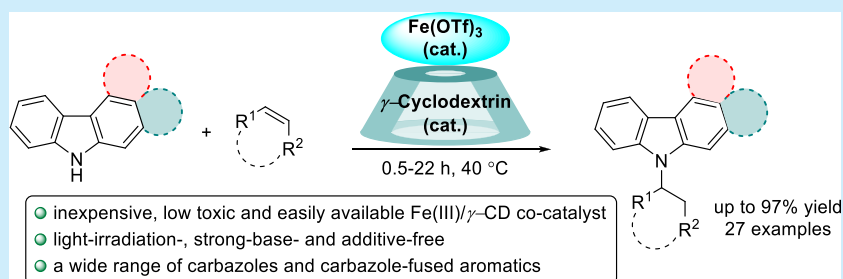
Metrics & More



Article Recommendations



Supporting Information



**ABSTRACT:** A Fe(OTf)<sub>3</sub>- and  $\gamma$ -cyclodextrin catalyzed hydroamination of alkenes with carbazoles is demonstrated. This biomimetic-catalyst-oriented sustainable and green method could deliver a wide scope of *N*-alkylated carbazoles and *N*-alkylated-carbazole-fused aromatics in up to 97% yield. The salient features of this transformation include simple and benign reaction conditions with no need for a strong base, additive, or the irradiation of light.

Carbazoles are privileged heterocyclic motifs that present in a wide variety of natural products,<sup>1</sup> bioactive molecules,<sup>2</sup> and functional materials (Figure 1).<sup>3</sup> The

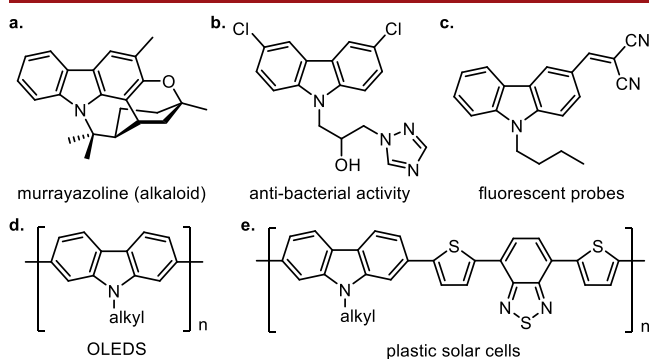


**Figure 1.** Selected applications of *N*-alkylated carbazoles.

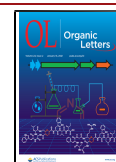
alkylation of the *N*-position of carbazoles is shown to further modulate their biological activities or photophysical properties. For example, alkyl substituents on nitrogen in a carbazole skeleton, shown in Figure 1b, are crucial antimicrobial moieties.<sup>2c</sup> Alkyl chains at the *N*-position of carbazoles can increase the two-photon absorption cross-section and the fluorescence quantum yield of the carbazole-cored two-photon fluorescent probes, such as in Figure 1c.<sup>3b,c</sup> Moreover, changing the structure and length of the alkyl substituents on the nitrogen of carbazoles, as in Figure 1d, e, can also fine-tune the solubility, molecular weight, and processability of

these materials to improve their performances in many aspects.<sup>3a</sup> Thus the development of an efficient and diverse synthesis of *N*-alkylated carbazoles is still highly desirable. The conventional *N*-alkylations of carbazoles are substitution reactions of aliphatic electrophiles, in which severe reaction conditions such as a strong base are generally needed and thus the functional group tolerance on carbazoles is limited.

The catalytic hydroamination of alkene is a very useful synthetic tool for the formation of valuable nitrogen building blocks. This transformation is also a promising green chemical method because it provides a direct and 100% atom-economical process from abundant, easily accessible, and low-cost amines and alkenes. Significant progress has been achieved in this field in recent years by employing a wide range of transition metals assisted by various ligands.<sup>4</sup> Despite the advances made in the hydroamination of alkenes with alkyl- or arylamines,<sup>5</sup> variants that accommodate amines that are embedded in aromatic systems are limited. This is because the lone pair on the nitrogen in aromatic rings participates in the  $\pi$ -system, which leads to the inertness of the *N*-H bond in the heteroaromatics. To date, only a few seminal examples having been reported that have focused on this challenging

Received: November 30, 2020

Published: December 23, 2020

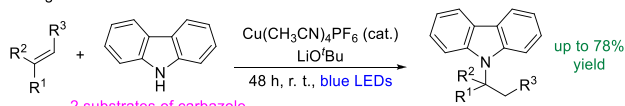


goal.<sup>6</sup> Therefore, the hydroamination of alkenes with nitrogen-containing heteroaromatics still remains elusive and is highly challenging. Two elegant examples have been reported by the Zhang<sup>6d</sup> and Zhu groups,<sup>6c</sup> respectively, very recently (Scheme 1a). Despite the significant progress achieved in these two

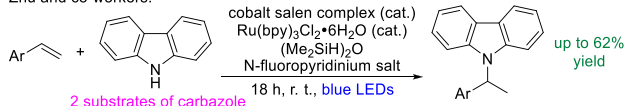
### Scheme 1. Hydroamination of Alkenes with Carbazoles

a) Previous hydroamination of alkenes with carbazoles

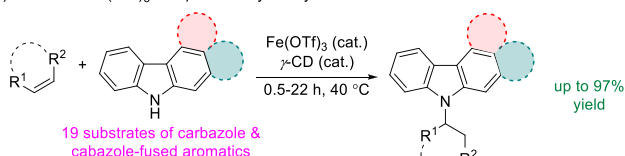
Zhang and co-workers:



Zhu and co-workers:



b) This work: Fe(OTf)<sub>3</sub> and  $\gamma$ -CD catalyzed hydroamination of alkenes with carbazoles



- inexpensive, low toxic and easily available Fe(III)/ $\gamma$ -CD co-catalyst
- light-irradiation-, strong-base- and additive-free
- a wide range of carbazoles and carbazole-fused aromatics

works, both of their successes relied on the induction of light. Thus the development of the hydroamination of alkenes with carbazoles under mild, green, and light-irradiation-free conditions still requires further improvements.

Iron is one of the most abundant metal on earth; therefore, various iron salts are readily available and inexpensive compared with the precious metals that are often applied. In addition, iron salts have low toxicity and are environmentally friendly and easy to handle. Iron salts have been widely investigated as powerful and promising catalysts for many organic transformations under mild and green reaction conditions.<sup>7</sup> On the other hand, cyclodextrins (CDs) are naturally occurring cyclic polymers composed of glucose monomers, which have been extensively studied as biomimetic catalysts.<sup>8</sup> The most commonly used CDs have three different sizes, a six-unit ring ( $\alpha$ -CD), a seven-unit ring ( $\beta$ -CD), or an eight-unit ring ( $\gamma$ -CD), and their hydrophobic cavities allow for the noncovalent selective binding of different sizes of varied organic small molecules in aqueous solution as well as organic solvents.<sup>9</sup> In particular, metal-associated CDs have attracted much attention because a metal center and a cavity of CD can form an artificial metalloenzyme to catalyze organic reactions with high efficiency and selectivity in the manner of enzymatic catalysis.<sup>10</sup> Compared with natural enzymes, these artificial metalloenzymes are cheaper, more durable, and easier to modify to enhance or alter the activity and selectivity. Despite these notable advances, most of the CDs in the metal-CD complexes need to be modified with several steps before combining with the metal core; organic transformations catalyzed by metal salts with unmodified CDs are rare. Herein we report our investigations into a Fe(OTf)<sub>3</sub>- and  $\gamma$ -cyclodextrin-catalyzed efficient and regioselective hydroamination of styrenes with carbazoles, which offers a range of valuable alkylated carbazoles in moderate to high yields

(Scheme 1b). The key features of this sustainable methodology include: (a) the use of inexpensive, low-toxicity, and easily available Fe(OTf)<sub>3</sub> and  $\gamma$ -cyclodextrin as catalysts, (b) a catalytic system that does not require the irradiation of light, (c) simple and benign reaction conditions with no strong base or additives, and (d) a broad substrate scope with respect to carbazoles and the demonstration of a wide range of carbazoles and carbazole-fused aromatics in moderate to high yields, beyond the scope and yields described in the previous work.

We initially investigated the hydroamination of styrenes with carbazoles by using carbazole **1a** and styrene **2a** in the presence of 20 mol % of Fe(OTf)<sub>3</sub> in DCE (Table 1). However, this

Table 1. Optimization of the Reaction Conditions<sup>a</sup>

entry	metal salt (mol %)	cyclodextrin (mol %)	solvent	yield (%) <sup>b</sup>	
				3aa	4
1	Fe(OTf) <sub>3</sub> (20)	none	DCE	trace	0
2	Fe(OTf) <sub>3</sub> (20)	$\alpha$ (20)	DCE	19	46
3	Fe(OTf) <sub>3</sub> (20)	$\beta$ (20)	DCE	31	39
4	Fe(OTf) <sub>3</sub> (20)	$\gamma$ (20)	DCE	60	12
5	FeCl <sub>3</sub> (20)	$\gamma$ (20)	DCE	trace	0
6	AgOTf (20)	$\gamma$ (20)	DCE	0	0
7	Sc(OTf) <sub>3</sub> (20)	$\gamma$ (20)	DCE	0	0
8	Fe(OTf) <sub>3</sub> (20)	$\gamma$ (30)	DCE	13	0
9	Fe(OTf) <sub>3</sub> (10)	$\gamma$ (10)	DCE	28	trace
10	Fe(OTf) <sub>3</sub> (20)	$\gamma$ (20)	DCM	31	5
11	Fe(OTf) <sub>3</sub> (20)	$\gamma$ (20)	toluene	<5	0

<sup>a</sup>Reactions were performed with 0.25 mmol of **1a**, 0.5 mmol of **2a**, and catalyst in 2 mL of solvent at 40 °C. <sup>b</sup>Isolated yield after column chromatography. DCE, 1,2-dichloroethane; DCM, dichloromethane.

system failed to provide product **3aa** (Table 1, entry 1), which indicated that Fe(OTf)<sub>3</sub> alone was not an effective catalyst to furnish the expected transformation. Notable progress was achieved by using cyclodextrin as the cocatalyst. The catalytic system became heterogeneous because of the insolubility of cyclodextrins in DCE. When  $\alpha$ -cyclodextrin was used together with Fe(OTf)<sub>3</sub>, the expected product **3aa** was obtained in 19% yield. Meanwhile, the further C3-alkylated **4** was detected as the main product in 46% yield in this transformation. The formation of byproduct **4** revealed that the C-3 and C-6 positions could compete with the N-9 position in carbazole to add to the vinyl group of styrene. Therefore, the regioselectivity of the reaction needs to be improved to increase the yield of the desired product **3aa**. Further screening of cyclodextrins showed that  $\beta$ -cyclodextrin could slightly improve the chemo- and regioselectivity (Table 1, entry 3). Unexpectedly, both the chemo- and regioselectivity of the reaction were increased dramatically by adding  $\gamma$ -cyclodextrin as the cocatalyst (Table 1, entry 4). These improvements might be because Fe(OTf)<sub>3</sub> can attach to the scaffold of cyclodextrins *in situ* to form a highly active Fe(OTf)<sub>3</sub>/CD complex in the reaction system (Table 1, complex A). Owing to the big size of Fe(OTf)<sub>3</sub> and the high activity and flexibility of the primary hydroxyl groups on the narrower rim of cyclodextrin, Fe(OTf)<sub>3</sub> could probably position at the

narrower rim of cyclodextrins through hydrogen bonds.<sup>10d,11</sup> As a result, Fe(OTf)<sub>3</sub> could exploit the inclusion ability of the cavity of cyclodextrin to assist and tune its interaction with a substrate that may be captured by the cavity. Therefore, Fe(OTf)<sub>3</sub>/CD complex **A**, which performed as a binding pocket of a natural enzyme, could promote the hydroamination reaction with high activity and selectivity compared with Fe(OTf)<sub>3</sub> alone. In addition, different Fe(OTf)<sub>3</sub>/CD pockets showed different product selectivities (Table 1, entries 2–4), which could further demonstrate the influence of the different-sized Fe(OTf)<sub>3</sub>/CD complexes on the outcome of the reaction. Furthermore, the type of the metal center was also crucial to the reaction. Other metallic salts such as FeCl<sub>3</sub>, AgOTf, and Sc(OTf)<sub>3</sub> were unable to facilitate the reaction (Table 1, entries 5–7). Increasing the amount of  $\gamma$ -cyclodextrin to 30 mol % or decreasing the loading of both Fe(OTf)<sub>3</sub> and  $\gamma$ -cyclodextrin to 10 mol % led to depressed chemoselectivities (Table 1, entries 8 and 9). Inferior performance was provided by solvents other than DCE (Table 1, entries 10 and 11). Thus the best result was observed when the reaction was run at 40 °C in DCE by using 20 mol % of Fe(OTf)<sub>3</sub> and 20 mol % of  $\gamma$ -cyclodextrin as the cocatalyst (Table 1, entry 4).

Using the superior Fe(OTf)<sub>3</sub>/ $\gamma$ -CD cocatalyst and the optimized reaction conditions (Table 1, entry 4), we evaluated various alkenes as substrates. First, styrenes bearing electron-donating groups such as a methyl group at the meta, ortho, and para positions of the phenyl rings gave rise to the desired hydroamination products in 51–68% yield (Scheme 2, 3ab–ad). Styrene bearing a bulky functional group like a tertiary butyl group at the para position could also be well tolerated (Scheme 2, 3ae, 63% yield). The electron-withdrawing-group-substituted styrenes proceeded smoothly to provide the

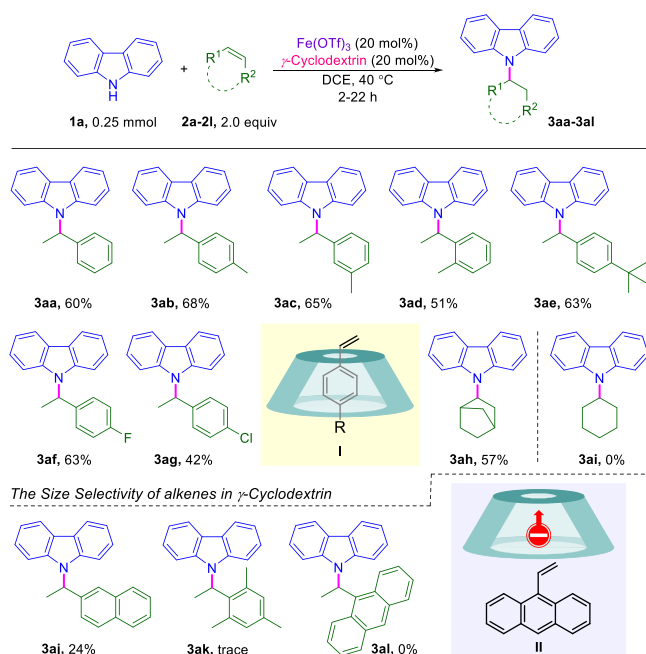
corresponding products 3af and 3ag in 63 and 42% yield, respectively. It is noteworthy that the subsequent attempts employing a nonactivated aliphatic alkene, norbornene 2h, also furnished the hydroamination product 3ah in 57% yield. However, cyclohexene 2i was found to be inert under the standard conditions.

It is well known that cyclodextrins allow for the noncovalent binding of small molecules in their hydrophobic cavities.<sup>8a–c</sup> To investigate the binding geometry between alkenes and  $\gamma$ -cyclodextrins in the hydroamination reaction, more bulky substrates 2j–l were also tested, which were larger than the monosubstituted styrenes or norbornene mentioned above. The reaction of the 2-vinylnaphthalene 2j and carbazole 1a proceeded to provide the corresponding product 3aj in dramatically decreased yield (24%). Moreover, when the size of the alkenes further increased (2k and 2l), which made it difficult for them to go inside into the cavity of  $\gamma$ -cyclodextrins (Scheme 2, diagram II), the system failed to provide the corresponding hydroamination products. These results definitely showed the size selectivity of alkenes in  $\gamma$ -cyclodextrins, which indicated that the alkenes were bound in the cavities of  $\gamma$ -cyclodextrins during the catalytic process of the hydroamination reaction (Scheme 2, diagram I).

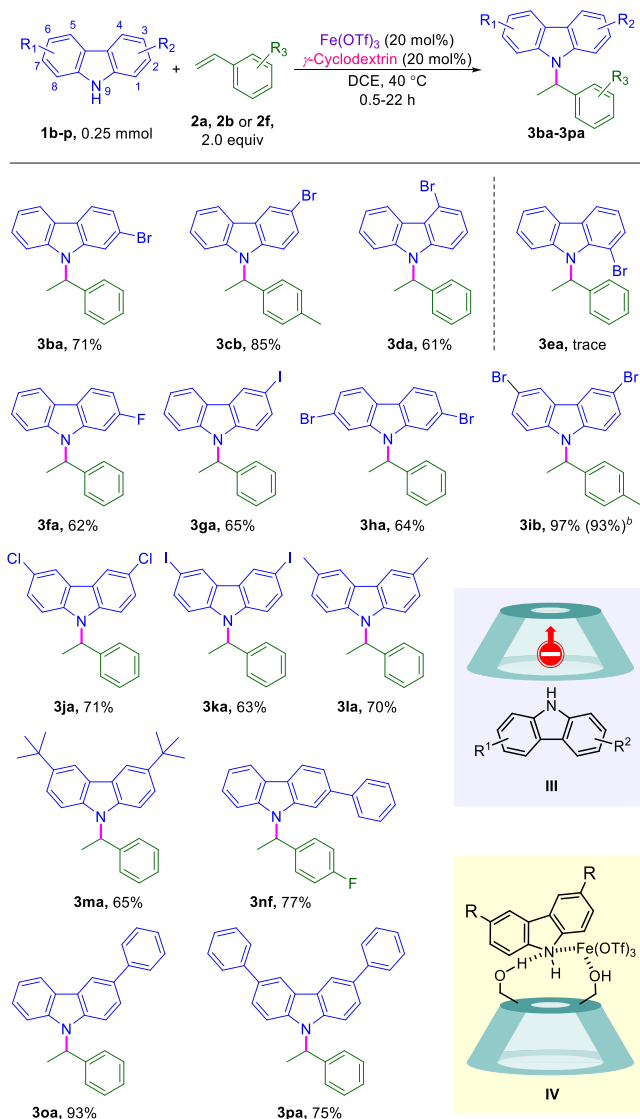
Encouraged by the above results, we next turned our attention to the scope of carbazoles that could be used in the hydroamination reaction. To our delight, a wide variety of commercially available carbazoles having electron-withdrawing or electron-donating groups at different positions were accommodated, and a series of hydroamination products based on these carbazoles were obtained in moderate to high yields. In previous work, both the scope of the carbazoles and the yields of the corresponding products were limited, in which only a few substituted carbazoles were tested and the yields were up to 68%. In this work, carbazoles 1b–d, 1f, and 1g bearing halogen groups on the C-2, C-3, or C-4 position could all give good yields for the products (3ba, 3cb, 3da, 3fa, and 3ga, 61–85% yield). However, 1-bromo-substituted carbazole 1e could not serve as a viable substrate, which might be because the steric hindrance provided by the large bromine substituent on the C-1 position of carbazole prevented the carbazole from undergoing the desired C–N bond formation under the standard conditions. Moreover, 2,7- and 3,6-halogen- or alkyl-disubstituted carbazoles 1h–m were also proven to be suitable substrates for this hydroamination reaction, affording the corresponding products 3ha, 3ib, 3ja, 3ka, 3la, and 3ma in 63–97% yield. Furthermore, carbazoles bearing mono- or diphenyl substituents also underwent this transformation to yield the products 3nf, 3oa, and 3pa in excellent yields (75–93%). On the basis of the results provided in Scheme 3, it is clear that there is no limit for the size of the carbazoles in these transformations, which was consistent with the fact that carbazoles 1a–p were too large to be bound into the cavities of  $\gamma$ -cyclodextrins (Scheme 3, diagram III). However, the carbazoles could still be trapped on the rim of the  $\gamma$ -cyclodextrins by both the hydroxyl groups and the metal center, which had also been captured by  $\gamma$ -cyclodextrins through noncovalent bonds (Scheme 3, diagram IV) to participate in the catalytic process.<sup>10d,12</sup>

Inspired by the above results, we next surveyed several carbazole-fused aromatics with styrene 2a under the standard conditions to further demonstrate the scope of the amines (Scheme 4). We were pleased to find that this system was also compatible with various carbazole-fused aromatics 5a–d, and

### Scheme 2. Substrate Scope and Limitation of Styrenes<sup>a</sup>



<sup>a</sup>Reactions were performed with 0.25 mmol of **1a**, 0.5 mmol of **2**, 20 mol % of Fe(OTf)<sub>3</sub>, and 20 mol % of  $\gamma$ -cyclodextrin in 2 mL of DCE at 40 °C. The percentages under the chemical structures are their isolated yields.

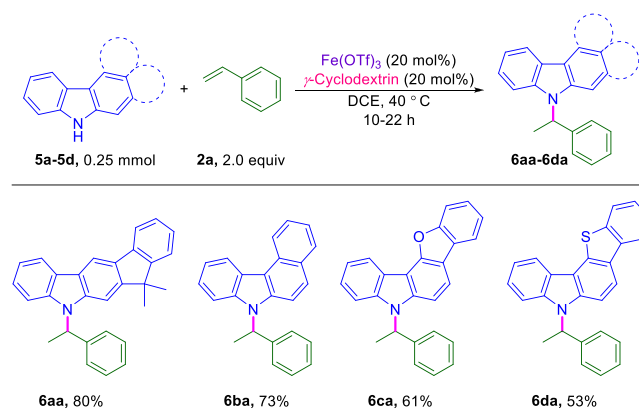
Scheme 3. Substrate Scope and Limitation of Carbazoles<sup>a</sup>

<sup>a</sup>Reactions were performed with 0.25 mmol of **1**, 0.5 mmol of **2**, 20 mol % of  $\text{Fe}(\text{OTf})_3$ , and 20 mol % of  $\gamma$ -cyclodextrin in 2 mL of DCE at 40 °C. The percentages under the chemical structures are their isolated yields. <sup>b</sup>Reaction was carried out on a 1 mmol scale of **1i**.

the corresponding hydroamination products **6aa–da** were isolated in moderate to good yields (53–80%).

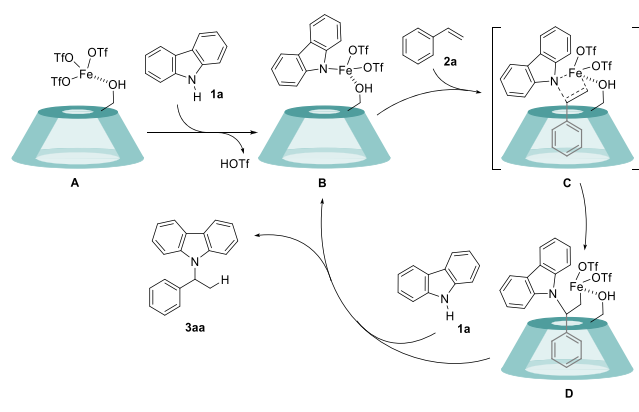
According to the observed binding geometry in Schemes 2 and 3 and on the basis of literature precedents,<sup>5a,10d,13</sup> a plausible mechanism is proposed in Scheme 5. The initial step is presumably the deprotonation of carbazole **1a** with the  $\text{Fe}(\text{OTf})_3/\gamma$ -cyclodextrin complex **A** to generate the catalytically active iron species **B**. Subsequently, styrene **2a** was captured by the cavity of the  $\gamma$ -cyclodextrin of active species **B** to form the intermediate **C**. The vinyl group of styrene **2a** in intermediate **C** would insert into the Fe–N bond to give the iron alkyl intermediate **D**. Finally, the Fe–C bond at the iron alkyl intermediate **D** would undergo protonolytic cleavage through the proton on the N-9 position of a new carbazole molecule to afford the desired hydroamination product **3aa** and release the catalytically active iron species **B**.

In summary, we have developed an efficient and general catalytic hydroamination of styrenes with carbazoles, wherein

Scheme 4. Substrate Scope and Limitation of Carbazole-Fused Aromatics<sup>a</sup>

<sup>a</sup>Reactions were performed with 0.25 mmol of **5**, 0.5 mmol of **2a**, 20 mol % of  $\text{Fe}(\text{OTf})_3$ , and 20 mol % of  $\gamma$ -cyclodextrin in 2 mL of DCE at 40 °C. The percentages under the chemical structures are their isolated yields.

Scheme 5. Proposed Mechanism for the N-Alkylation Reaction



the  $\text{Fe}(\text{OTf})_3$  and  $\gamma$ -CD complex are used for the first time as an inexpensive, low-toxicity, and facile cocatalyst that performed as an artificial metalloenzyme with high activity and selectivity. This simple cocatalyst enables the transformation of a wide variety of readily available alkenes and carbazoles as well as carbazole-fused aromatics into hydroamination products with moderate to high yields, whereas most of the carbazoles and carbazole-fused aromatics were not involved in previous reports. One of the distinctive features of this catalytic system is the simple and benign reaction conditions with no need for a strong base, additive, or the irradiation of light. The  $\text{Fe}(\text{OTf})_3$  and  $\gamma$ -cyclodextrin cocatalyst is of great potential for the exploration of organic transformations under atom-economic and sustainable reaction conditions.

## ■ ASSOCIATED CONTENT

### Supporting Information

The Supporting Information is available free of charge at <https://pubs.acs.org/doi/10.1021/acs.orglett.0c03959>.

Experimental procedures, characterization data, and copies of NMR spectra for substrates and products (PDF)

## ■ AUTHOR INFORMATION

## Corresponding Authors

**Peng Chen** – School of Materials Science and Chemical Engineering, Institute of Drug Discovery Technology, Ningbo University, Ningbo 315211, P. R. China; [orcid.org/0000-0001-8970-0967](https://orcid.org/0000-0001-8970-0967); Email: [chenpeng@nbu.edu.cn](mailto:chenpeng@nbu.edu.cn)

**Yi-Jun Jiang** – School of Materials Science and Chemical Engineering, Institute of Drug Discovery Technology, Ningbo University, Ningbo 315211, P. R. China; [orcid.org/0000-0003-1872-8721](https://orcid.org/0000-0003-1872-8721); Email: [jiangyijun@nbu.edu.cn](mailto:jiangyijun@nbu.edu.cn)

## Authors

**En-Kai Xiao** – School of Materials Science and Chemical Engineering, Institute of Drug Discovery Technology, Ningbo University, Ningbo 315211, P. R. China

**Xian-Tao Wu** – School of Materials Science and Chemical Engineering, Institute of Drug Discovery Technology, Ningbo University, Ningbo 315211, P. R. China

**Feng Ma** – School of Materials Science and Chemical Engineering, Institute of Drug Discovery Technology, Ningbo University, Ningbo 315211, P. R. China

**Xiaohua Feng** – Zhejiang Engineering Research Center for Biomedical Materials, Cixi Institute of BioMedical Engineering, Ningbo Institute of Materials Technology and Engineering, Chinese Academy of Sciences, Cixi 315300, P. R. China; [orcid.org/0000-0001-5931-9321](https://orcid.org/0000-0001-5931-9321)

Complete contact information is available at:

<https://pubs.acs.org/10.1021/acs.orglett.0c03959>

## Notes

The authors declare no competing financial interest.

## ■ ACKNOWLEDGMENTS

This research was supported by the Zhejiang Provincial Natural Science Foundation of China (grant nos. LY20B020004 and LY19B020003), Programs Supported by Ningbo Natural Science Foundation (grant no. 202003N4009), and A Project Supported by Scientific Research Fund of Zhejiang Provincial Education Department (grant no. Y201941353).

## ■ REFERENCES

- (1) (a) Knolker, H. J.; Reddy, K. R. *Chem. Rev.* **2002**, *102*, 4303. (b) Schmidt, A. W.; Reddy, K. R.; Knolker, H. J. *Chem. Rev.* **2012**, *112*, 3193.
- (2) (a) Choi, T. A.; Czerwonka, R.; Forke, R.; Jäger, A.; Knöll, J.; Krahl, M. P.; Krause, T.; Reddy, K. R.; Franzblau, S. G.; Knölker, H.-J. *Med. Chem. Res.* **2008**, *17*, 374. (b) Börger, C.; Brutting, C.; Julich-Gruner, K. K.; Hesse, R.; Kumar, V. P.; Kutz, S. K.; Ronnefahrt, M.; Thomas, C.; Wan, B.; Franzblau, S. G.; Knolker, H. J. *Bioorg. Med. Chem.* **2017**, *25*, 6167. (c) Zhang, Y.; Tanganchu, V. K. R.; Cheng, Y.; Yang, R. G.; Lin, J. M.; Zhou, C. H. *ACS Med. Chem. Lett.* **2018**, *9*, 244. (d) Caruso, A.; Ceramella, J.; Iacopetta, D.; Saturnino, C.; Mauro, M. V.; Bruno, R.; Aquaro, S.; Sinicropi, M. S. *Molecules* **2019**, *24*, 1912. (e) Kumar, N.; Lal, N.; Nemaysh, V.; Luthra, P. M. *Bioorg. Chem.* **2020**, *100*, 103911.
- (3) (a) Gendron, D.; Leclerc, M. *Energy Environ. Sci.* **2011**, *4*, 1225. (b) Hao, X. L.; Zhang, L.; Wang, D.; Zhang, C.; Guo, J. F.; Ren, A. M. *J. Phys. Chem. C* **2018**, *122*, 6273. (c) Yin, J.; Ma, Y.; Li, G.; Peng, M.; Lin, W. *Coord. Chem. Rev.* **2020**, *412*, 213257.
- (4) (a) Bernoud, E.; Lepori, C.; Mellah, M.; Schulz, E.; Hannedouche, J. *Catal. Sci. Technol.* **2015**, *5*, 2017. (b) Greenhalgh, M. D.; Jones, A. S.; Thomas, S. P. *ChemCatChem* **2015**, *7*, 190.
- (c) Huang, L. B.; Arndt, M.; Goossen, K.; Heydt, H.; Goossen, L. J. *Chem. Rev.* **2015**, *115*, 2596. (d) Hannedouche, J.; Lepori, C. *Synthesis* **2017**, *49*, 1158. (e) Trowbridge, A.; Walton, S. M.; Gaunt, M. J. *Chem. Rev.* **2020**, *120*, 2613.
- (5) (a) Bernoud, E.; Oulie, P.; Guillot, R.; Mellah, M.; Hannedouche, J. *Angew. Chem., Int. Ed.* **2014**, *53*, 4930. (b) Nguyen, H. N.; Lee, H.; Audörsch, S.; Reznichenko, A. L.; Nawara-Hultzs, A. J.; Schmidt, B.; Hultzs, K. C. *Organometallics* **2018**, *37*, 4358. (c) Kang, O. Y.; Kim, B. E.; Park, S. J.; Ryu, D. H.; Lim, H. J. *Asian J. Org. Chem.* **2018**, *7*, 451. (d) Ma, W.; Zhang, X.; Fan, J.; Liu, Y.; Tang, W.; Xue, D.; Li, C.; Xiao, J.; Wang, C. *J. Am. Chem. Soc.* **2019**, *141*, 13506. (e) Miller, D. C.; Ganley, J. M.; Musacchio, A. J.; Sherwood, T. C.; Ewing, W. R.; Knowles, R. R. *J. Am. Chem. Soc.* **2019**, *141*, 16590. (f) Takata, T.; Hirano, K.; Miura, M. *Org. Lett.* **2019**, *21*, 4284. (g) Tran, G.; Shao, W.; Mazet, C. *J. Am. Chem. Soc.* **2019**, *141*, 14814. (h) Vanable, E. P.; Kennemur, J. L.; Joyce, L. A.; Ruck, R. T.; Schultz, D. M.; Hull, K. L. *J. Am. Chem. Soc.* **2019**, *141*, 739.
- (6) (a) Sevov, C. S.; Zhou, J. S.; Hartwig, J. F. *J. Am. Chem. Soc.* **2014**, *136*, 3200. (b) Sunaba, H.; Kamata, K.; Mizuno, N. *ChemCatChem* **2014**, *6*, 2333. (c) Ye, Y.; Kim, S. T.; Jeong, J.; Baik, M. H.; Buchwald, S. L. *J. Am. Chem. Soc.* **2019**, *141*, 3901. (d) Xiong, Y.; Zhang, G. *Org. Lett.* **2019**, *21*, 7873. (e) Sun, H. L.; Yang, F.; Ye, W. T.; Wang, J. J.; Zhu, R. *ACS Catal.* **2020**, *10*, 4983. (f) Yahata, K.; Kaneko, Y.; Akai, S. *Org. Lett.* **2020**, *22*, 598.
- (7) Bauer, I.; Knolker, H. J. *Chem. Rev.* **2015**, *115*, 3170.
- (8) (a) Breslow, R.; Dong, S. D. *Chem. Rev.* **1998**, *98*, 1997. (b) Takahashi, K. *Chem. Rev.* **1998**, *98*, 2013. (c) Marchetti, L.; Levine, M. *ACS Catal.* **2011**, *1*, 1090. (d) Hong, S. B.; Liu, M. Y.; Zhang, W.; Deng, W. *Chin. J. Org. Chem.* **2015**, *35*, 325.
- (9) (a) Kanagaraj, K.; Suresh, P.; Pitchumani, K. *Org. Lett.* **2010**, *12*, 4070. (b) Kumar, A.; Tripathi, V. D.; Kumar, P. *Green Chem.* **2011**, *13*, 51. (c) Kanagaraj, K.; Pitchumani, K. *J. Org. Chem.* **2013**, *78*, 744. (d) Kumar, A.; Shukla, R. D. *Green Chem.* **2015**, *17*, 848.
- (10) (a) Thompson, Z.; Cowan, J. A. *Small* **2020**, *16*, No. 2000392. (b) Iwasawa, T. *Tetrahedron Lett.* **2017**, *58*, 4217. (c) Jouffroy, M.; Gramage-Doria, R.; Armspach, D.; Sémeril, D.; Oberhauser, W.; Matt, D.; Toupet, L. *Angew. Chem., Int. Ed.* **2014**, *53*, 3937. (d) Khan, R. I.; Pitchumani, K. *Green Chem.* **2016**, *18*, 5518. (e) Wang, B.; Bols, M. *Chem. - Eur. J.* **2017**, *23*, 13766. (f) Zhang, P. L.; Tugny, C.; Mejjide Suárez, J.; Guitet, M.; Derat, E.; Vanthuyne, N.; Zhang, Y. M.; Bistri, O.; Mouriès-Mansuy, V.; Ménand, M.; Roland, S.; Fensterbank, L.; Sollogoub, M. *Chem.* **2017**, *3*, 174. (g) Zhang, P.; Mejjide Suárez, J.; Driant, T.; Derat, E.; Zhang, Y.; Ménand, M.; Roland, S.; Sollogoub, M. *Angew. Chem., Int. Ed.* **2017**, *56*, 10821.
- (11) (a) Suresh, P.; Pitchumani, K. *J. Org. Chem.* **2008**, *73*, 9121. (b) Guitet, M.; Zhang, P.; Marcelo, F.; Tugny, C.; Jiménez-Barbero, J.; Buriez, O.; Amatore, C.; Mouriès-Mansuy, V.; Goddard, J. P.; Fensterbank, L.; Zhang, Y.; Roland, S.; Ménand, M.; Sollogoub, M. *Angew. Chem., Int. Ed.* **2013**, *52*, 7213.
- (12) (a) Sridhar, R.; Srinivas, B.; Kumar, V. P.; Reddy, V. P.; Kumar, A. V.; Rao, K. R. *Adv. Synth. Catal.* **2008**, *350*, 1489. (b) Tayade, Y. A.; Padvi, S. A.; Wagh, Y. B.; Dalal, D. S. *Tetrahedron Lett.* **2015**, *56*, 2441.
- (13) (a) Lepori, C.; Bernoud, E.; Guillot, R.; Tobisch, S.; Hannedouche, J. *Chem. - Eur. J.* **2019**, *25*, 835. (b) Hannedouche, J. *Chimia* **2018**, *72*, 635.

*Supporting Information for*

## **Fe(OTf)<sub>3</sub> and $\gamma$ -Cyclodextrin Catalyzed Hydroamination of Alkenes with Carbazoles**

En-Kai Xiao,<sup>a</sup> Xian-Tao Wu,<sup>a</sup> Feng Ma,<sup>a</sup> Xiaohua Feng,<sup>b</sup> Peng Chen<sup>\*a</sup> and Yi-Jun Jiang<sup>\*a</sup> .

<sup>a</sup>School of Materials Science and Chemical Engineering, Institute of Drug Discovery Technology, Ningbo University, Ningbo 315211 (P. R. China)

<sup>b</sup>Zhejiang Engineering Research Center for Biomedical Materials, Cixi Institute of BioMedical Engineering, Ningbo Institute of Materials Technology and Engineering, Chinese Academy of Sciences, Cixi 315300 (P. R. China)

*Corresponding Author Emails: chenpeng@nbu.edu.cn; jiangyijun@nbu.edu.cn*

## TABLE OF CONTENTS:

1. General .....	S1
2. Fe(OTf) <sub>3</sub> /γ-CD Catalyzed Hydroamination of Alkenes with Carbazoles.....	S1
3.References .....	S11
4.Copies of NMR Spectra .....	S11

## 1. General

All moisture or oxygen-sensitive reactions were carried out under a nitrogen atmosphere in oven or heat-dried flasks or Schlenk tubes. All commercially available reagents were directly used as received without further purification. All reactions were monitored by thin-layer chromatography (TLC) on gel F<sub>254</sub> plates using UV light as visualizing agent (if applicable), and a solution of phosphomolybdic acid hydrate (50 g/L) in EtOH followed by heating as developing agents. The products were purified by flash column chromatography on silica gel (200-300 meshes) from the Qingdao Marine Chemical Factory in China.

<sup>1</sup>H NMR and <sup>13</sup>C NMR spectra were recorded in CDCl<sub>3</sub> solution on a Bruker AVANCE II 400 MHz or Bruker Ascend 500 MHz instrument. Chemical shifts were denoted in ppm (δ), and calibrated by using residual undeuterated solvent (CHCl<sub>3</sub> (7.26 ppm) or tetramethylsilane (0.00 ppm)) as internal reference for <sup>1</sup>H NMR and the deuterated solvent (CDCl<sub>3</sub> (77.16 ppm) or tetramethylsilane (0.00 ppm)) as internal standard for <sup>13</sup>C NMR. The coupling constants were reported in Hz. The following abbreviations were used to explain the multiplicities: s = singlet, d = doublet, t = triplet, q = quartet, br = broad, td = triple doublet, dt = double triplet, m = multiplet. High-resolution mass spectral analysis (HRMS) data were measured on a Thermo Scientific TM Q Exactive Plus<sup>TM</sup> mass spectrometer by means of the ESI technique.

## 2. Fe(OTf)<sub>3</sub>/γ-CD Catalyzed Hydroamination of Alkenes with Carbazoles

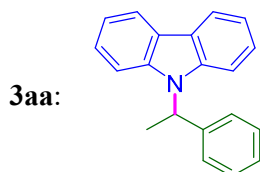
General experimental procedure was described as follows:

The compounds **1a-1p**, **2a-2l** and **5a-5d** used in this work are commercially available from Adamas, Innochem or TCI.

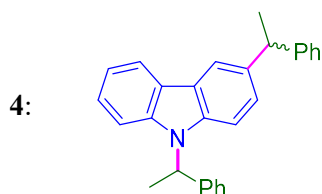
To an oven-dried Schlenk tube were sequentially added carbazole or its derivatives (0.25 mmol), γ-cyclodextrin (64.9 mg, 0.05 mmol), iron (III) trifluoromethanesulfonate (25.2 mg, 0.05 mmol) and 1,2-dichloroethane (2.0 mL). The reaction mixture was stirred at 40°C for 5 min. Then, alkene substrate (0.5 mmol, 2.0 equiv) was added to the reaction mixture. The resultant mixture was stirred at 40°C for 0.5–22h (monitored by thin layer chromatography until the carbazole or its derivatives had disappeared or the system no longer changed). Then the reaction mixture was cooled to room temperature and quenched with water (10 mL). Following addition of ethyl acetate (AcOEt) (10 mL), the organic layer was separated, and the aqueous phase was extracted with AcOEt (10 mL). The combined organic extracts were washed with H<sub>2</sub>O (4 mL) and brine (10 mL), dried over anhydrous Na<sub>2</sub>SO<sub>4</sub>, and concentrated under reduced pressure. The residue was purified by flash column chromatography on silica gel with an eluent (for **3aj** the eluant is *n*-hexane/AcOEt (250:1), and for all the other products the eluant is *n*-hexane) to afford the product.



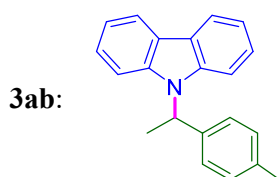
Except for special notes, all the products was obtained following the above general experimental procedure.



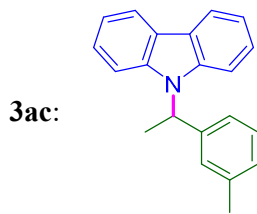
The general experimental procedure was followed to afford product **3aa** as yellow oil (40.7 mg, 60% yield).  $^1\text{H}$  NMR (400 MHz,  $\text{CDCl}_3$ ):  $\delta$  (ppm) 8.09 (d,  $J = 7.6$  Hz, 2H), 7.33–7.27 (m, 2H), 7.26–7.09 (m, 9H), 6.01 (q,  $J = 7.2$  Hz, 1H), 1.93 (d,  $J = 7.2$  Hz, 3H).  $^{13}\text{C}$  NMR (126 MHz,  $\text{CDCl}_3$ ):  $\delta$  (ppm) 140.8, 139.9, 128.7, 127.4, 126.6, 125.6, 123.6, 120.4, 119.1, 110.2, 52.4, 17.5. HRMS (ESI)  $m/z$ :  $[M+H]^+$  Calcd for  $\text{C}_{20}\text{H}_{18}\text{N}$  272.1434; Found 272.1427.



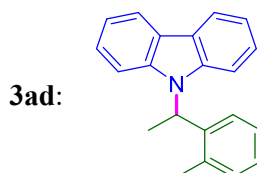
**4** is a byproduct from the reaction to synthesize **3aa**.  $^1\text{H}$  NMR (400 MHz,  $\text{CDCl}_3$ ):  $\delta$  (ppm) 8.08 (d,  $J = 7.6$  Hz, 1H), 7.98 (s, 1H), 7.36–7.09 (m, 15H), 6.02 (q,  $J = 6.8$  Hz, 1H), 4.32 (q,  $J = 6.8$  Hz, 1H), 1.95 (d,  $J = 6.8$  Hz, 3H), 1.74 (d,  $J = 6.8$  Hz, 3H).  $^{13}\text{C}$  NMR (126 MHz,  $\text{CDCl}_3$ ):  $\delta$  (ppm) 147.4, 141.0, 140.3, 138.6, 137.2, 128.8, 128.5, 127.8, 127.4, 126.6, 126.0, 125.83, 125.79, 125.4, 123.6, 123.5, 120.4, 118.9, 110.2, 110.1, 52.4, 44.8, 22.6, 17.6. HRMS (ESI)  $m/z$ :  $[M+H]^+$  Calcd for  $\text{C}_{28}\text{H}_{26}\text{N}$  376.2060; Found 376.2056.



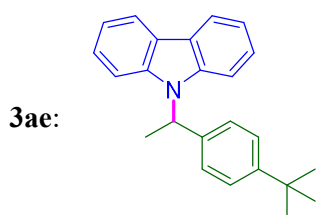
The general experimental procedure was followed to afford product **3ab** as yellow oil (48.5 mg, 68% yield).  $^1\text{H}$  NMR (400 MHz,  $\text{CDCl}_3$ ):  $\delta$  (ppm) 8.11 (d,  $J = 8.0$  Hz, 2H), 7.36–7.30 (m, 2H), 7.26–7.15 (m, 6H), 7.10 (d,  $J = 8.0$  Hz, 2H), 6.03 (q,  $J = 7.2$  Hz, 1H), 2.31 (s, 3H), 1.96 (d,  $J = 7.2$  Hz, 3H).  $^{13}\text{C}$  NMR (126 MHz,  $\text{CDCl}_3$ ):  $\delta$  (ppm) 140.0, 137.8, 137.1, 129.4, 126.5, 125.5, 123.5, 120.4, 119.0, 110.3, 52.2, 21.2, 17.6. HRMS (ESI)  $m/z$ :  $[M+H]^+$  Calcd for  $\text{C}_{21}\text{H}_{20}\text{N}$  286.1590; Found 286.1585.



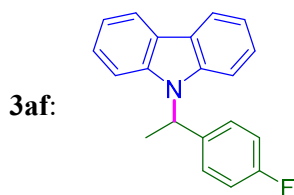
The general experimental procedure was followed to afford product **3ac** as yellow oil (46.4 mg, 65% yield).  $^1\text{H}$  NMR (400 MHz,  $\text{CDCl}_3$ ):  $\delta$  (ppm) 8.09 (d,  $J = 7.6$  Hz, 2H), 7.33–7.28 (m, 2H), 7.24–7.12 (m, 5H), 7.11–7.01 (m, 3H), 5.98 (q,  $J = 7.2$  Hz, 1H), 2.23 (s, 3H), 1.91 (d,  $J = 7.2$  Hz, 3H).  $^{13}\text{C}$  NMR (126 MHz,  $\text{CDCl}_3$ ):  $\delta$  (ppm) 140.8, 140.0, 138.4, 128.6, 128.2, 127.4, 125.6, 123.63, 123.55, 120.4, 119.0, 110.3, 52.4, 21.6, 17.5. HRMS (ESI)  $m/z$ :  $[M+H]^+$  Calcd for  $\text{C}_{21}\text{H}_{20}\text{N}$  286.1590; Found 286.1584.



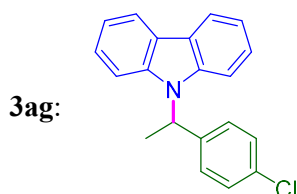
The general experimental procedure was followed to afford product **3ad** as yellow oil (36.6 mg, 51% yield).  $^1\text{H}$  NMR (400 MHz,  $\text{CDCl}_3$ ):  $\delta$  (ppm) 8.08 (d,  $J = 8.0$  Hz, 2H), 7.75 (d,  $J = 7.6$  Hz, 1H), 7.38–7.15 (m, 8H), 7.08 (d,  $J = 7.2$  Hz, 1H), 5.98 (q,  $J = 7.2$  Hz, 1H), 1.94 (d,  $J = 7.2$  Hz, 3H), 1.81 (s, 3H).  $^{13}\text{C}$  NMR (126 MHz,  $\text{CDCl}_3$ ):  $\delta$  (ppm) 139.8, 138.3, 138.2, 131.3, 128.1, 126.8, 126.1, 125.6, 123.4, 120.4, 119.0, 109.8, 51.4, 19.8, 17.6. HRMS (ESI)  $m/z$ :  $[M+H]^+$  Calcd for  $\text{C}_{21}\text{H}_{20}\text{N}$  286.1590; Found 286.1585.



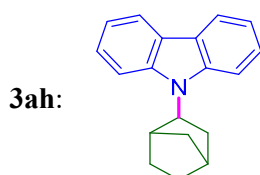
The general experimental procedure was followed to afford product **3ae** as yellow oil (51.6 mg, 63% yield).  $^1\text{H}$  NMR (400 MHz,  $\text{CDCl}_3$ ):  $\delta$  (ppm) 8.10 (d,  $J = 7.6$  Hz, 2H), 7.34–7.11 (m, 10H), 6.00 (q,  $J = 7.2$  Hz, 1H), 1.94 (d,  $J = 7.2$  Hz, 3H), 1.26 (s, 9H).  $^{13}\text{C}$  NMR (126 MHz,  $\text{CDCl}_3$ ):  $\delta$  (ppm) 150.3, 140.0, 137.8, 126.3, 125.6, 125.5, 123.6, 120.4, 119.0, 110.4, 52.2, 34.6, 31.4, 17.6. The NMR analytic data of **3ae** is consistent with the literature.<sup>[1]</sup>



The general experimental procedure was followed to afford product **3af** as yellow oil (45.6 mg, 63% yield).  $^1\text{H}$  NMR (400 MHz,  $\text{CDCl}_3$ ):  $\delta$  (ppm) 8.08 (d,  $J = 8.0$  Hz, 2H), 7.34–7.28 (m, 2H), 7.22–7.12 (m, 6H), 6.93 (t,  $J = 8.8$  Hz, 2H), 5.96 (q,  $J = 7.2$  Hz, 1H), 1.91 (d,  $J = 7.2$  Hz, 3H).  $^{13}\text{C}$  NMR (126 MHz,  $\text{CDCl}_3$ ):  $\delta$  (ppm) 162.1 (d,  $^1J_{\text{C-F}} = 247.0$  Hz), 139.8, 136.6, 128.3 (d,  $^3J_{\text{C-F}} = 7.6$  Hz), 125.7, 123.6, 120.5, 119.2, 115.6 (d,  $^2J_{\text{C-F}} = 21.4$  Hz), 110.1, 51.8, 17.6. HRMS (ESI)  $m/z$ :  $[M+H]^+$  Calcd for  $\text{C}_{20}\text{H}_{17}\text{FN}$  290.1340; Found 290.1333.

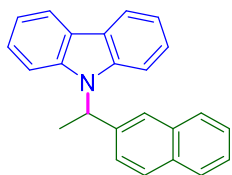


The general experimental procedure was followed to afford product **3ag** as yellow oil (32.1 mg, 42% yield).  $^1\text{H}$  NMR (400 MHz,  $\text{CDCl}_3$ ):  $\delta$  (ppm) 8.10 (d,  $J = 7.2$  Hz, 2H), 7.36–7.29 (m, 2H), 7.26–7.14 (m, 8H), 5.97 (q,  $J = 6.4$  Hz, 1H), 1.93 (d,  $J = 6.4$  Hz, 3H).  $^{13}\text{C}$  NMR (126 MHz,  $\text{CDCl}_3$ ):  $\delta$  (ppm) 139.8, 139.4, 133.3, 128.9, 128.0, 125.7, 123.6, 120.5, 119.3, 110.1, 51.9, 17.5. HRMS (ESI)  $m/z$ :  $[M+H]^+$  Calcd for  $\text{C}_{20}\text{H}_{17}\text{ClN}$  306.1044; Found 306.1042.



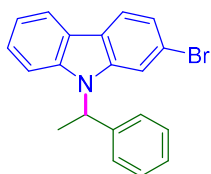
The general experimental procedure was followed to afford product **3ah** as colorless oil (37.2 mg, 57% yield).  $^1\text{H}$  NMR (400 MHz,  $\text{CDCl}_3$ ) (major isomer):  $\delta$  (ppm) 8.06 (d,  $J = 7.6$  Hz, 2H), 7.55 (d,  $J = 7.6$  Hz, 2H), 7.38 (t,  $J = 7.6$  Hz, 2H), 7.18 (t,  $J = 7.6$  Hz, 2H), 4.53–4.48 (m, 1H), 3.02–2.98 (m, 1H), 2.49–2.43 (m, 1H), 2.11–2.04 (m, 2H), 1.74–1.62 (m, 2H), 1.52–1.30 (m, 4H).  $^{13}\text{C}$  NMR (126 MHz,  $\text{CDCl}_3$ ) (major isomer):  $\delta$  (ppm) 140.2, 125.5, 123.6, 120.1, 118.7, 111.0, 61.4, 41.3, 39.2, 38.2, 35.8, 29.1, 28.6. HRMS (ESI)  $m/z$ :  $[M+H]^+$  Calcd for  $\text{C}_{19}\text{H}_{20}\text{N}$  262.1590; Found 262.1588.

**3aj:**



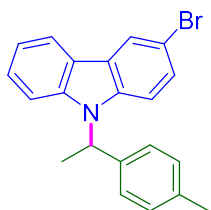
The general experimental procedure was followed to afford product **3aj** as a white solid (19.2 mg, 24% yield). <sup>1</sup>H NMR (400 MHz, CDCl<sub>3</sub>): δ (ppm) 8.11 (d, *J* = 7.6 Hz, 2H), 7.86 (s, 1H), 7.80–7.72 (m, 2H), 7.64 (d, *J* = 8.8 Hz, 1H), 7.47–7.40 (m, 2H), 7.31–7.14 (m, 7H), 6.14 (q, *J* = 7.2 Hz, 1H), 2.04 (d, *J* = 7.2 Hz, 3H). <sup>13</sup>C NMR (126 MHz, CDCl<sub>3</sub>): δ (ppm) 140.0, 138.5, 133.4, 132.8, 128.6, 128.2, 127.8, 126.4, 126.2, 125.6, 125.3, 124.8, 123.6, 120.5, 119.1, 110.2, 52.5, 17.4. The NMR analytic data of **3aj** is consistent with the literature.<sup>[1]</sup>

**3ba:**

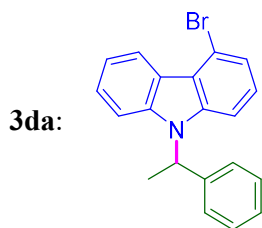


The general experimental procedure was followed to afford product **3ba** as colorless oil (62.2 mg, 71% yield). <sup>1</sup>H NMR (400 MHz, CDCl<sub>3</sub>): δ (ppm) 8.03 (d, *J* = 7.6 Hz, 1H), 7.91 (d, *J* = 8.0 Hz, 1H), 7.40 (d, *J* = 1.6 Hz, 1H), 7.34–7.15 (m, 9H), 5.96 (q, *J* = 7.2 Hz, 1H), 1.94 (d, *J* = 7.2 Hz, 3H). <sup>13</sup>C NMR (126 MHz, CDCl<sub>3</sub>): δ (ppm) 140.7, 140.0, 139.8, 128.7, 127.5, 126.3, 125.9, 122.9, 122.3, 122.1, 121.4, 120.2, 119.5, 119.1, 113.0, 110.5, 52.5, 17.4. HRMS (ESI) *m/z*: [*M*+H]<sup>+</sup> Calcd for C<sub>20</sub>H<sub>17</sub>BrN 350.0539; Found 350.0528.

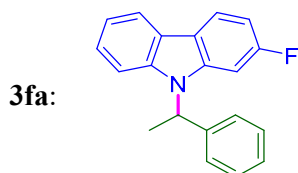
**3cb:**



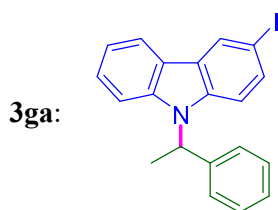
The general experimental procedure was followed to afford product **3cb** as colorless oil (77.3 mg, 85% yield). <sup>1</sup>H NMR (400 MHz, CDCl<sub>3</sub>): δ (ppm) 8.20 (d, *J* = 1.6 Hz, 1H), 8.04 (d, *J* = 8.0 Hz, 1H), 7.39–7.34 (m, 2H), 7.28–7.18 (m, 2H), 7.15–7.03 (m, 5H), 5.98 (q, *J* = 6.8 Hz, 1H), 2.30 (s, 3H), 1.93 (d, *J* = 6.8 Hz, 3H). <sup>13</sup>C NMR (126 MHz, CDCl<sub>3</sub>): δ (ppm) 140.4, 138.5, 137.34, 137.31, 129.5, 128.2, 126.5, 126.3, 125.4, 123.1, 122.5, 120.6, 119.5, 111.91, 111.86, 110.3, 52.4, 21.2, 17.5. HRMS (ESI) *m/z*: [*M*+H]<sup>+</sup> Calcd for C<sub>21</sub>H<sub>19</sub>BrN 364.0695; Found 364.0691.



The general experimental procedure was followed to afford product **3da** as colorless oil (53.4 mg, 61% yield).  $^1\text{H}$  NMR (400 MHz,  $\text{CDCl}_3$ ):  $\delta$  (ppm) 8.85 (d,  $J = 8.0$  Hz, 1H), 7.39–7.33 (m, 2H), 7.28–7.19 (m, 7H), 7.16–7.07 (m, 2H), 6.02 (q,  $J = 7.2$  Hz, 1H), 1.92 (d,  $J = 7.2$  Hz, 3H).  $^{13}\text{C}$  NMR (126 MHz,  $\text{CDCl}_3$ ):  $\delta$  (ppm) 141.0, 140.3, 140.1, 128.8, 127.6, 126.5, 126.3, 125.9, 123.3, 123.1, 122.9, 122.0, 119.2, 117.0, 110.0, 109.1, 52.4, 17.3. HRMS (ESI)  $m/z$ :  $[M+H]^+$  Calcd for  $\text{C}_{20}\text{H}_{17}\text{BrN}$  350.0539; Found 350.0534.

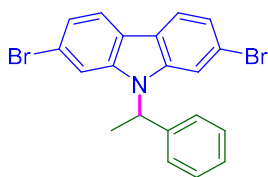


The general experimental procedure was followed to afford product **3fa** as colorless oil (44.8 mg, 62% yield).  $^1\text{H}$  NMR (400 MHz,  $\text{CDCl}_3$ ):  $\delta$  (ppm) 8.01 (d,  $J = 8.0$  Hz, 1H), 7.96 (dd,  $J = 8.4, 5.6$  Hz, 1H), 7.32–7.12 (m, 8H), 6.94–6.83 (m, 2H), 5.92 (q,  $J = 7.2$  Hz, 1H), 1.91 (d,  $J = 7.2$  Hz, 3H).  $^{13}\text{C}$  NMR (126 MHz,  $\text{CDCl}_3$ ):  $\delta$  (ppm) 161.8 (d,  $^1J_{\text{C-F}} = 241.9$  Hz), 140.6, 140.3, 128.8, 127.6, 126.6, 125.2, 123.2, 121.3, 121.2, 120.04, 119.95, 119.6, 110.2, 107.2 (d,  $^2J_{\text{C-F}} = 23.9$  Hz), 97.3 (d,  $^2J_{\text{C-F}} = 27.7$  Hz), 52.6, 17.3. HRMS (ESI)  $m/z$ :  $[M+H]^+$  Calcd for  $\text{C}_{20}\text{H}_{17}\text{FN}$  290.1340; Found 290.1336.



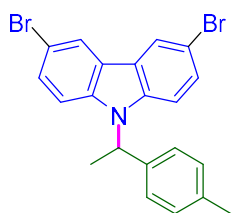
The general experimental procedure was followed to afford product **3ga** as a white solid (64.5 mg, 65% yield).  $^1\text{H}$  NMR (400 MHz,  $\text{CDCl}_3$ ):  $\delta$  (ppm) 8.39 (d,  $J = 1.6$  Hz, 1H), 8.02 (d,  $J = 7.6$  Hz, 1H), 7.52 (dd,  $J = 8.4, 1.6$  Hz, 1H), 7.34 (t,  $J = 7.2$  Hz, 1H), 7.30–7.16 (m, 7H), 6.94 (d,  $J = 8.8$  Hz, 1H), 5.97 (q,  $J = 7.2$  Hz, 1H), 1.92 (d,  $J = 7.2$  Hz, 3H).  $^{13}\text{C}$  NMR (126 MHz,  $\text{CDCl}_3$ )  $\delta$  (ppm) 140.4, 140.1, 139.0, 133.8, 129.3, 128.9, 127.7, 126.6, 126.4, 126.2, 122.3, 120.7, 119.7, 112.4, 110.3, 81.8, 52.6, 17.6. HRMS (ESI)  $m/z$ :  $[M+H]^+$  Calcd for  $\text{C}_{20}\text{H}_{17}\text{IN}$  398.0400; Found 398.0398.

**3ha:**



The general experimental procedure was followed to afford product **3ha** as a white solid (68.6 mg, 64% yield).  $^1\text{H}$  NMR (400 MHz,  $\text{CDCl}_3$ ):  $\delta$  (ppm) 7.88 (d,  $J = 8.4$  Hz, 2H), 7.37 (d,  $J = 1.6$  Hz, 2H), 7.35–7.21 (m, 7H), 5.92 (q,  $J = 7.2$  Hz, 1H), 1.95 (d,  $J = 7.2$  Hz, 3H).  $^{13}\text{C}$  NMR (126 MHz,  $\text{CDCl}_3$ ):  $\delta$  (ppm) 140.9, 139.6, 129.0, 127.9, 126.4, 122.9, 122.0, 121.5, 119.7, 113.5, 52.9, 17.5. HRMS (ESI)  $m/z$ :  $[M+H]^+$  Calcd for  $\text{C}_{20}\text{H}_{16}\text{Br}_2\text{N}$  429.9624; Found 429.9623.

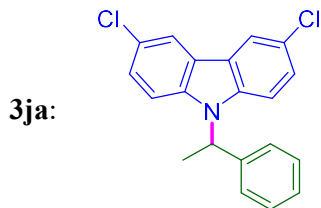
**3ib:**



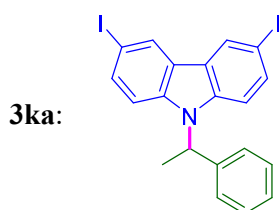
The general experimental procedure was followed to afford product **3ib** as a white solid (107.4 mg, 97% yield).  $^1\text{H}$  NMR (400 MHz,  $\text{CDCl}_3$ ):  $\delta$  (ppm) 8.16 (d,  $J = 2.0$  Hz, 2H), 7.44 (dd,  $J = 8.8, 2.0$  Hz, 2H), 7.15–7.09 (m, 6H), 5.96 (q,  $J = 7.2$  Hz, 1H), 2.33 (s, 3H), 1.94 (d,  $J = 6.8$  Hz, 3H).  $^{13}\text{C}$  NMR (126 MHz,  $\text{CDCl}_3$ ):  $\delta$  (ppm) 138.9, 137.6, 136.9, 129.6, 129.0, 126.4, 124.2, 123.3, 112.3, 111.9, 52.6, 21.2, 17.5. HRMS (ESI)  $m/z$ :  $[M+H]^+$  Calcd for  $\text{C}_{21}\text{H}_{18}\text{Br}_2\text{N}$  443.9780; Found 443.9738.

For a 1 mmol scale example, the experimental procedure was as follows:

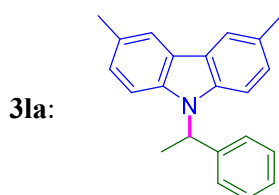
To an oven-dried Schlenk tube were sequentially added 3,6-Dibromocarbazole **1i** (325.0 mg, 1.0 mmol),  $\gamma$ -cyclodextrin (259.4 mg, 0.2 mmol), iron (III) trifluoromethanesulfonate (100.6 mg, 0.2 mmol) and 1,2-dichloroethane (4.0 mL). The reaction mixture was stirred at 40°C for 5 min. Then, 4-Methylstyrene **2b** (236.4 mg, 2.0 mmol, 2.0 equiv) was added to the reaction mixture. The resultant mixture was stirred at 40°C for 1h (monitored by thin layer chromatography until 2-bromocarbazole had disappeared). Then the reaction mixture was cooled to room temperature and quenched with water (20 mL). Following addition of ethyl acetate (AcOEt) (60 mL), the organic layer was separated, and the aqueous phase was extracted with AcOEt (60 mL). The combined organic extracts were washed with  $\text{H}_2\text{O}$  (20 mL) and brine (20 mL), dried over anhydrous  $\text{Na}_2\text{SO}_4$ , and concentrated under reduced pressure. The residue was purified by flash column chromatography on silica gel with an eluent of *n*-hexane to afford the product **3ib** (413.5 mg, 93% yield).



The general experimental procedure was followed to afford product **3ja** as a white solid (60.4 mg, 71% yield). <sup>1</sup>H NMR (400 MHz, CDCl<sub>3</sub>): δ (ppm) 7.96 (d, *J* = 2.0 Hz, 2H), 7.31–7.17 (m, 7H), 7.09 (d, *J* = 8.8 Hz, 2H), 5.93 (q, *J* = 7.2 Hz, 1H), 1.91 (d, *J* = 7.2 Hz, 3H). <sup>13</sup>C NMR (126 MHz, CDCl<sub>3</sub>): δ (ppm) 140.0, 138.7, 128.9, 127.8, 126.44, 126.37, 125.0, 123.7, 120.3, 111.4, 52.8, 17.5. HRMS (ESI) *m/z*: [*M*+H]<sup>+</sup> Calcd for C<sub>20</sub>H<sub>16</sub>Cl<sub>2</sub>N 340.0654; Found 340.0648.

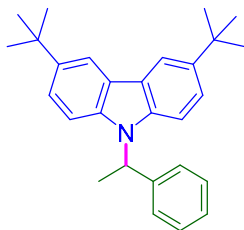


The general experimental procedure was followed to afford product **3ka** as a white solid (82.4 mg, 63% yield). <sup>1</sup>H NMR (400 MHz, CDCl<sub>3</sub>): δ (ppm) 8.31 (d, *J* = 1.6 Hz, 2H), 7.54 (dd, *J* = 8.4, 1.6 Hz, 2H), 7.31–7.17 (m, 5H), 6.96 (d, *J* = 8.8 Hz, 2H), 5.92 (q, *J* = 7.2 Hz, 1H), 1.90 (d, *J* = 7.2 Hz, 3H). <sup>13</sup>C NMR (126 MHz, CDCl<sub>3</sub>): δ (ppm) 139.9, 139.1, 134.6, 129.5, 129.0, 127.8, 126.4, 124.7, 112.4, 82.2, 52.7, 17.5. HRMS (ESI) *m/z*: [*M*+H]<sup>+</sup> Calcd for C<sub>20</sub>H<sub>16</sub>I<sub>2</sub>N 523.9367; Found 523.9335.



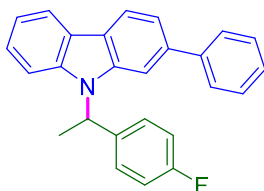
The general experimental procedure was followed to afford product **3la** as a white solid (52.4 mg, 70% yield). <sup>1</sup>H NMR (400 MHz, CDCl<sub>3</sub>): δ (ppm) 7.86 (s, 2H), 7.25–7.16 (m, 5H), 7.09 (d, *J* = 8.0 Hz, 2H), 7.04 (d, *J* = 8.0 Hz, 2H), 5.91 (q, *J* = 7.2 Hz, 1H), 2.47 (s, 6H), 1.88 (d, *J* = 7.2 Hz, 3H). <sup>13</sup>C NMR (126 MHz, CDCl<sub>3</sub>): δ (ppm) 141.1, 138.5, 128.7, 128.0, 127.3, 126.7, 126.6, 123.5, 120.4, 109.8, 52.4, 21.4, 17.5. HRMS (ESI) *m/z*: [*M*+H]<sup>+</sup> Calcd for C<sub>22</sub>H<sub>22</sub>N 300.1747; Found 300.1740.

**3ma:**



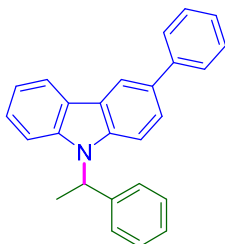
The general experimental procedure was followed to afford product **3ma** as a white solid (62.3 mg, 65% yield). <sup>1</sup>H NMR (400 MHz, CDCl<sub>3</sub>): δ (ppm) 8.12 (d, *J* = 1.6 Hz, 2H), 7.36 (dd, *J* = 8.8, 1.6 Hz, 2H), 7.31–7.19 (m, 5H), 7.11 (d, *J* = 8.8 Hz, 2H), 5.96 (q, *J* = 7.2 Hz, 1H), 1.92 (d, *J* = 7.2 Hz, 3H), 1.43 (s, 18H). <sup>13</sup>C NMR (126 MHz, CDCl<sub>3</sub>): δ (ppm) 141.6, 141.1, 138.3, 128.5, 127.2, 126.5, 123.3, 123.1, 116.2, 109.5, 52.3, 34.6, 32.0, 17.5. HRMS (ESI) *m/z*: [*M*+H]<sup>+</sup> Calcd for C<sub>28</sub>H<sub>34</sub>N 384.2686; Found 384.2678.

**3nf:**



The general experimental procedure was followed to afford product **3nf** as a white solid (70.3 mg, 77% yield). <sup>1</sup>H NMR (400 MHz, CDCl<sub>3</sub>): δ (ppm) 8.20–8.07 (m, 2H), 7.58 (d, *J* = 7.2 Hz, 2H), 7.51–7.17 (m, 10H), 7.00 (t, *J* = 8.4 Hz, 2H), 6.08 (q, *J* = 6.8 Hz, 1H), 2.00 (d, *J* = 6.8 Hz, 3H). <sup>13</sup>C NMR (126 MHz, CDCl<sub>3</sub>): δ (ppm) 162.2 (d, <sup>1</sup>*J*<sub>C-F</sub> = 247.0 Hz), 142.2, 140.4, 140.2, 139.2, 136.5 (d, <sup>4</sup>*J*<sub>C-F</sub> = 2.5 Hz), 128.9, 128.4 (d, <sup>3</sup>*J*<sub>C-F</sub> = 8.8 Hz), 127.7, 127.2, 125.7, 123.5, 122.9, 120.7, 120.6, 119.4, 119.0, 115.7 (d, <sup>2</sup>*J*<sub>C-F</sub> = 21.4 Hz), 110.3, 108.6, 51.9, 17.8. HRMS (ESI) *m/z*: [*M*+H]<sup>+</sup> Calcd for C<sub>26</sub>H<sub>21</sub>FN 366.1653; Found 366.1644.

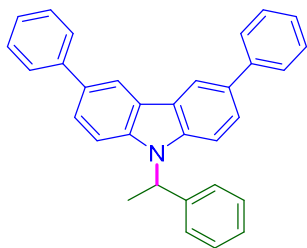
**3oa:**



The general experimental procedure was followed to afford product **3oa** as a white solid (80.6 mg, 93% yield). <sup>1</sup>H NMR (400 MHz, CDCl<sub>3</sub>): δ (ppm) 8.31 (d, *J* = 1.2 Hz, 1H), 8.13 (dd, *J* = 7.6, 1.2 Hz, 1H), 7.67–7.63 (m, 2H), 7.52 (dd, *J* = 8.8, 2.0 Hz, 1H), 7.40 (t, *J* = 7.6 Hz, 2H), 7.33–7.15 (m, 10H), 5.97 (q, *J* = 7.2 Hz, 1H), 1.91 (d, *J* = 7.2 Hz, 3H). <sup>13</sup>C NMR (126 MHz, CDCl<sub>3</sub>): δ (ppm) 142.1, 140.7, 140.4, 139.4, 132.6, 128.85, 128.76, 127.5, 127.4, 126.6, 125.8, 125.1, 124.1, 123.7, 120.5, 119.2, 118.9, 110.5, 110.3, 52.5, 17.5. HRMS (ESI) *m/z*: [*M*+H]<sup>+</sup> Calcd for C<sub>26</sub>H<sub>22</sub>N 348.1747; Found 348.1742.

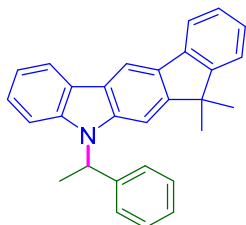


**3pa:**



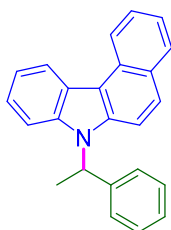
The general experimental procedure was followed to afford product **3pa** as a white solid (79.8 mg, 75% yield). <sup>1</sup>H NMR (400 MHz, CDCl<sub>3</sub>): δ (ppm) 8.37 (s, 2H), 7.67 (d, *J* = 7.6 Hz, 4H), 7.54 (dd, *J* = 8.4, 0.8 Hz, 2H), 7.41 (t, *J* = 7.6 Hz, 4H), 7.30–7.18 (m, 9H), 5.98 (q, *J* = 7.2 Hz, 1H), 1.93 (d, *J* = 6.8 Hz, 3H). <sup>13</sup>C NMR (126 MHz, CDCl<sub>3</sub>): δ (ppm) 142.0, 140.6, 139.9, 132.7, 128.9, 128.8, 127.6, 127.4, 126.6, 125.3, 124.2, 119.0, 110.6, 52.7, 17.6. HRMS (ESI) *m/z*: [*M*+H]<sup>+</sup> Calcd for C<sub>32</sub>H<sub>26</sub>N 424.2060; Found 424.2052.

**6aa:**

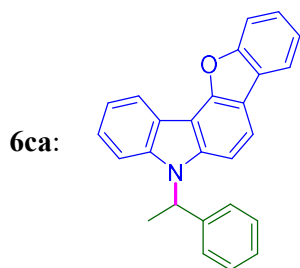


The general experimental procedure was followed to afford product **6aa** as a white solid (77.5 mg, 80% yield). <sup>1</sup>H NMR (400 MHz, CDCl<sub>3</sub>): δ (ppm) 8.40 (s, 1H), 8.15 (d, *J* = 7.6 Hz, 1H), 7.81 (d, *J* = 7.6 Hz, 1H), 7.39 (d, *J* = 7.2 Hz, 1H), 7.35–7.13 (m, 11H), 6.09 (q, *J* = 7.2 Hz, 1H), 1.99 (d, *J* = 7.2 Hz, 3H), 1.50 (s, 3H), 1.42 (s, 3H). <sup>13</sup>C NMR (126 MHz, CDCl<sub>3</sub>): δ (ppm) 153.3, 152.7, 140.8, 140.6, 140.2, 140.0, 131.5, 128.7, 127.4, 127.1, 126.7, 126.2, 125.2, 123.9, 123.0, 122.6, 120.3, 119.4, 119.1, 111.4, 110.6, 104.1, 52.5, 46.7, 28.2, 28.1, 17.5. HRMS (ESI) *m/z*: [*M*+H]<sup>+</sup> Calcd for C<sub>29</sub>H<sub>26</sub>N 388.2060; Found 388.2039.

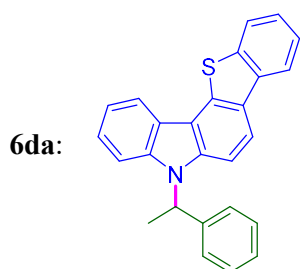
**6ba:**



The general experimental procedure was followed to afford product **6ba** as a white solid (58.7 mg, 73% yield). <sup>1</sup>H NMR (400 MHz, CDCl<sub>3</sub>): δ (ppm) 8.81 (d, *J* = 8.4 Hz, 1H), 8.63–8.59 (m, 1H), 7.89 (d, *J* = 8.0 Hz, 1H), 7.65 (t, *J* = 8.4 Hz, 2H), 7.43–7.29 (m, 5H), 7.23–7.15 (m, 5H), 6.10 (q, *J* = 7.2 Hz, 1H), 1.93 (d, *J* = 7.2 Hz, 3H). <sup>13</sup>C NMR (126 MHz, CDCl<sub>3</sub>): δ (ppm) 140.8, 139.0, 137.6, 130.1, 129.2, 128.9, 128.8, 127.5, 127.0, 126.5, 124.2, 124.0, 123.2, 123.0, 122.3, 120.0, 115.6, 112.2, 110.7, 52.4, 18.0. HRMS (ESI) *m/z*: [*M*+H]<sup>+</sup> Calcd for C<sub>24</sub>H<sub>20</sub>N 322.1590; Found 322.1587.



The general experimental procedure was followed to afford product **6ca** as a white solid (55.1 mg, 61% yield).  $^1\text{H}$  NMR (400 MHz,  $\text{CDCl}_3$ ):  $\delta$  (ppm) 8.56 (d,  $J = 7.2$  Hz, 1H), 7.89 (dd,  $J = 7.2, 0.4$  Hz, 1H), 7.81 (d,  $J = 8.4$  Hz, 1H), 7.69 (d,  $J = 8.0$  Hz, 1H), 7.41–7.15 (m, 11H), 6.10 (q,  $J = 7.2$  Hz, 1H), 1.99 (d,  $J = 7.2$  Hz, 3H).  $^{13}\text{C}$  NMR (126 MHz,  $\text{CDCl}_3$ ):  $\delta$  (ppm) 156.3, 151.6, 140.6, 140.4, 139.5, 128.8, 127.5, 126.6, 125.4, 125.2, 123.0, 122.9, 121.2, 119.9, 119.7, 117.6, 115.8, 111.7, 110.3, 108.8, 106.0, 52.9, 17.6. HRMS (ESI)  $m/z$ :  $[M+H]^+$  Calcd for  $\text{C}_{26}\text{H}_{20}\text{NO}$  362.1539; Found 362.1534.



The general experimental procedure was followed to afford product **6da** as a white solid (50.0 mg, 53% yield).  $^1\text{H}$  NMR (400 MHz,  $\text{CDCl}_3$ ):  $\delta$  (ppm) 8.29 (d,  $J = 7.2$  Hz, 1H), 8.10 (d,  $J = 7.6$  Hz, 1H), 8.03 (d,  $J = 8.8$  Hz, 1H), 7.93 (d,  $J = 7.6$  Hz, 1H), 7.46–7.16 (m, 11H), 6.12 (q,  $J = 7.2$  Hz, 1H), 2.00 (d,  $J = 7.2$  Hz, 3H).  $^{13}\text{C}$  NMR (126 MHz,  $\text{CDCl}_3$ ):  $\delta$  (ppm) 140.6, 139.8, 139.0, 138.7, 136.2, 133.0, 128.8, 128.4, 127.6, 126.6, 125.4, 125.3, 124.7, 123.1, 122.7, 121.9, 120.9, 119.8, 118.9, 117.2, 110.4, 108.1, 52.8, 17.7. HRMS (ESI)  $m/z$ :  $[M+H]^+$  Calcd for  $\text{C}_{26}\text{H}_{20}\text{NS}$  378.1311; Found 378.1309.

### 3. References

[1] Y. Xiong, G. Zhang, *Org. Lett.* **2019**, *21*, 7873-7877.

### 4. Copies of NMR Spectra

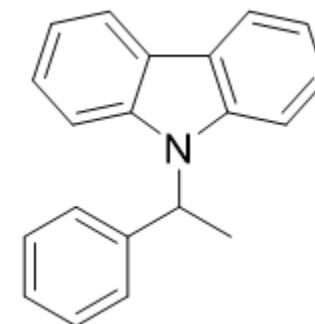
See the next page!

8.097  
8.078  
7.322  
7.320  
7.302  
7.284  
7.281  
7.254  
7.243  
7.227  
7.219  
7.206  
7.198  
7.184  
7.179  
7.159  
7.102  
6.032  
6.015  
5.997  
5.979

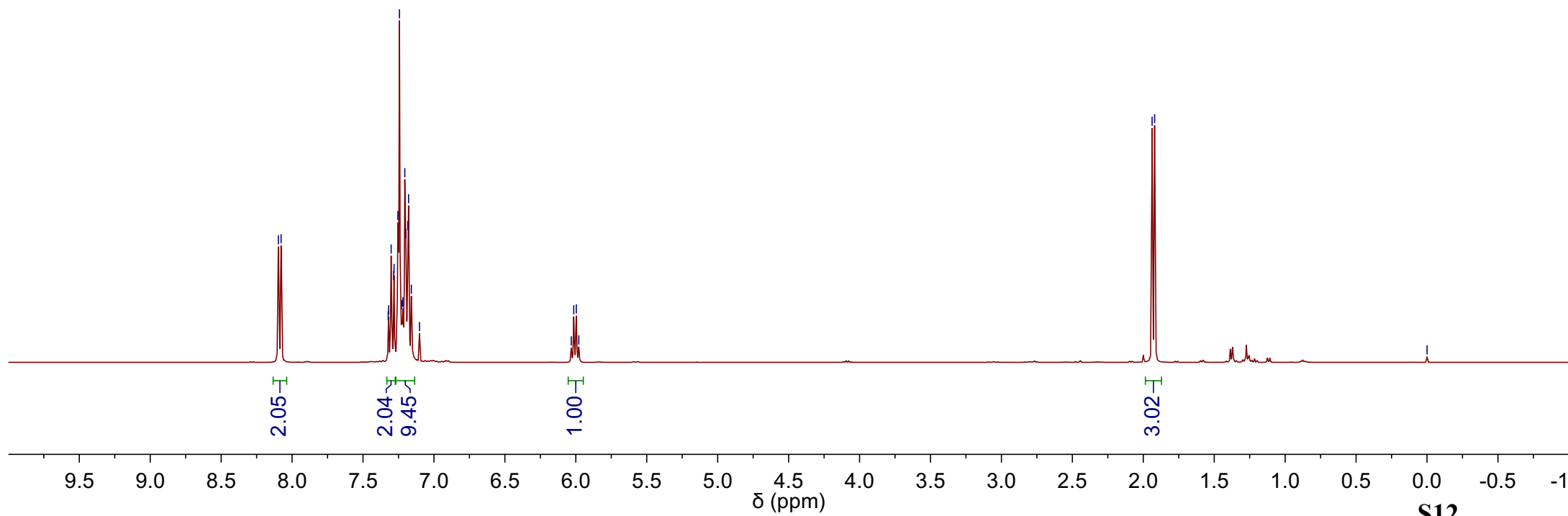
1.938  
1.920

0.000

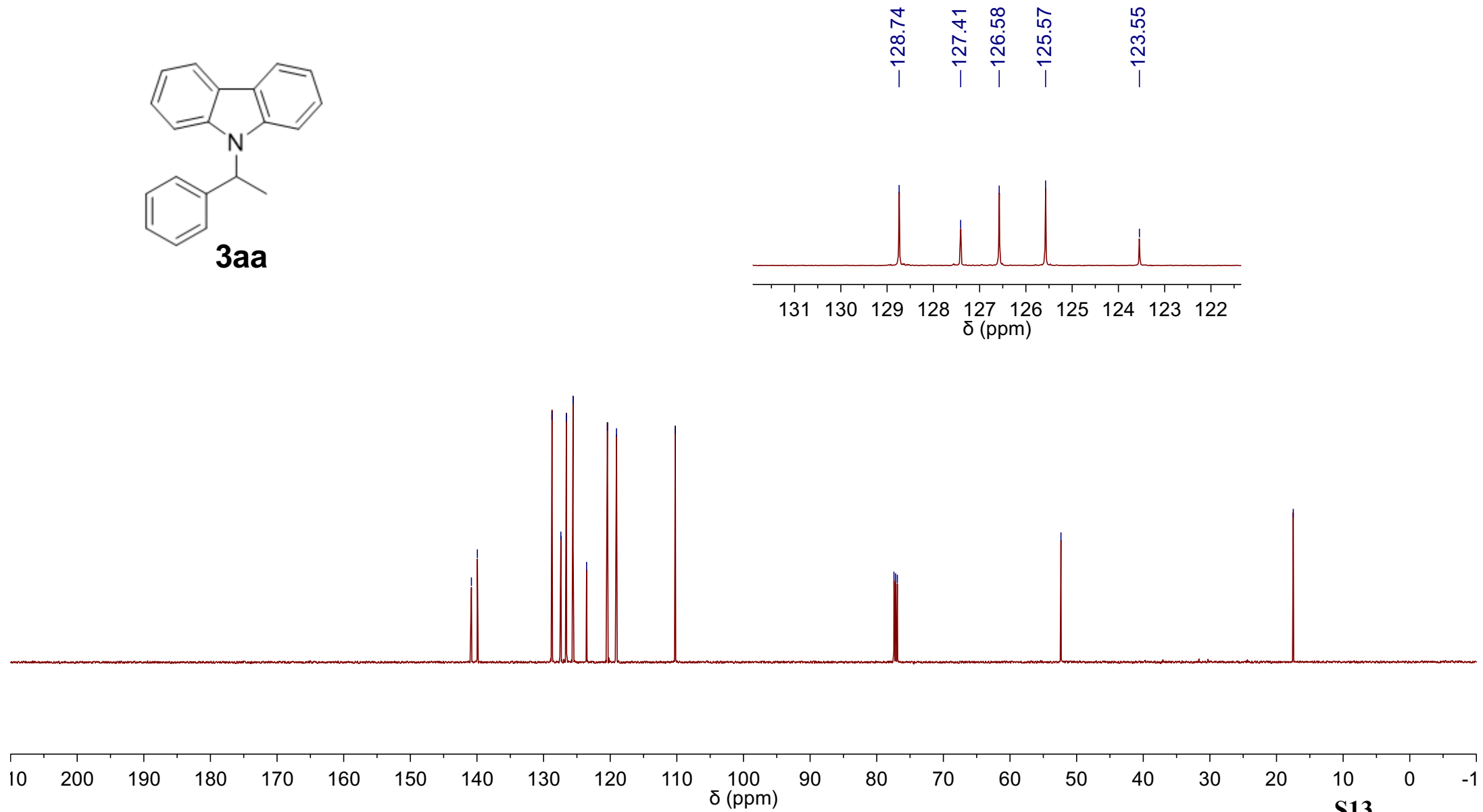
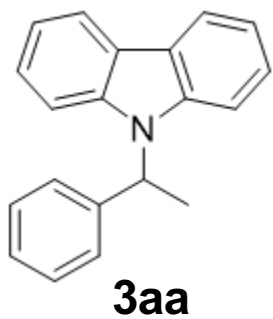
<sup>1</sup>H NMR (400 MHz, CDCl<sub>3</sub>)

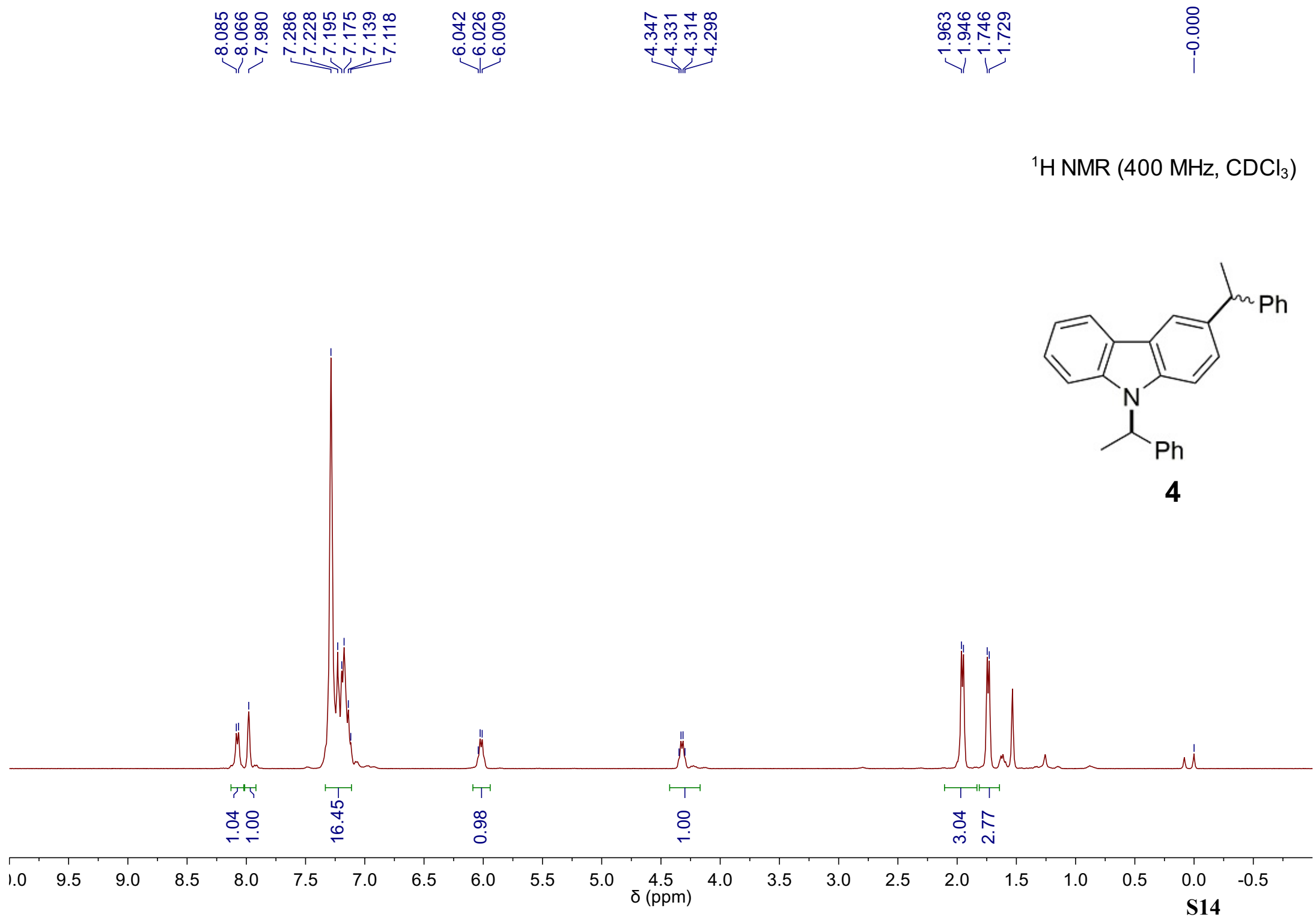


**3aa**

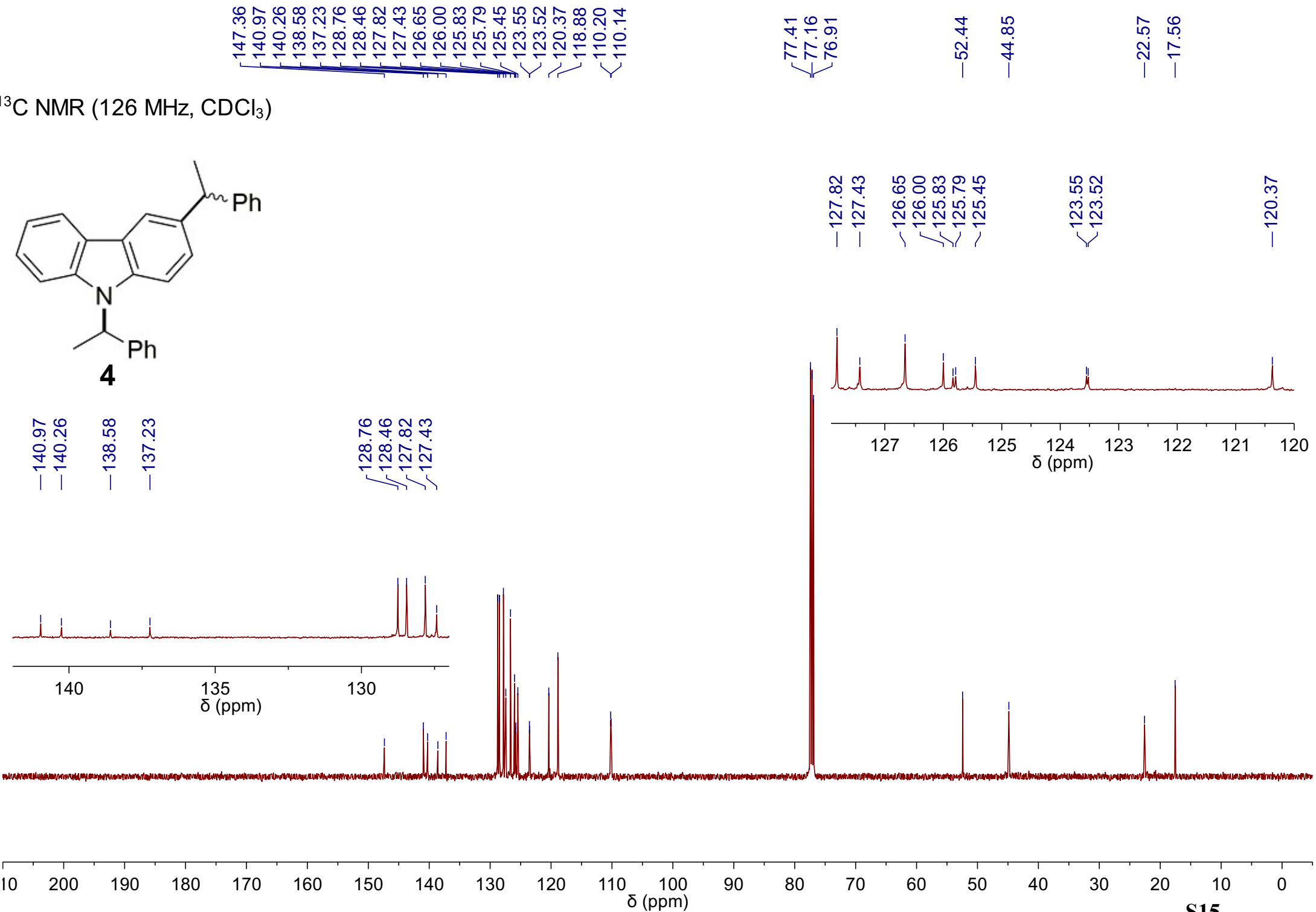
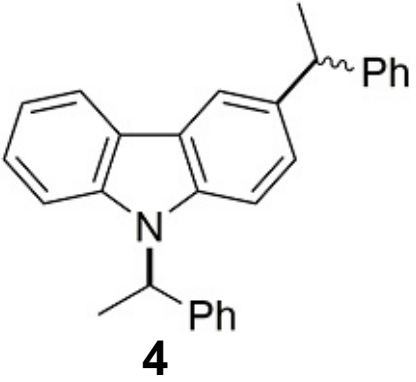


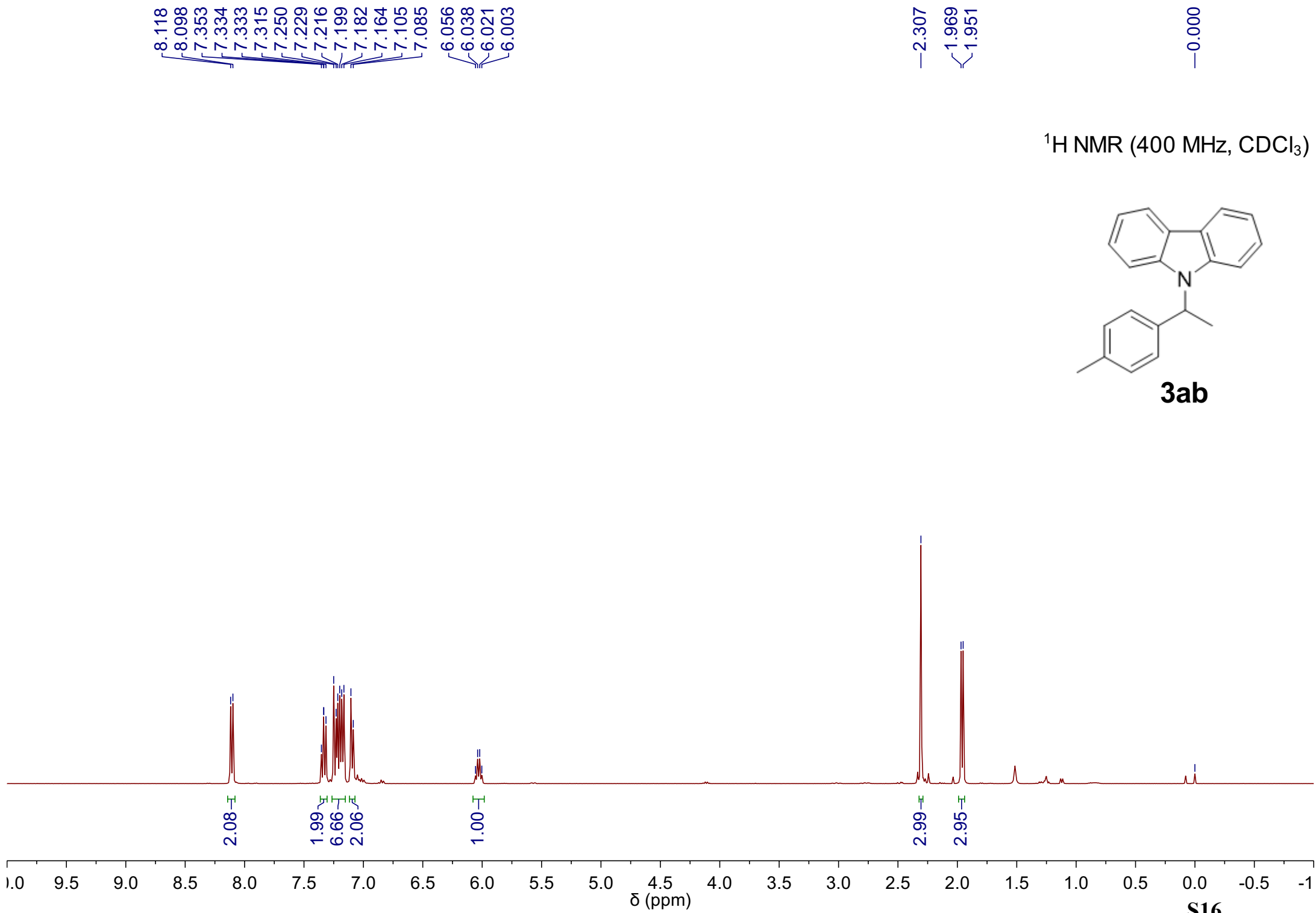
$^{13}\text{C}$  NMR (126 MHz,  $\text{CDCl}_3$ )



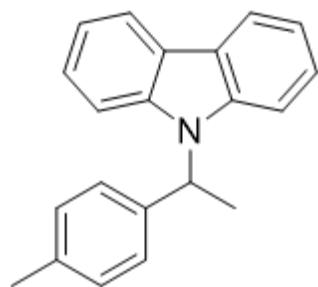


<sup>13</sup>C NMR (126 MHz, CDCl<sub>3</sub>)





$^{13}\text{C}$  NMR (126 MHz,  $\text{CDCl}_3$ )



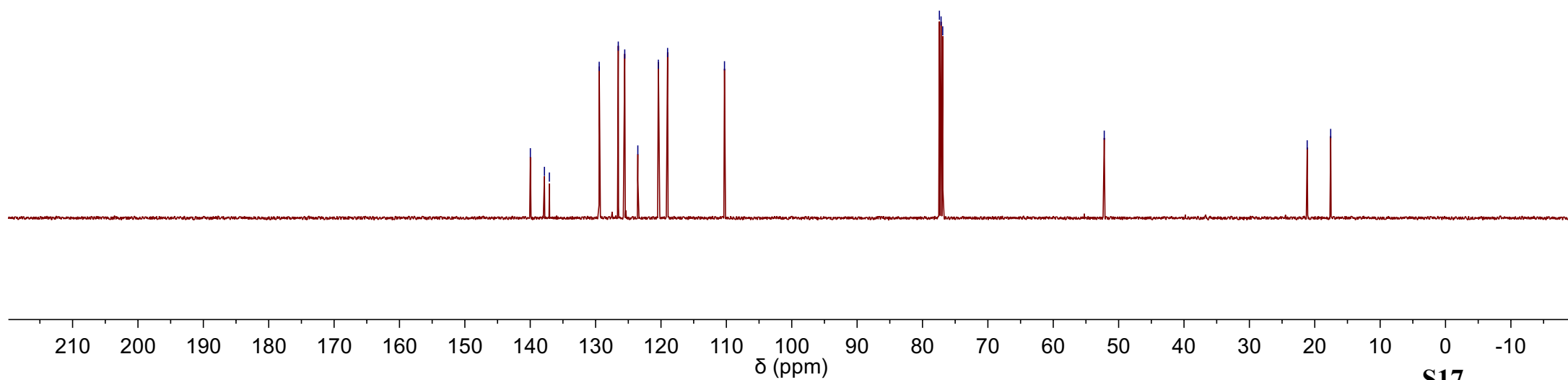
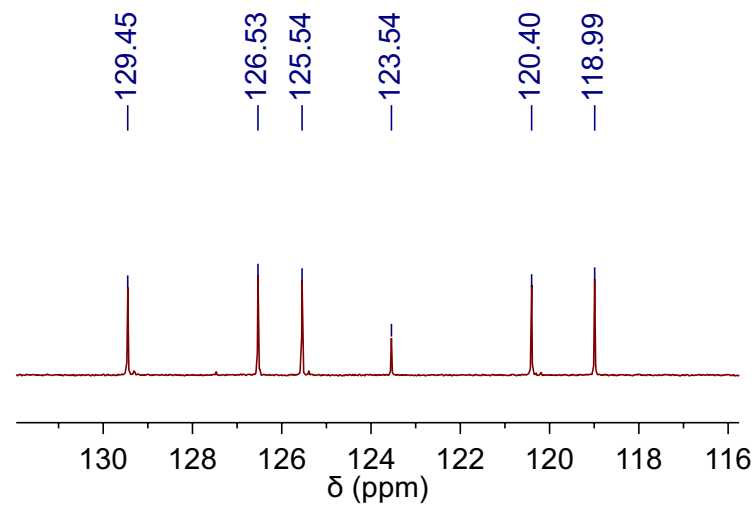
**3ab**

139.98  
137.83  
137.07  
129.45  
126.53  
125.54  
123.54  
120.40  
118.99  
110.29

77.41  
77.16  
76.91

52.20

21.16  
17.56



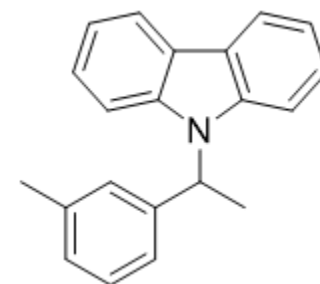


8.095  
8.076  
7.329  
7.327  
7.309  
7.291  
7.289  
7.227  
7.206  
7.197  
7.178  
7.170  
7.160  
7.151  
7.132  
7.096  
7.080  
7.061  
7.044  
7.026  
6.004  
5.986  
5.968  
5.950

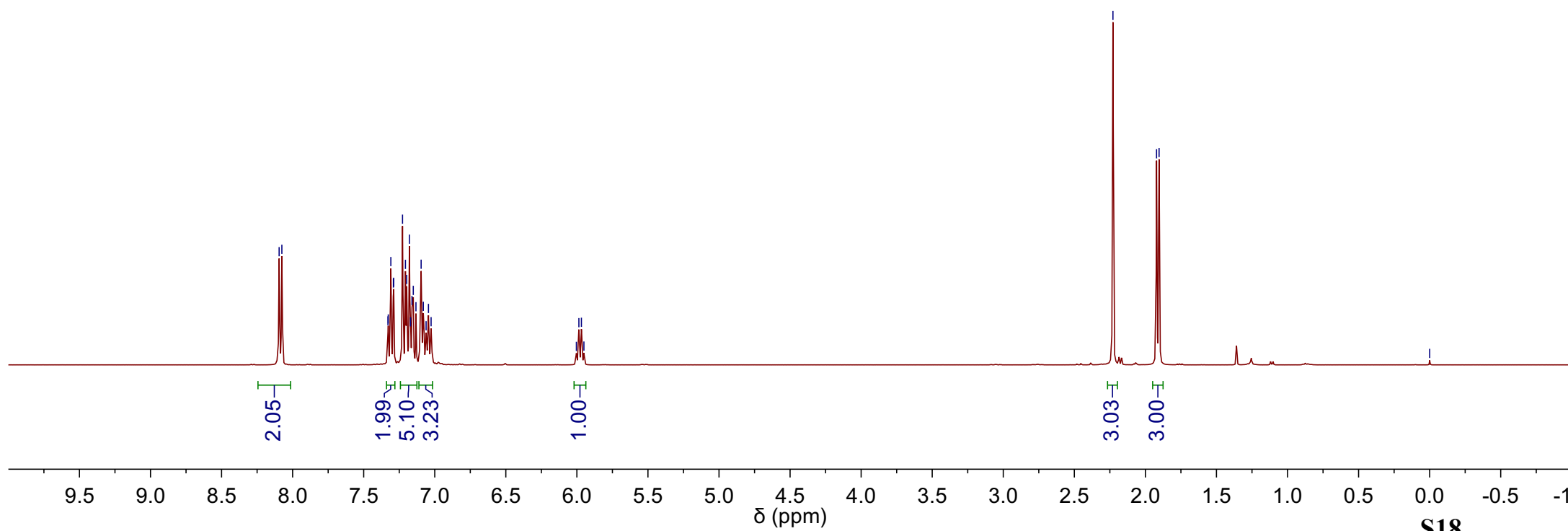
-2.228  
1.921  
1.904

-0.000

<sup>1</sup>H NMR (400 MHz, CDCl<sub>3</sub>)

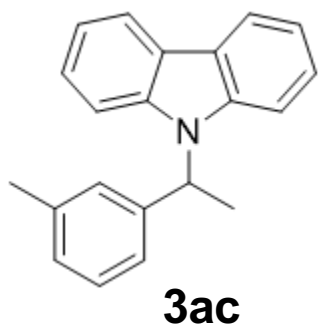


**3ac**



**S18**

$^{13}\text{C}$  NMR (126 MHz,  $\text{CDCl}_3$ )

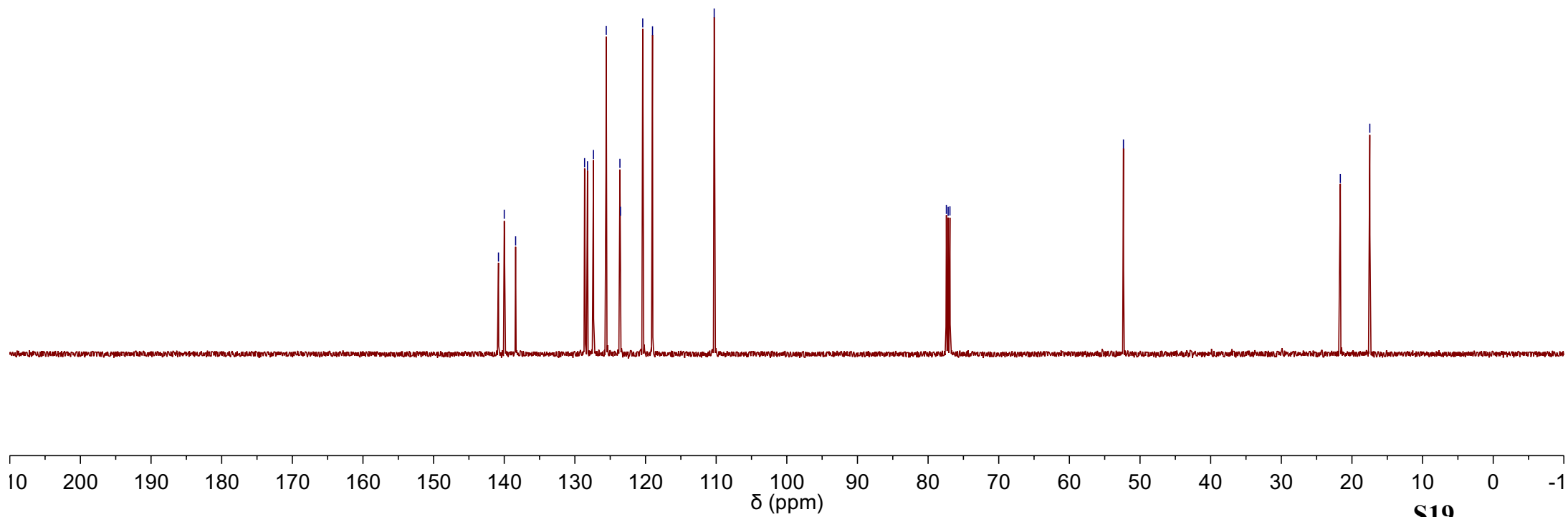
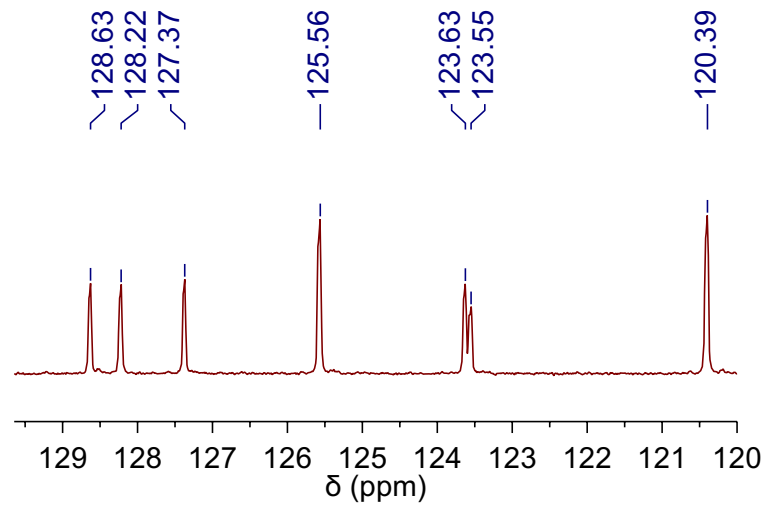


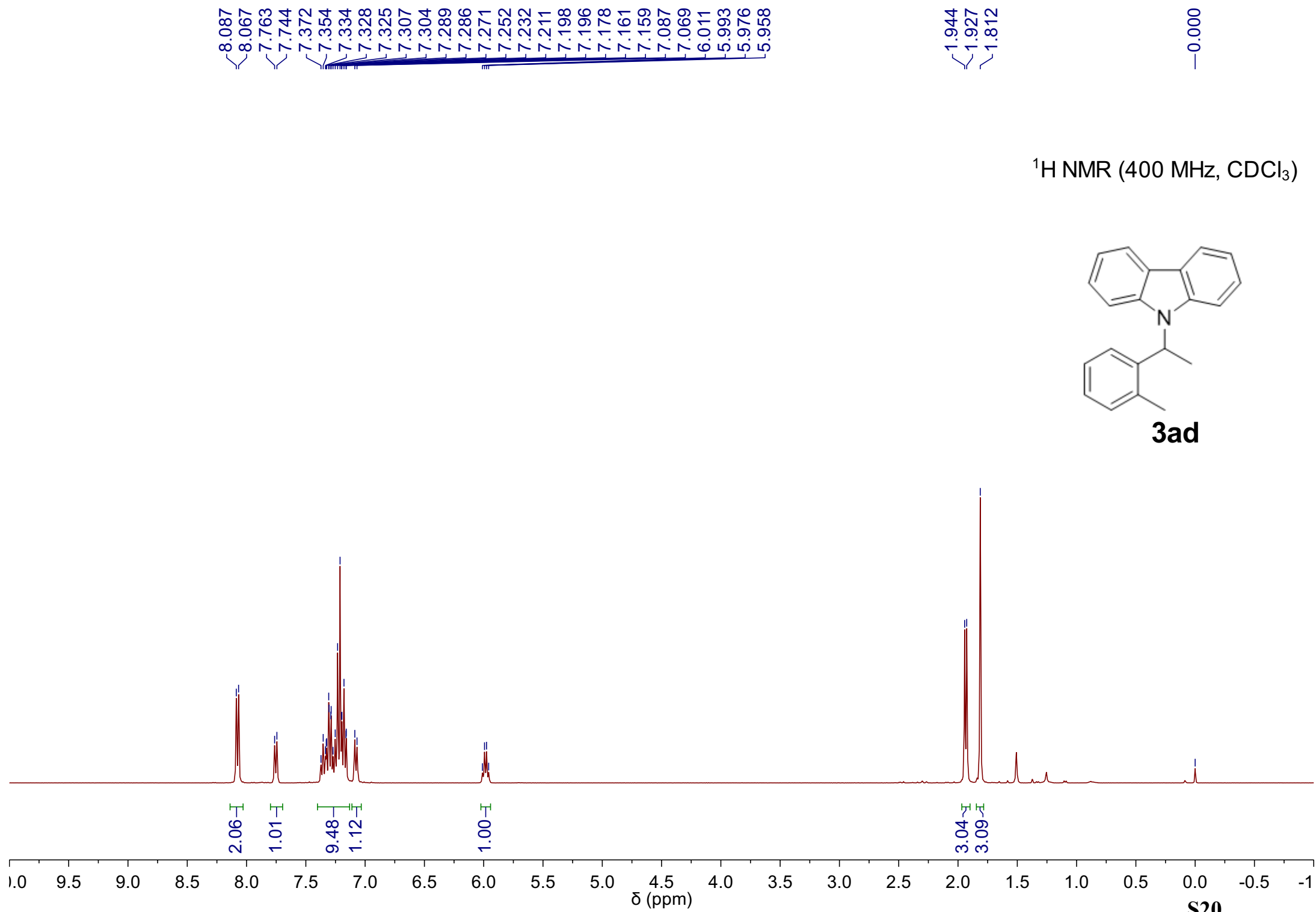
140.82  
140.00  
138.39  
128.63  
128.22  
127.37  
125.56  
123.63  
123.55  
120.39  
119.01  
110.28

77.41  
77.16  
76.91

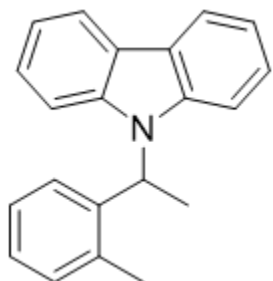
52.35

21.65  
17.47





<sup>13</sup>C NMR (126 MHz, CDCl<sub>3</sub>)



**3ad**

139.82  
138.28  
138.22  
131.29  
128.08  
126.77  
126.13  
125.59  
123.40  
120.39  
118.98  
109.84

77.41  
77.16  
76.91

51.42

19.83  
17.58

131.29

128.08

126.77

126.13

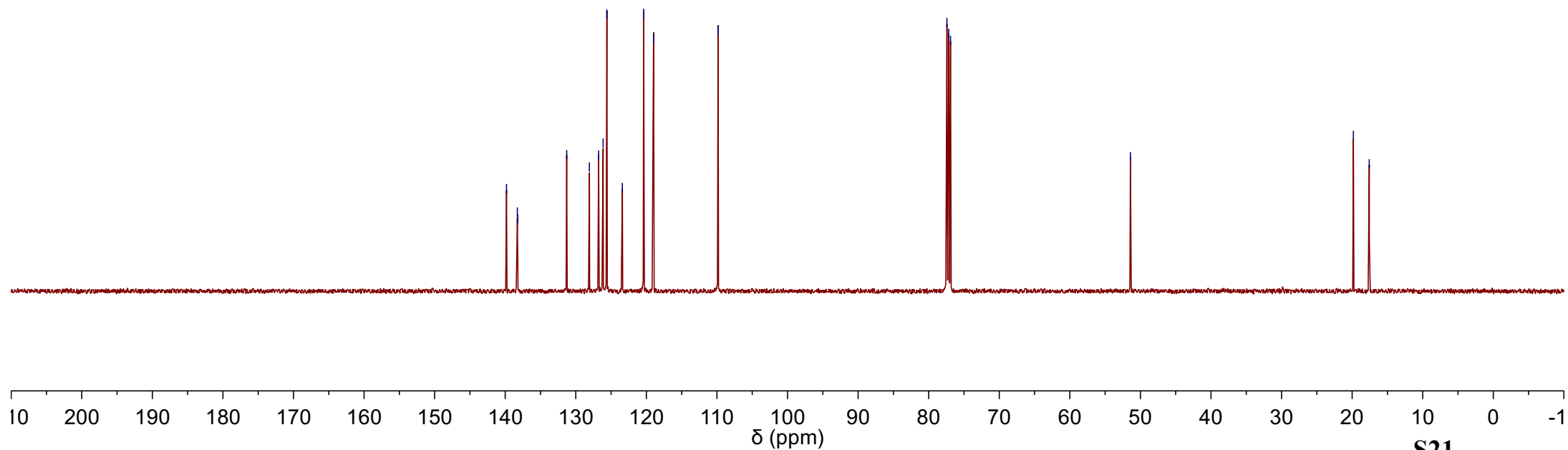
125.59

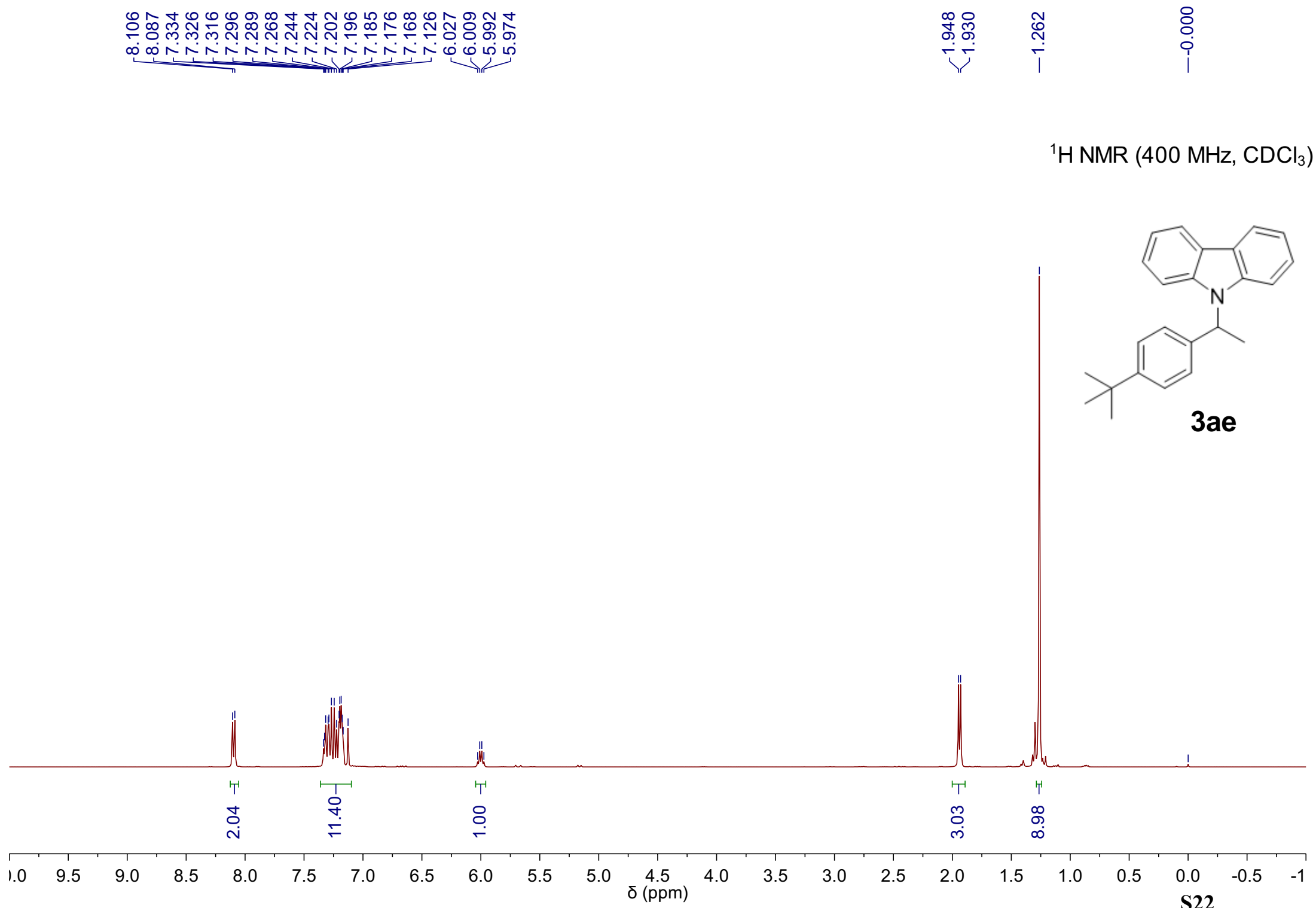
123.40

120.39

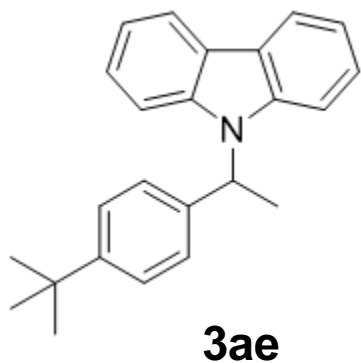
118.98

136 134 132 130 128 126 124 122 120 118 116 114  
δ (ppm)





<sup>13</sup>C NMR (126 MHz, CDCl<sub>3</sub>)



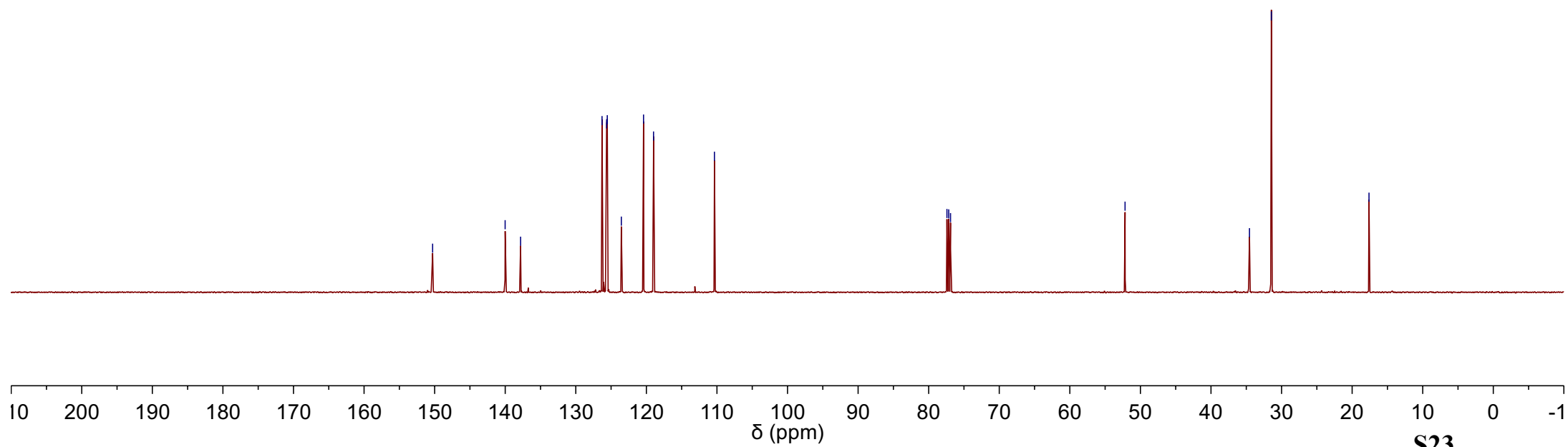
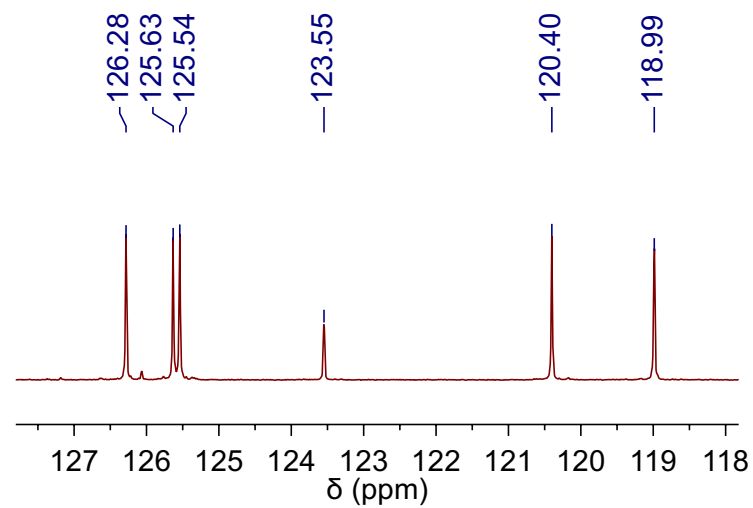
—150.29  
~140.01  
~137.82  
126.28  
125.63  
125.54  
123.55  
120.40  
118.99  
—110.36

77.41  
77.16  
76.91

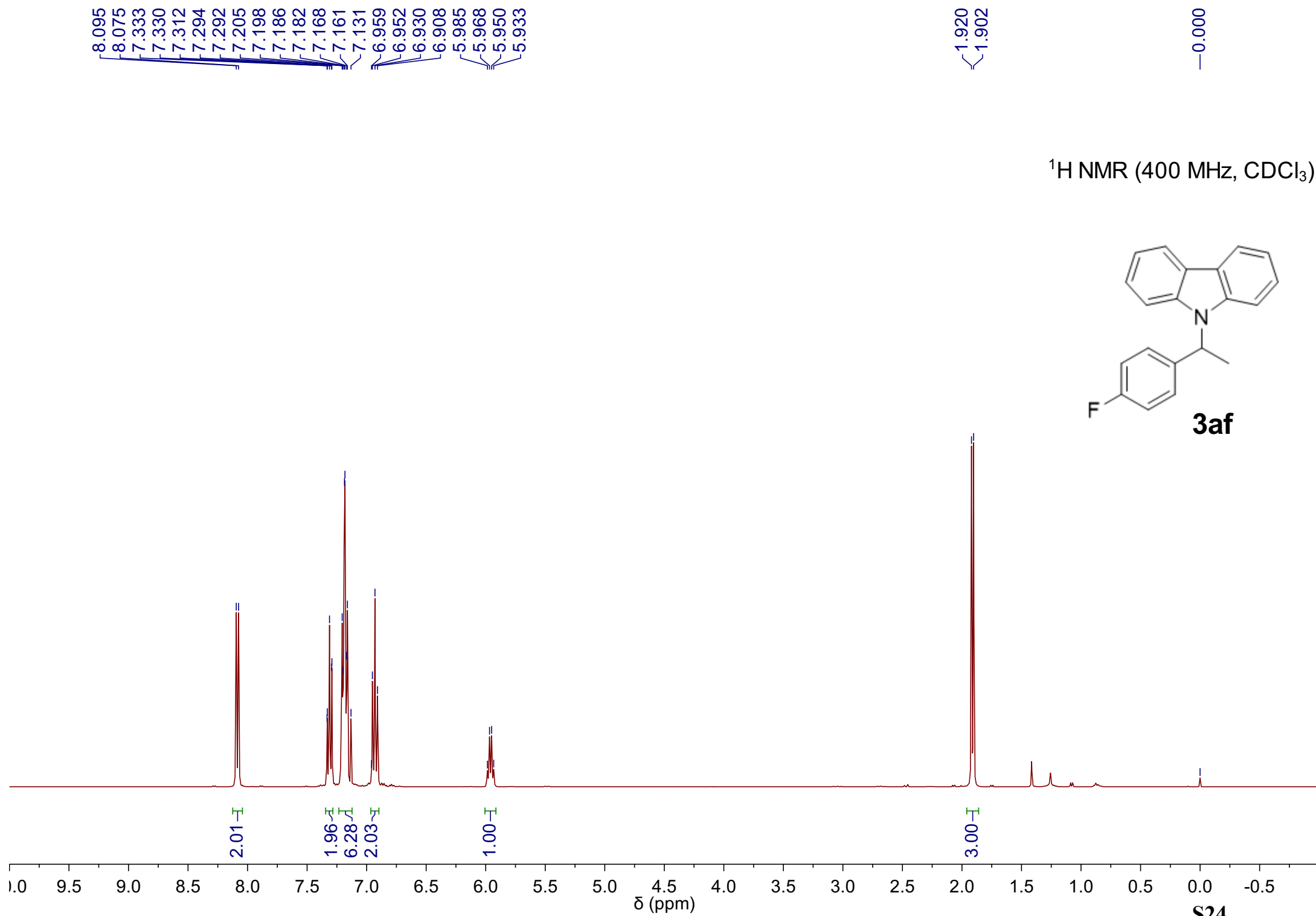
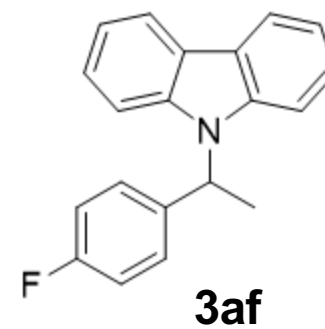
—52.18

—34.55  
—31.45

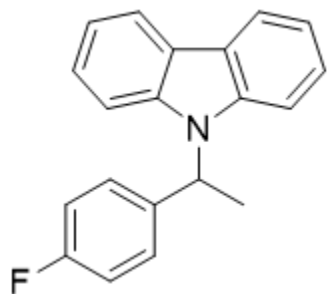
—17.61



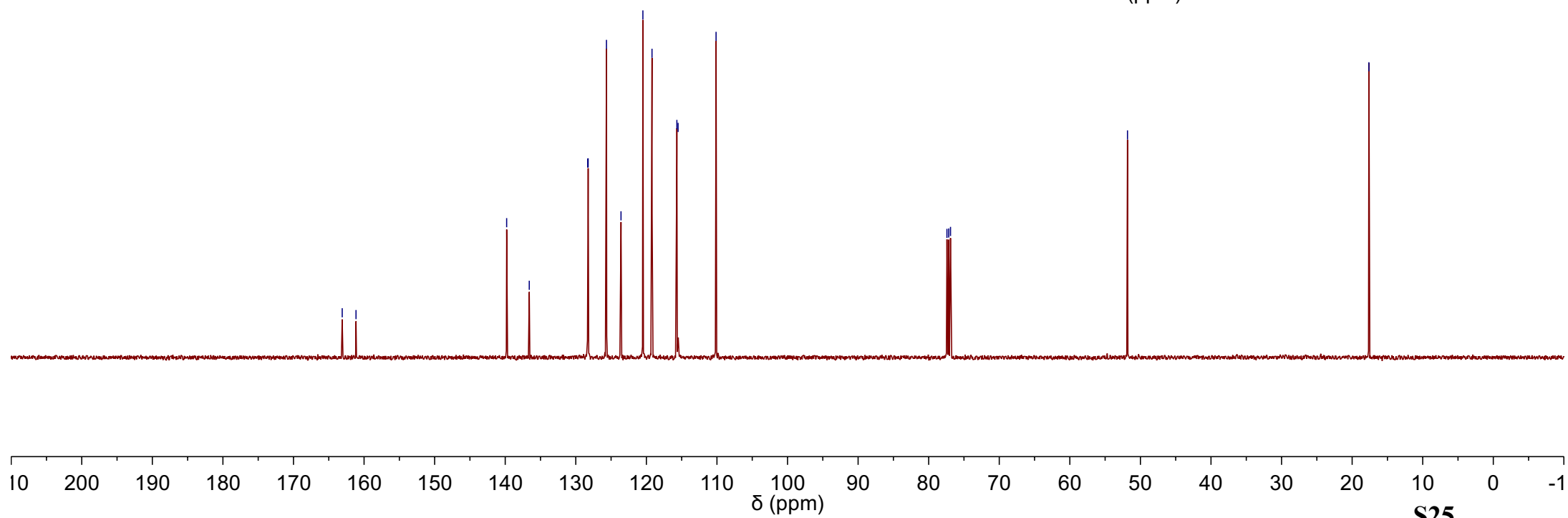
<sup>1</sup>H NMR (400 MHz, CDCl<sub>3</sub>)



$^{13}\text{C}$  NMR (126 MHz,  $\text{CDCl}_3$ )

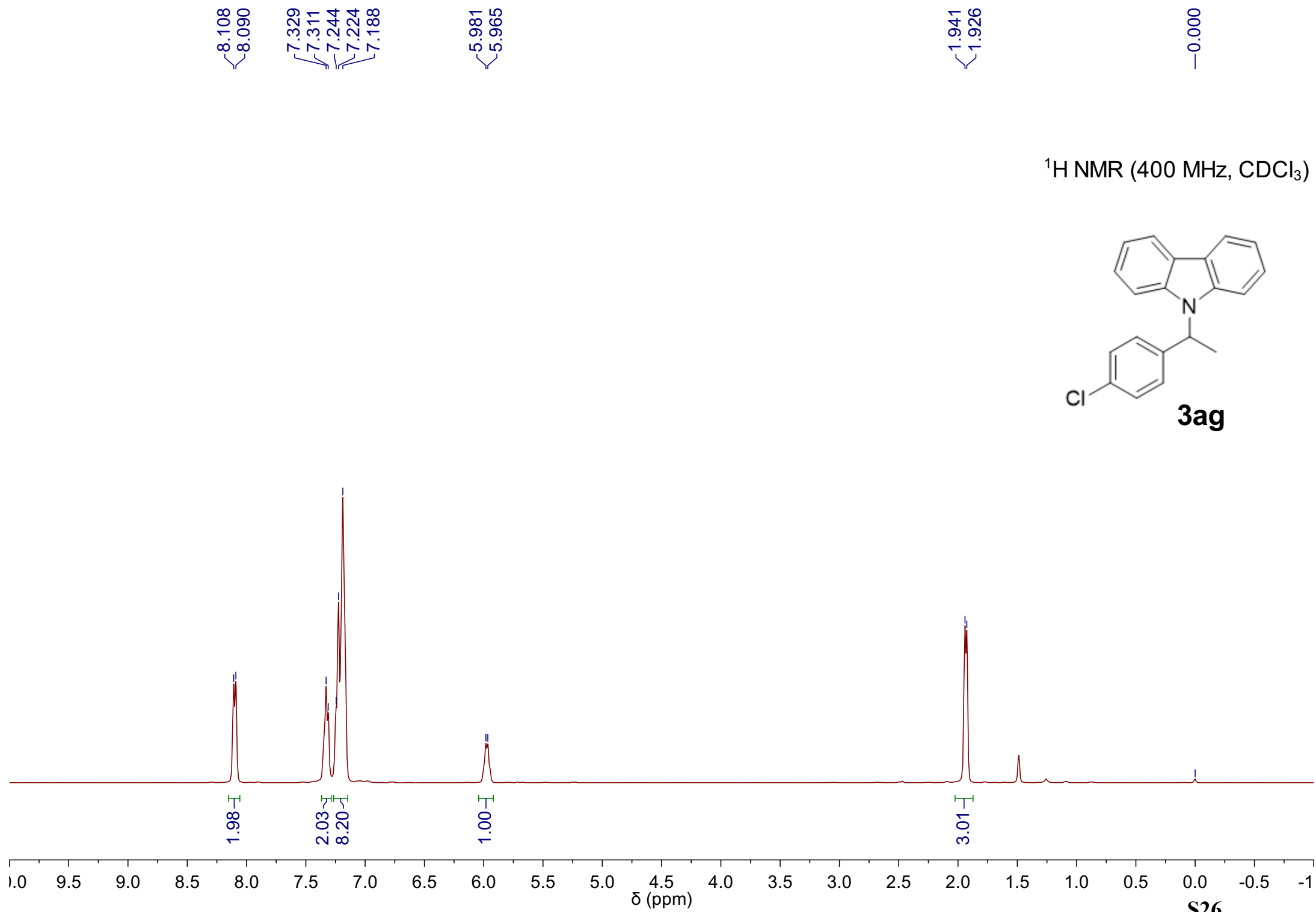
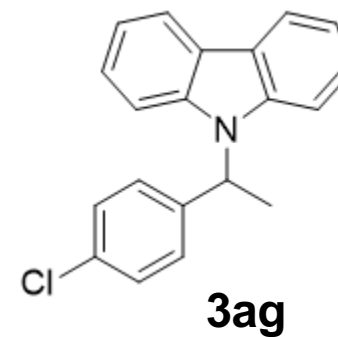


**3af**

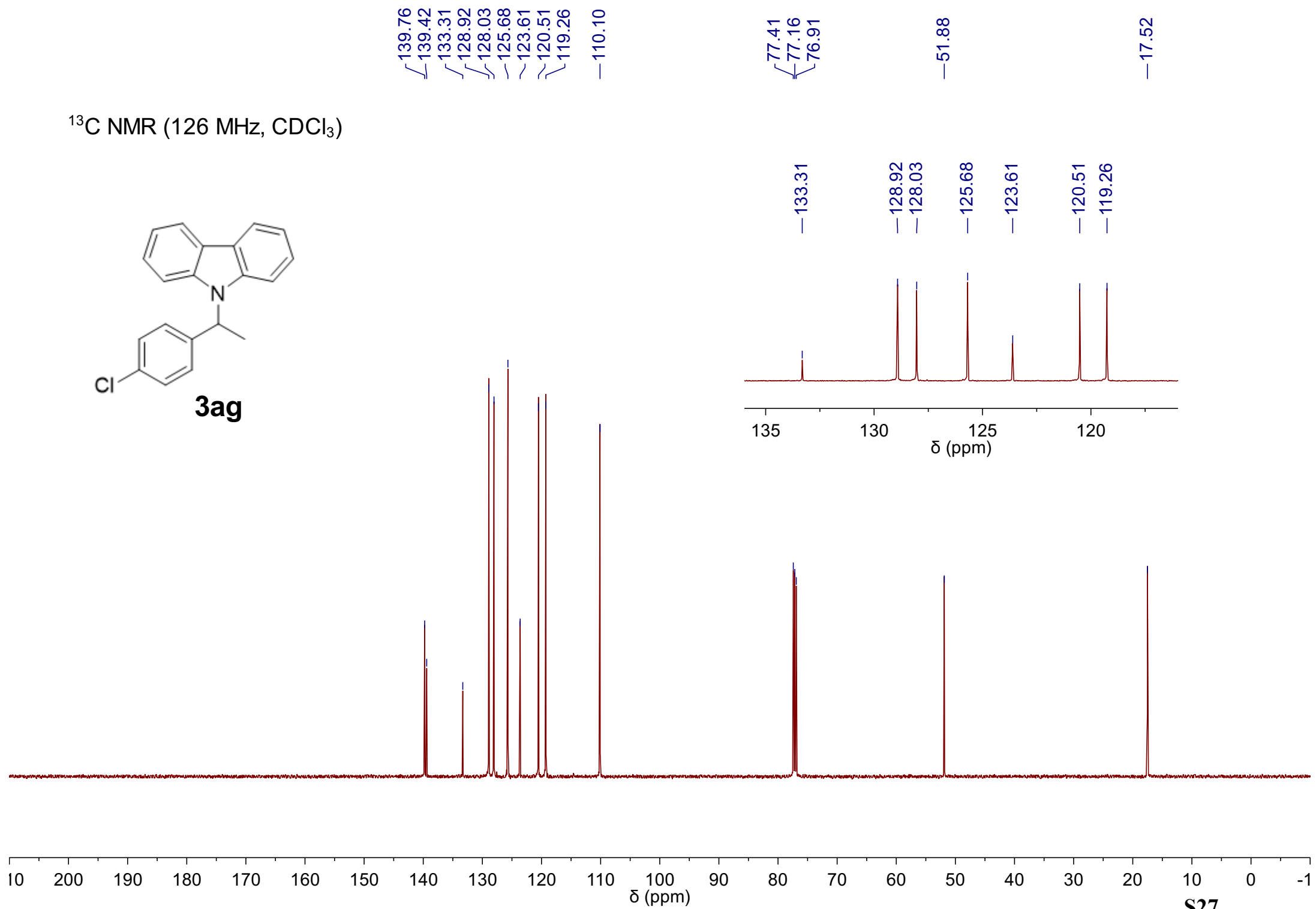
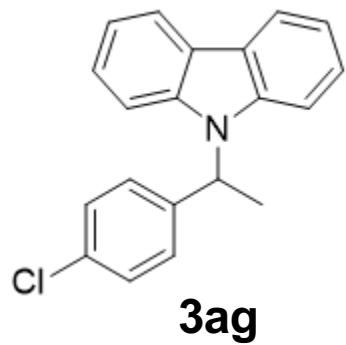


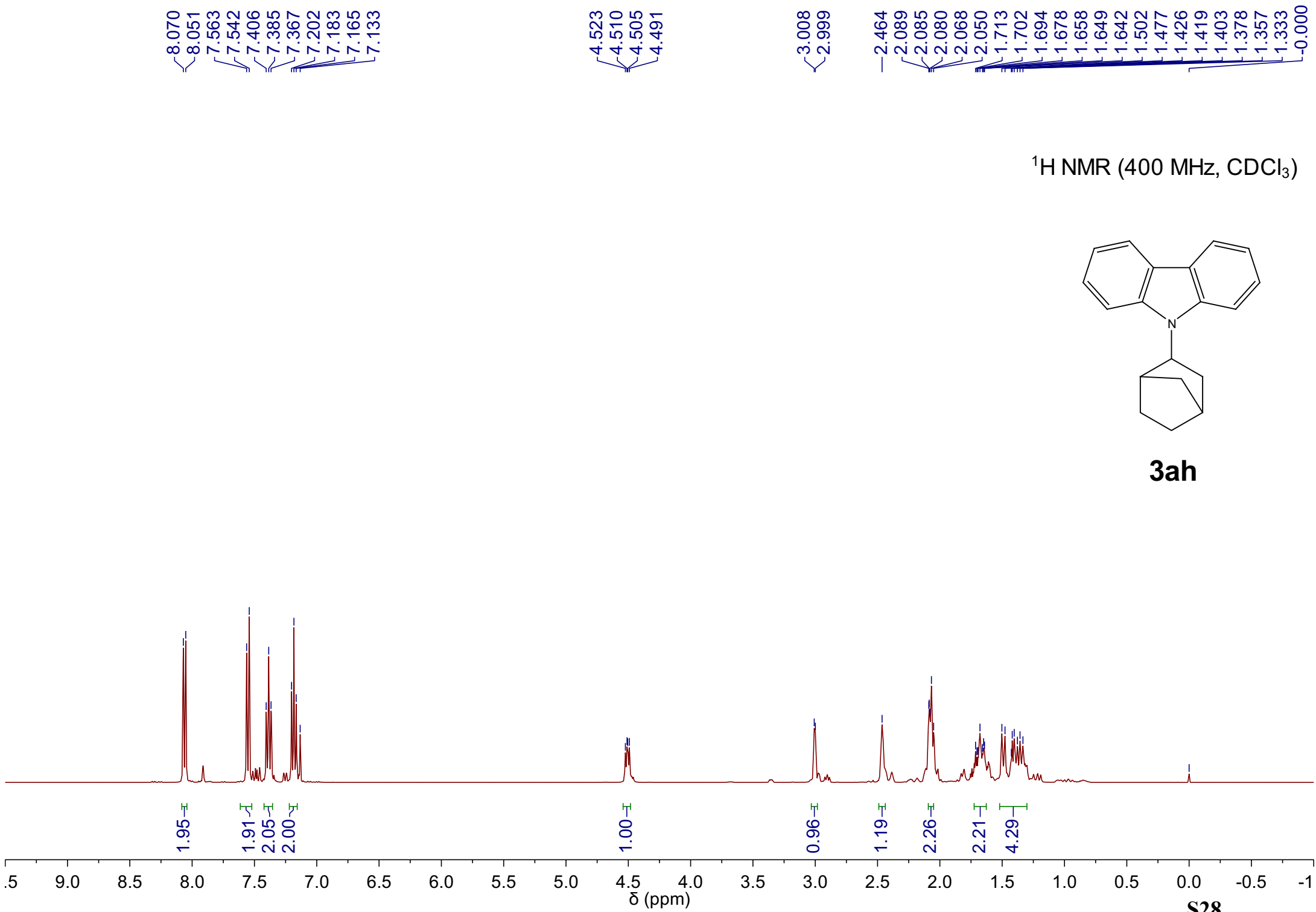


<sup>1</sup>H NMR (400 MHz, CDCl<sub>3</sub>)

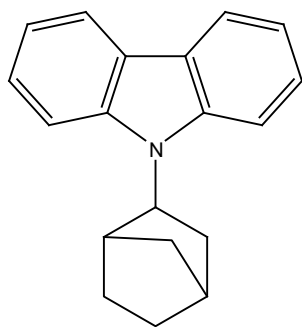


$^{13}\text{C}$  NMR (126 MHz,  $\text{CDCl}_3$ )



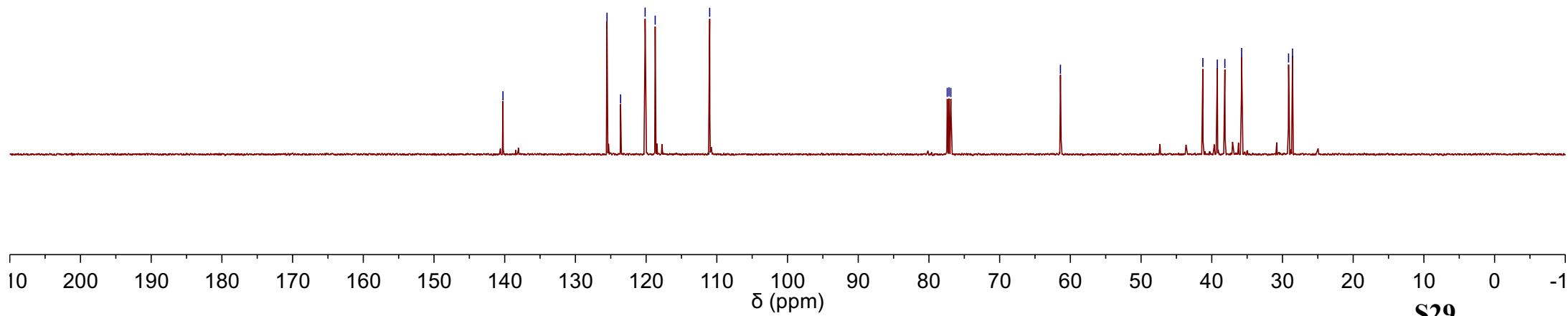


$^{13}\text{C}$  NMR (126 MHz,  $\text{CDCl}_3$ )



**3ah**

— 140.25  
/ 125.53  
— 123.61  
/ 120.14  
/ 118.72  
— 111.01  
  
/ 77.41  
/ 77.16  
/ 76.91  
— 61.40  
  
/ 41.26  
/ 39.22  
/ 38.15  
/ 35.78  
/ 29.14  
/ 28.58

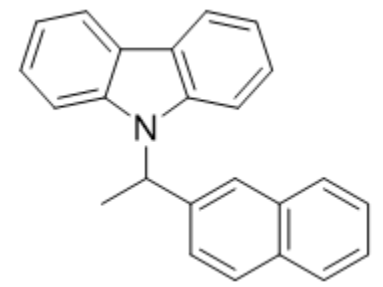


8.116  
8.097  
7.862  
7.785  
7.768  
7.752  
7.736  
7.731  
7.654  
7.632  
7.450  
7.443  
7.435  
7.427  
7.420  
7.305  
7.287  
7.284  
7.267  
7.239  
7.227  
7.220  
7.204  
7.186  
7.169  
7.167  
7.152  
6.165  
6.148  
6.130  
6.113

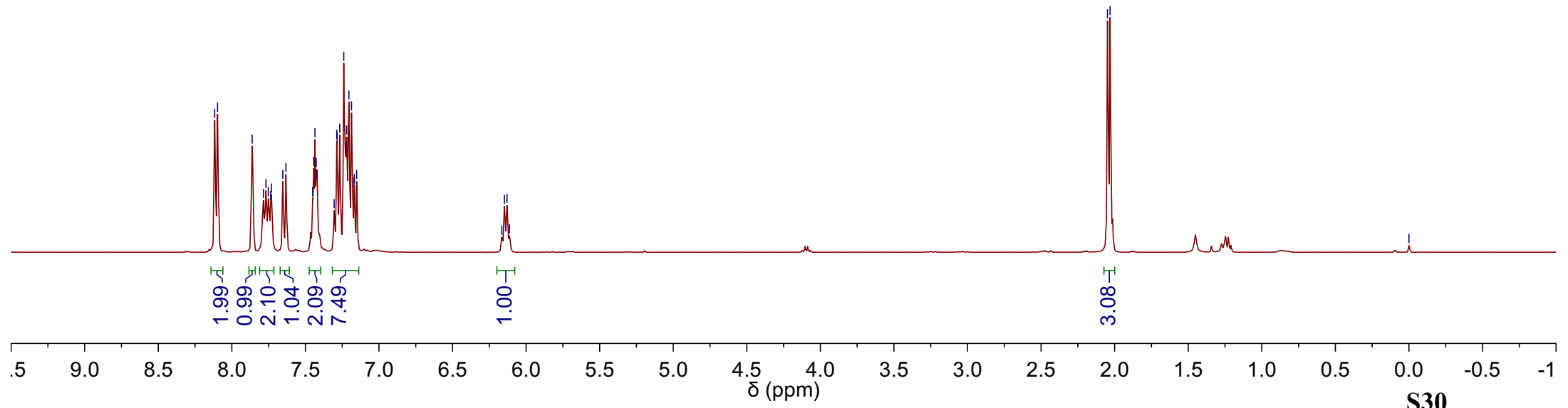
2.049  
2.031

0.000

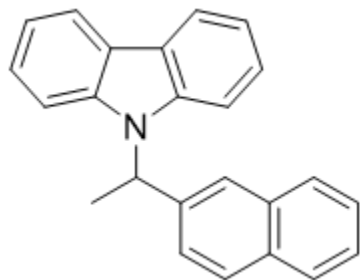
<sup>1</sup>H NMR (400 MHz, CDCl<sub>3</sub>)



**3aj**



<sup>13</sup>C NMR (126 MHz, CDCl<sub>3</sub>)



**3aj**

140.04  
138.51  
133.41  
132.76  
128.64  
128.21  
127.76  
126.38  
126.18  
125.65  
125.29  
124.85  
123.62  
120.46  
119.14  
110.23

77.41  
77.16  
76.91

52.54

17.38

133.41  
132.76

128.64  
128.21  
127.76

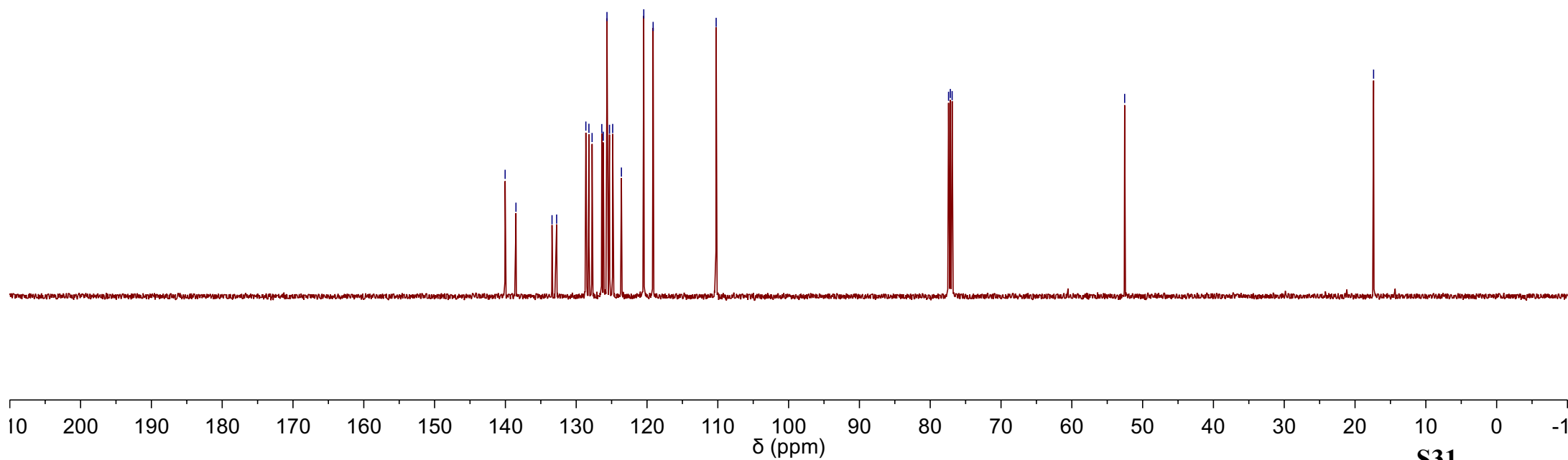
126.38  
126.18  
125.65  
125.29  
124.85

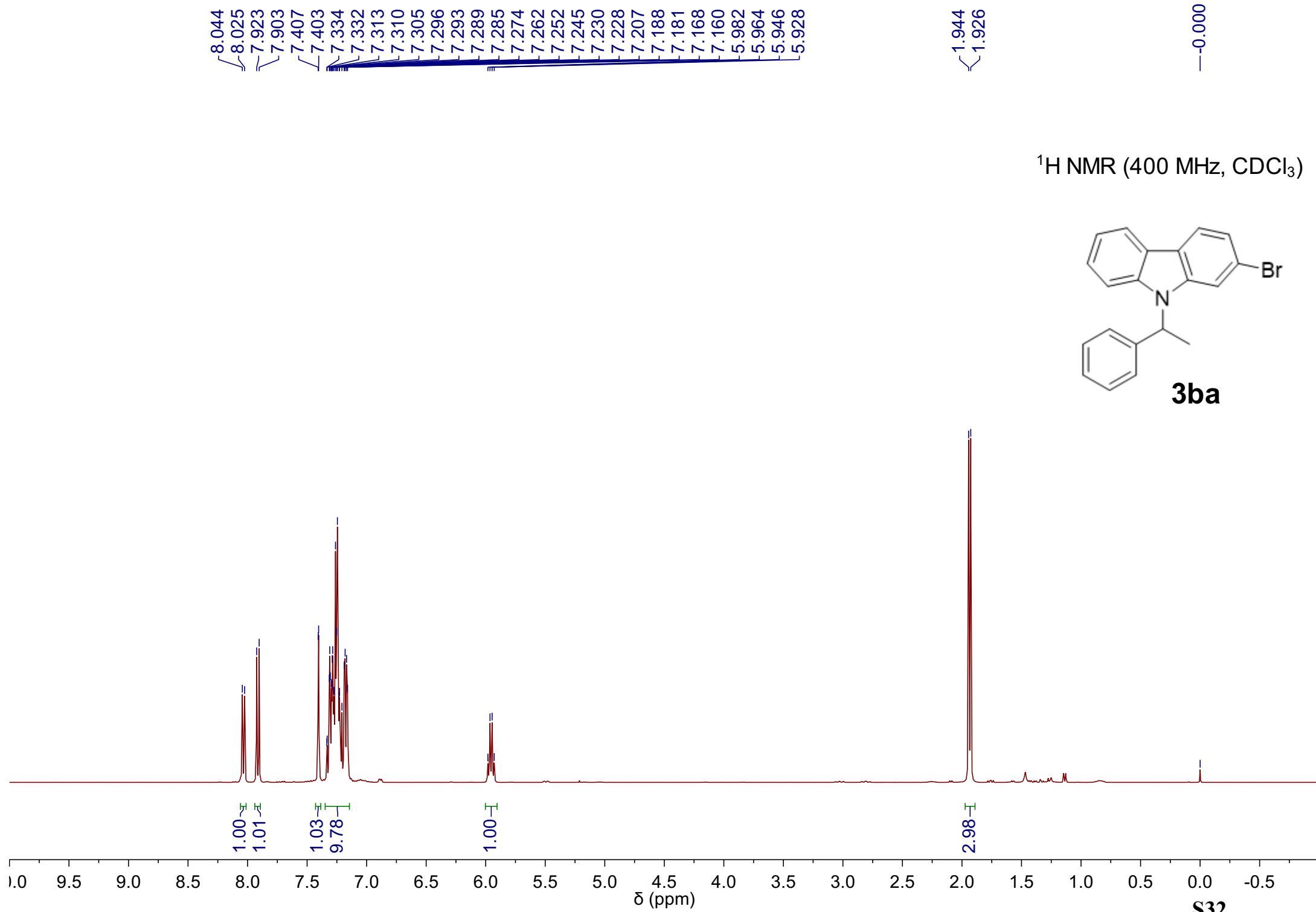
123.62

120.46

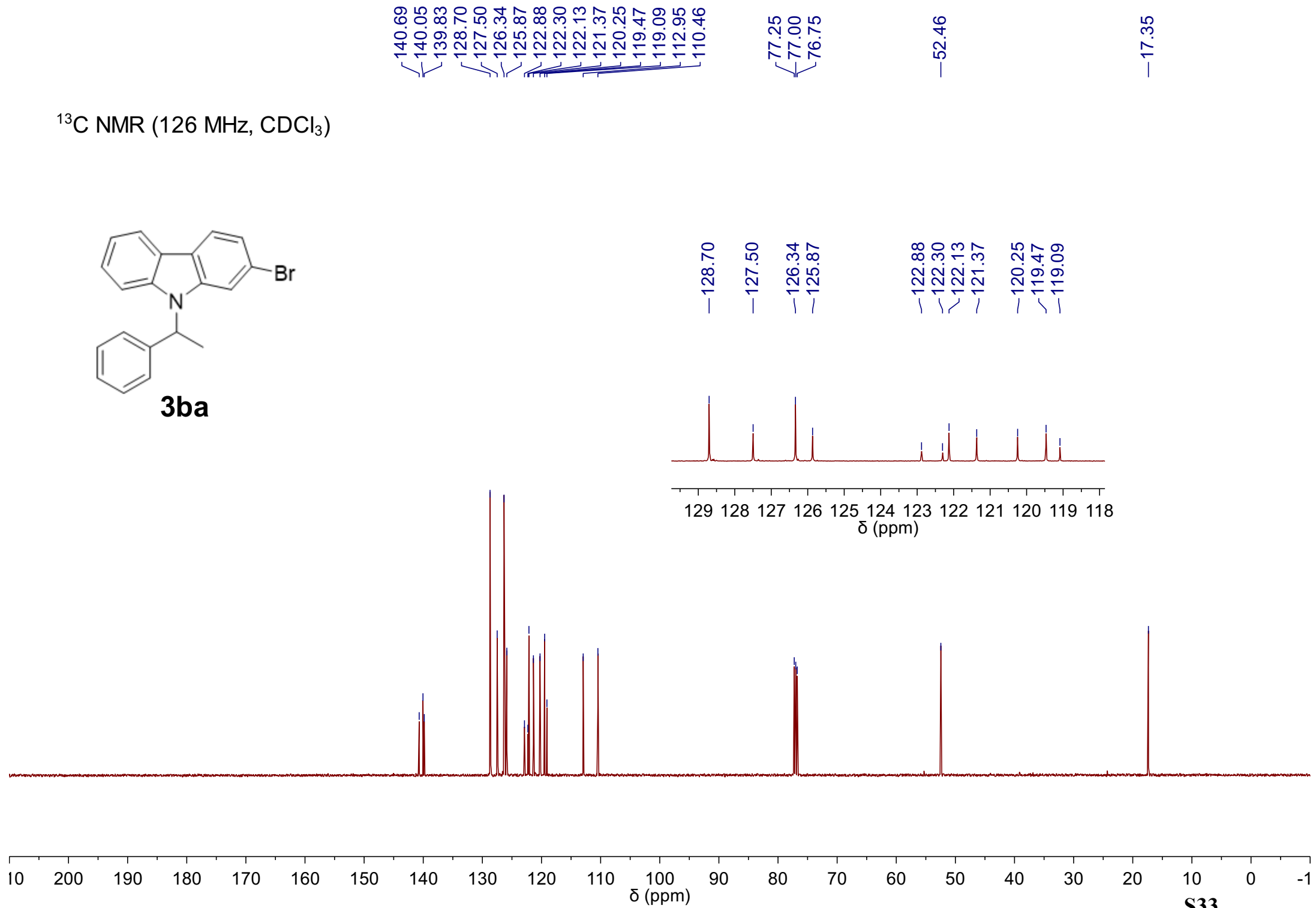
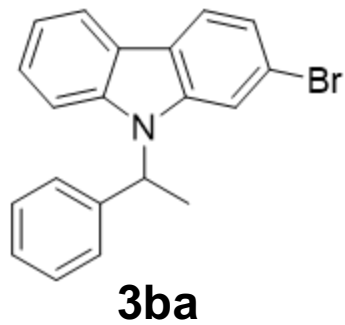
119.14

134 133 132 131 130 129 128 127 126 125 124 123 122 121 120 119 118  
δ (ppm)

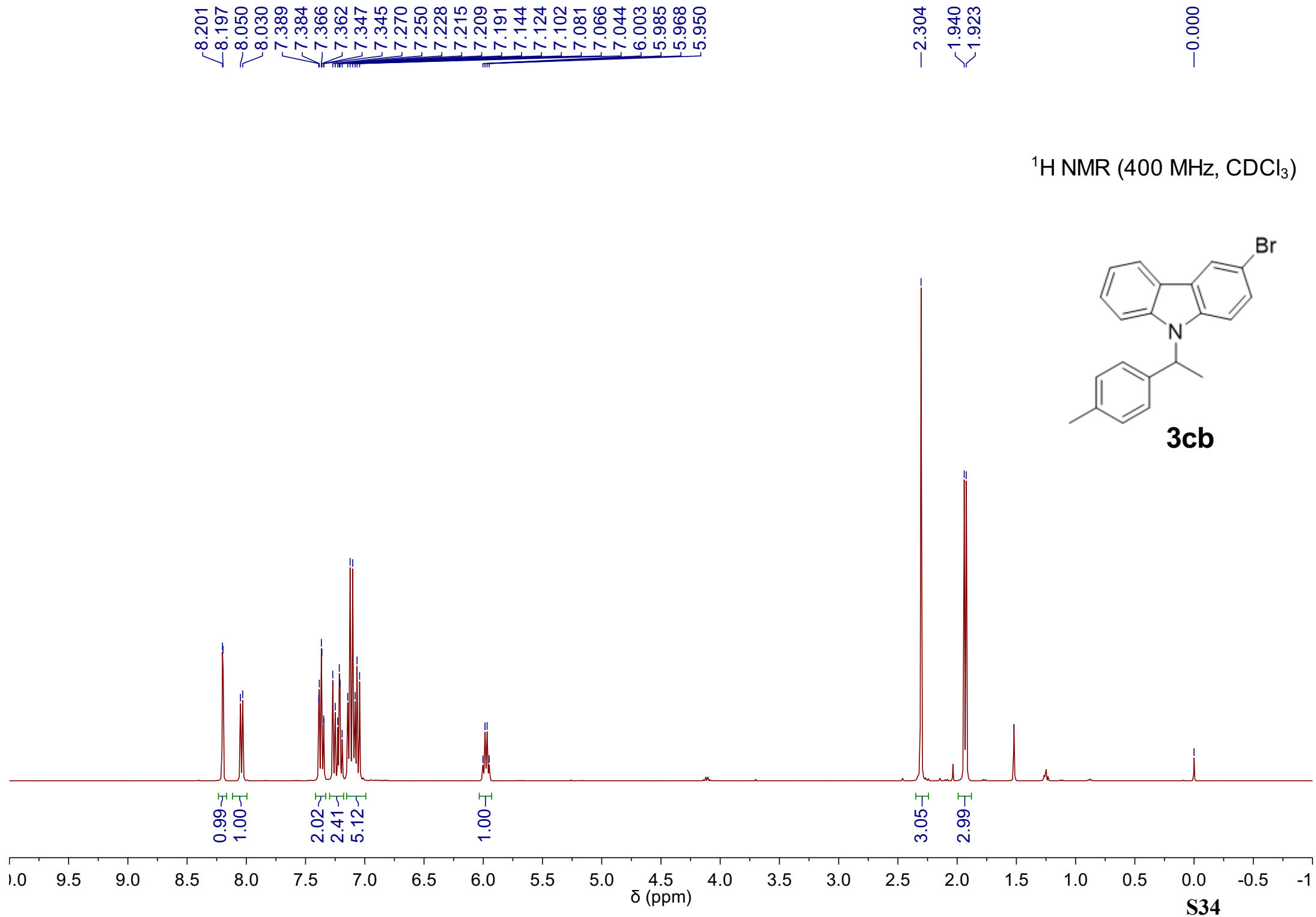




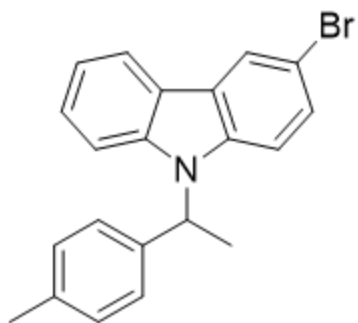
$^{13}\text{C}$  NMR (126 MHz,  $\text{CDCl}_3$ )







$^{13}\text{C}$  NMR (126 MHz,  $\text{CDCl}_3$ )



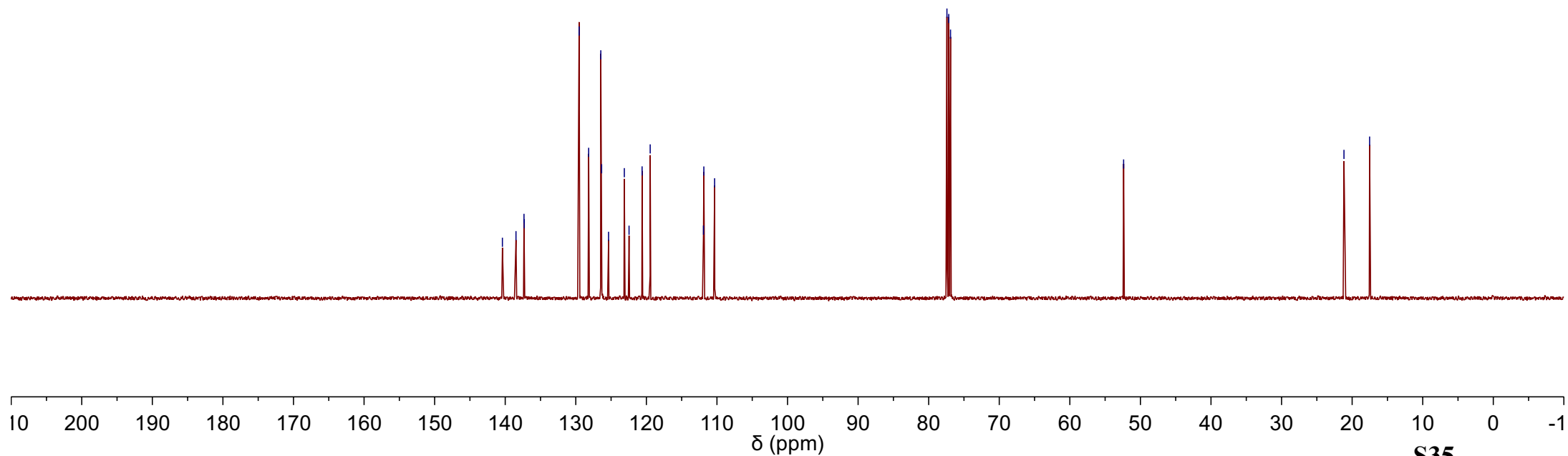
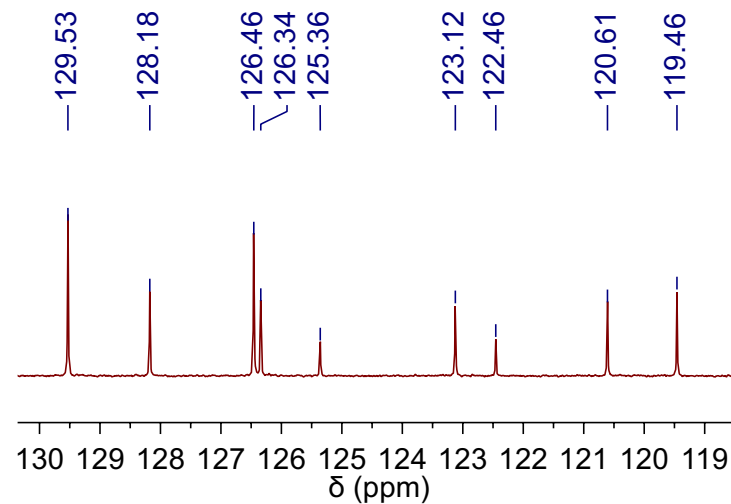
**3cb**

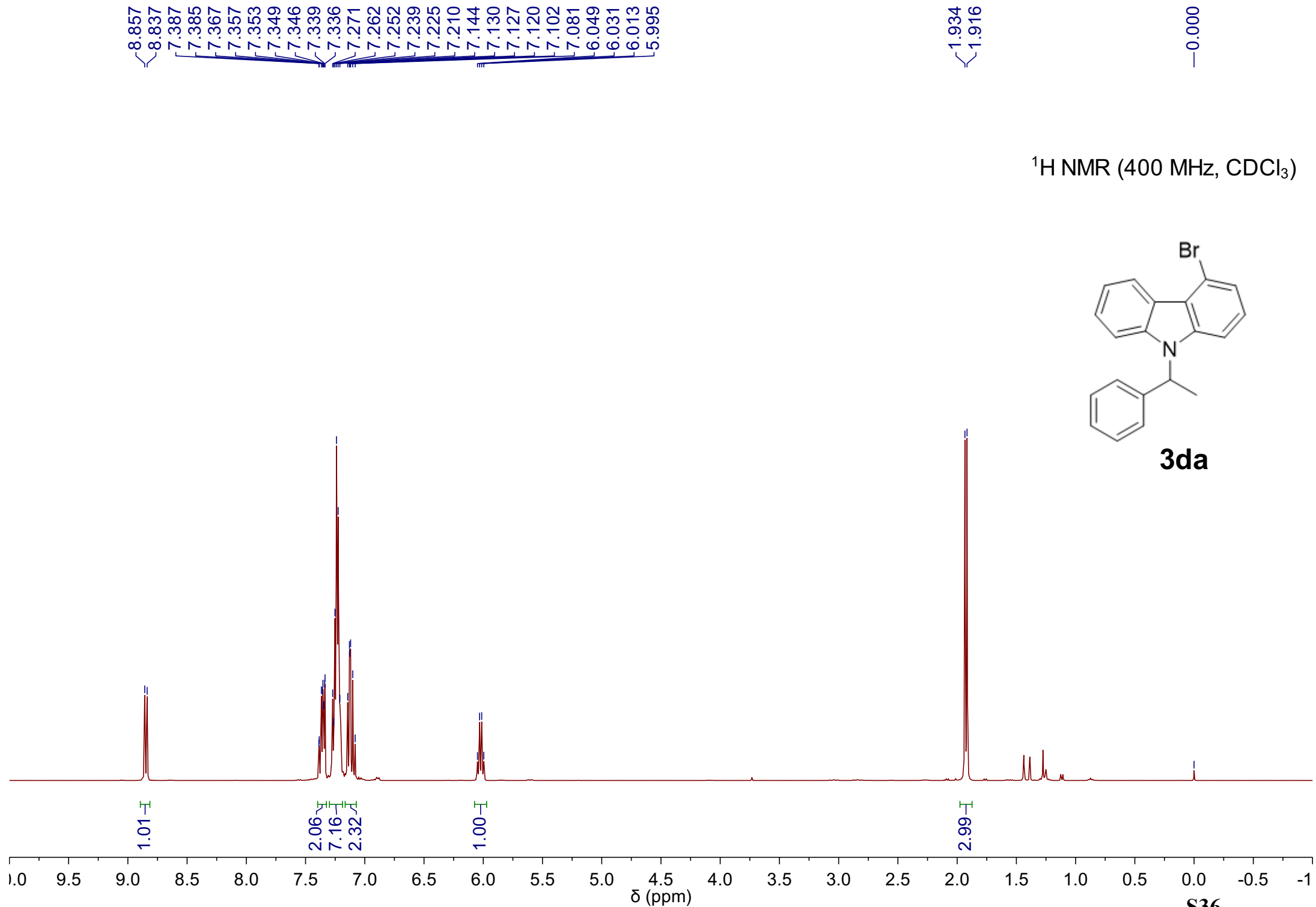
140.40  
138.47  
137.34  
137.31  
129.53  
128.18  
126.46  
126.34  
125.36  
123.12  
122.46  
120.61  
119.46  
111.91  
111.86  
110.33

77.41  
77.16  
76.91

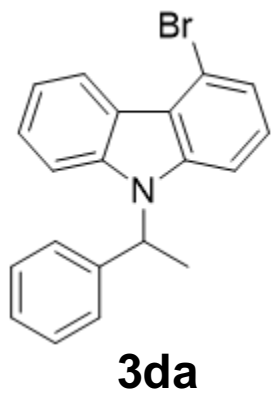
52.38

21.16  
17.52





$^{13}\text{C}$  NMR (126 MHz,  $\text{CDCl}_3$ )

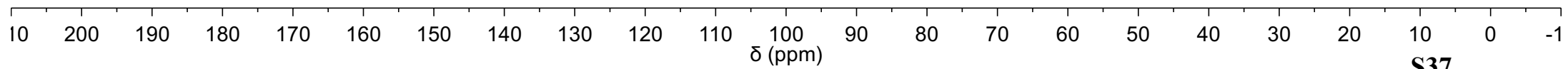
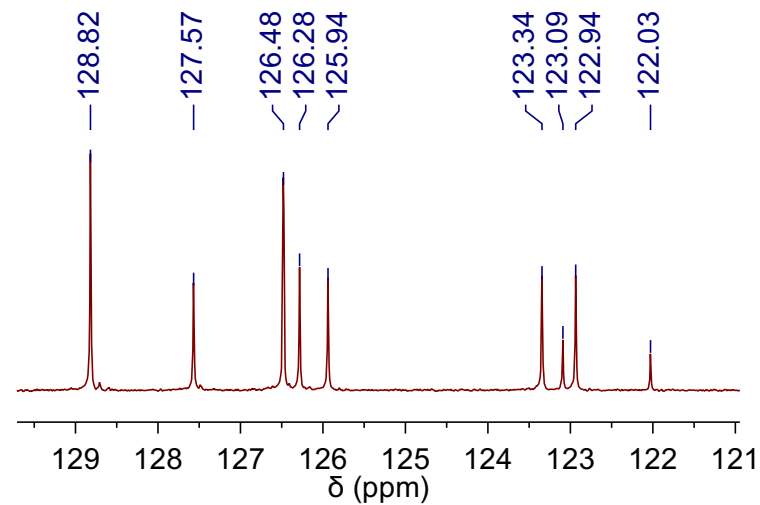


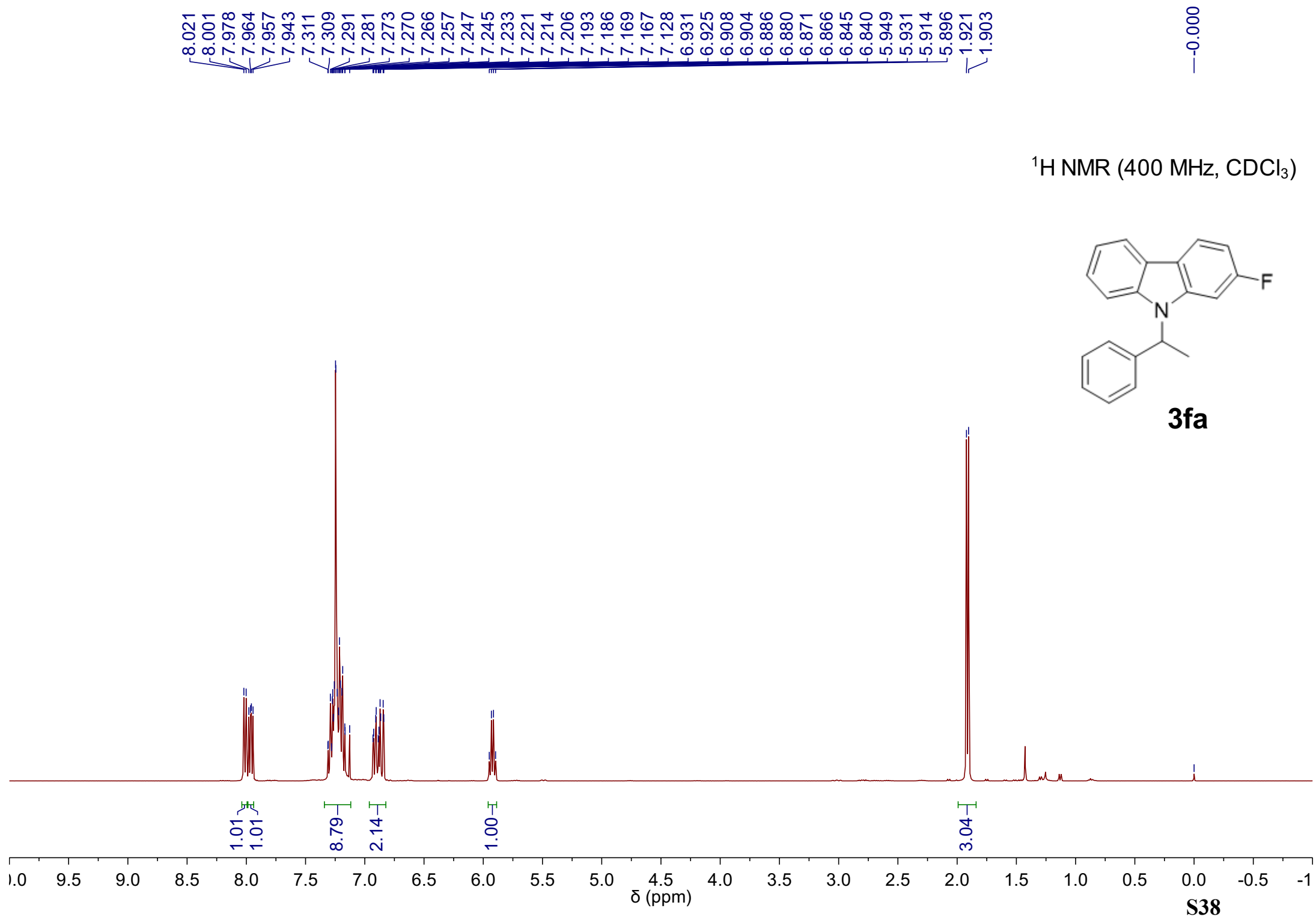
141.02  
140.28  
140.12  
128.82  
127.57  
126.48  
126.28  
125.94  
123.34  
123.09  
122.94  
122.03  
119.25  
116.95  
110.01  
109.14

77.41  
77.16  
76.91

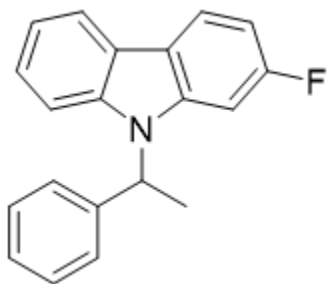
52.44

17.29

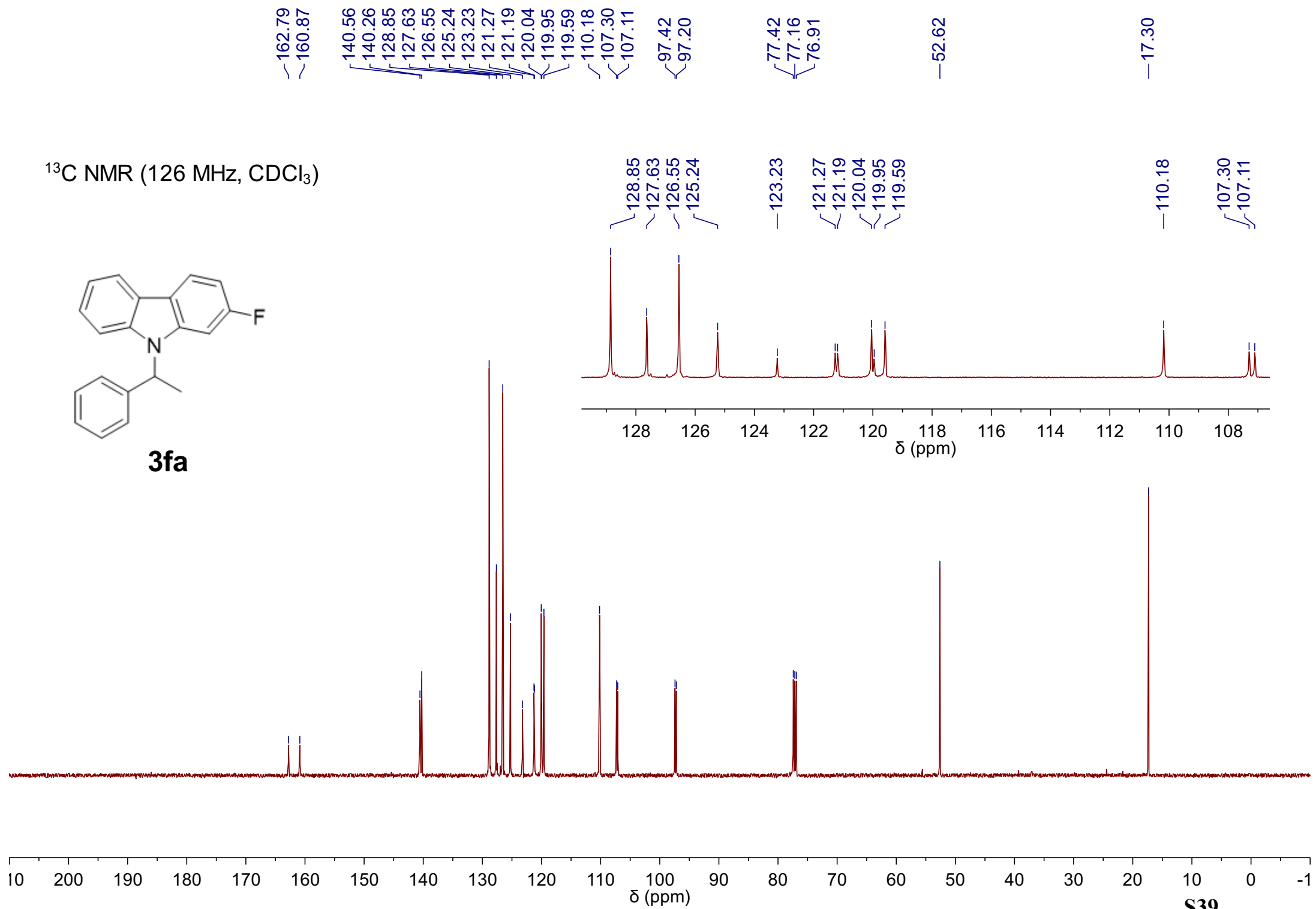


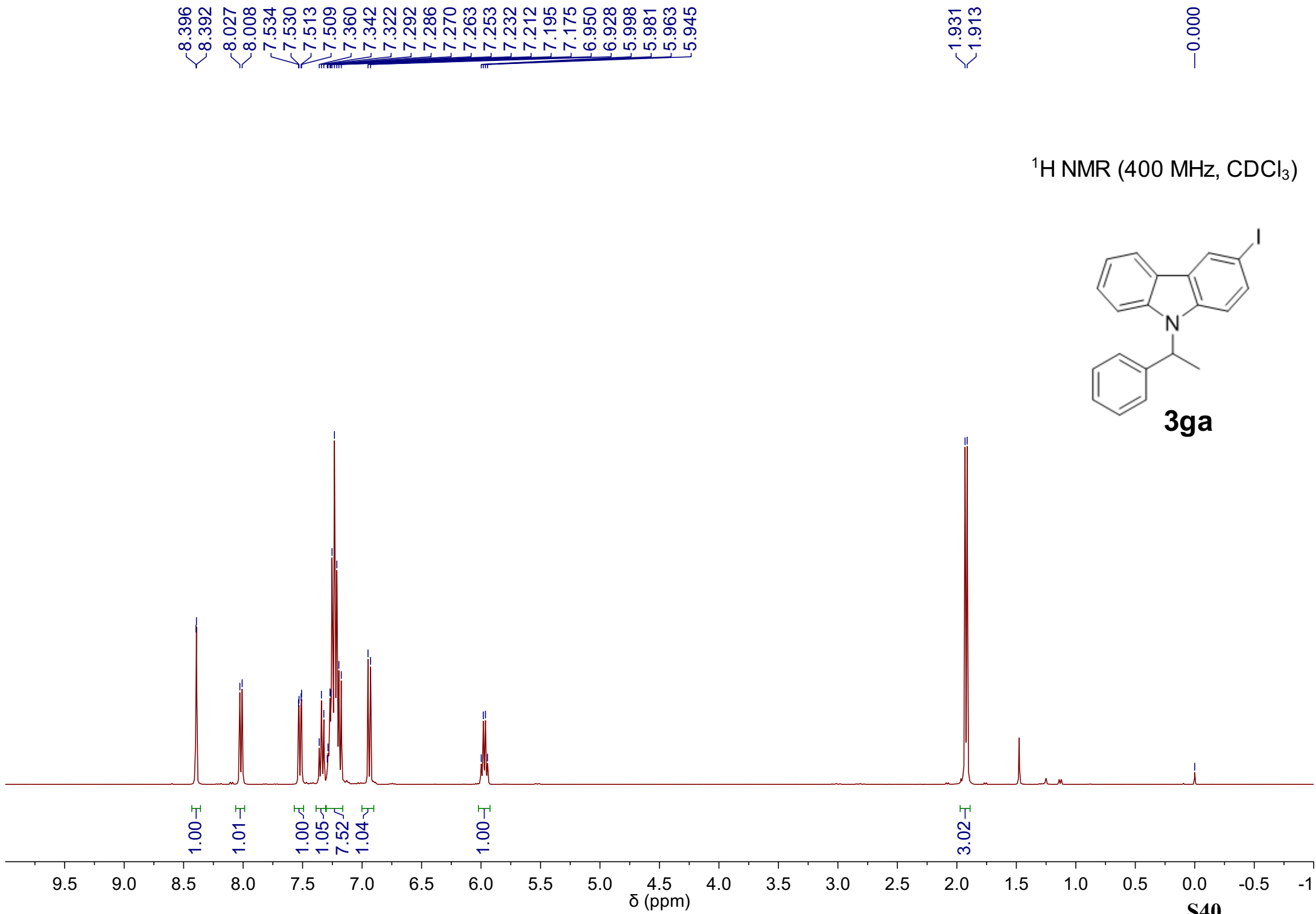


$^{13}\text{C}$  NMR (126 MHz,  $\text{CDCl}_3$ )

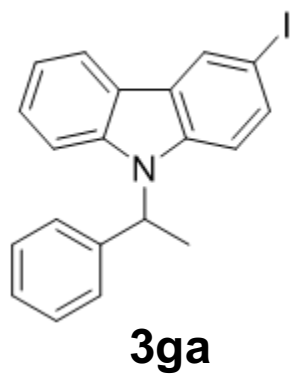


**3fa**





$^{13}\text{C}$  NMR (126 MHz,  $\text{CDCl}_3$ )

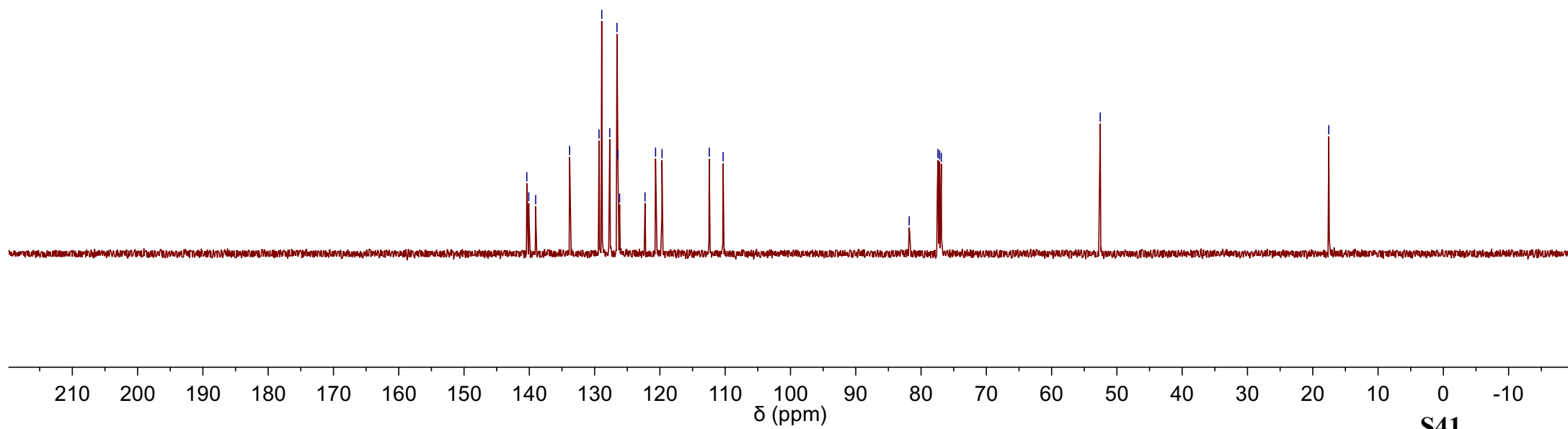
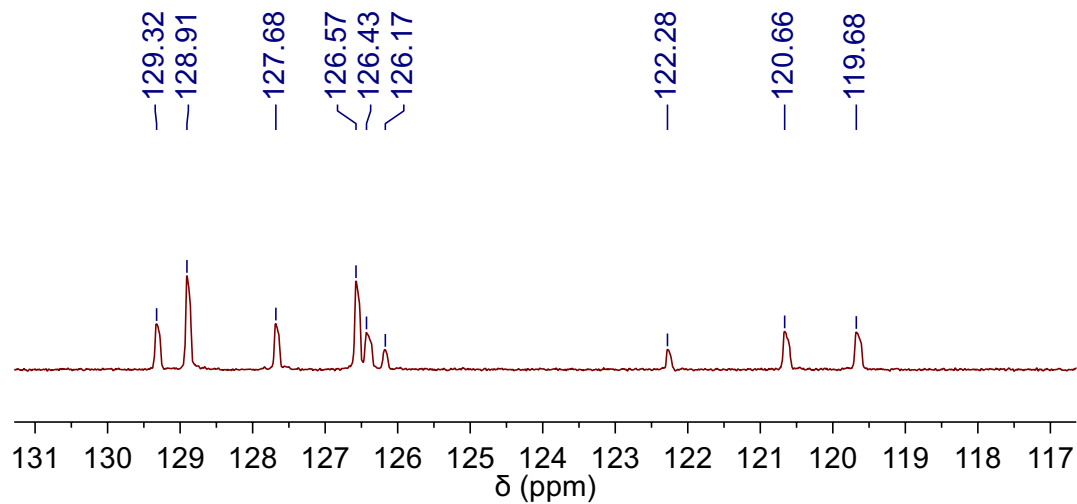


140.39  
140.09  
139.02  
133.83  
129.32  
128.91  
127.68  
126.57  
126.43  
126.17  
122.28  
120.66  
119.68  
112.44  
110.32

81.82  
77.41  
77.16  
76.90

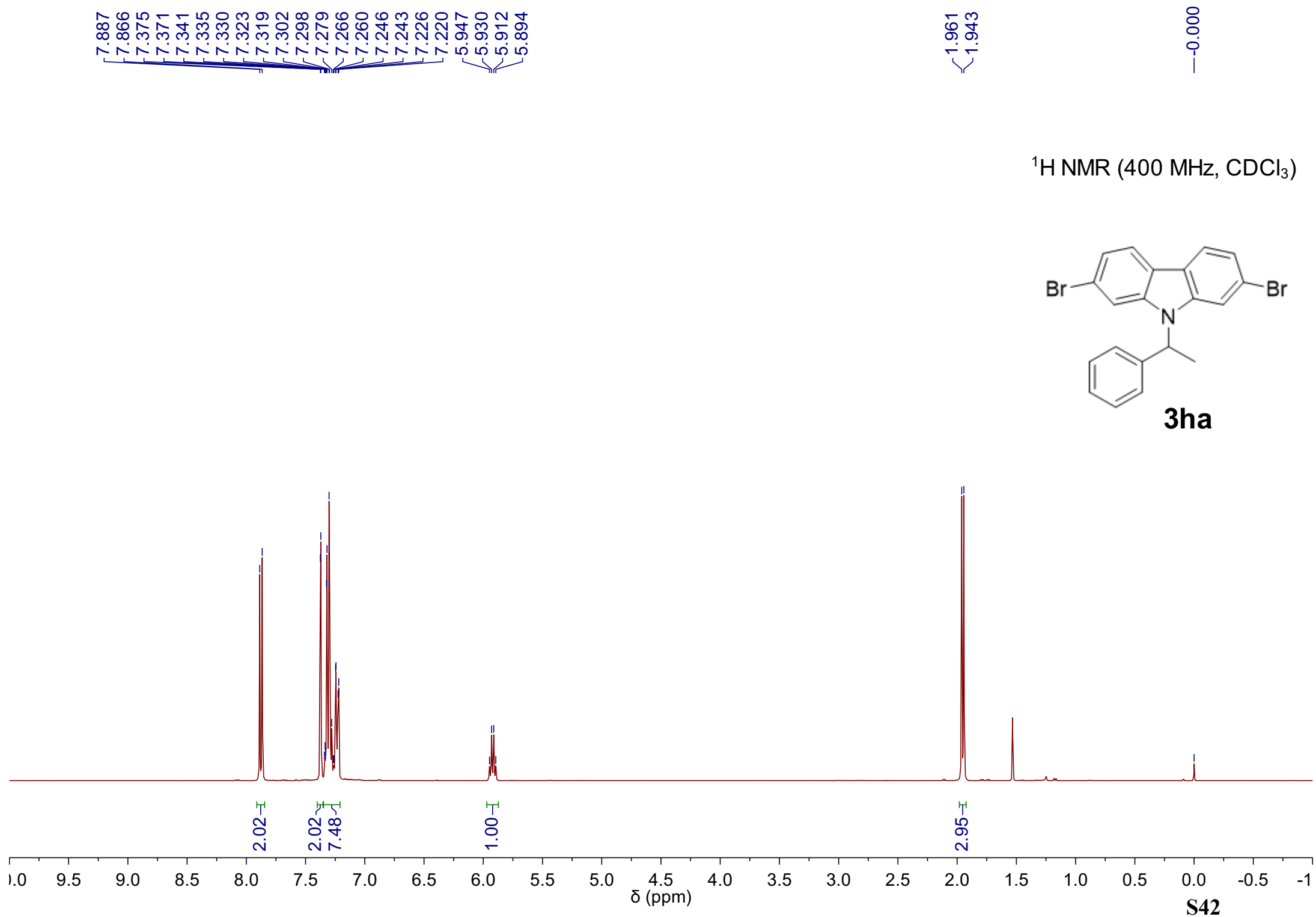
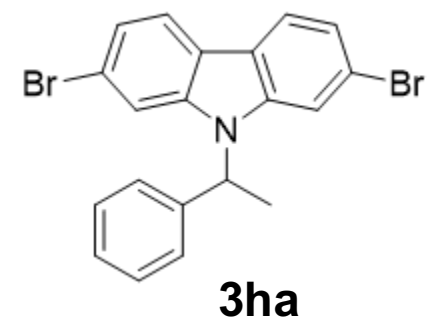
—52.56

—17.55

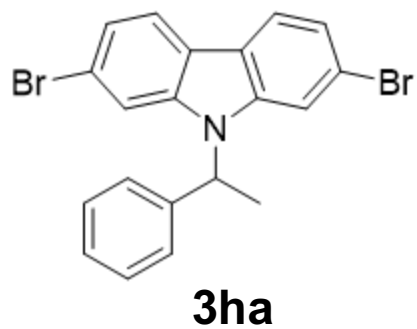




<sup>1</sup>H NMR (400 MHz, CDCl<sub>3</sub>)



$^{13}\text{C}$  NMR (126 MHz,  $\text{CDCl}_3$ )



140.87  
139.59  
129.00  
127.92  
126.42  
122.89  
121.96  
121.52  
119.70  
113.50

77.35  
77.16  
76.91

52.88

17.54

129.00

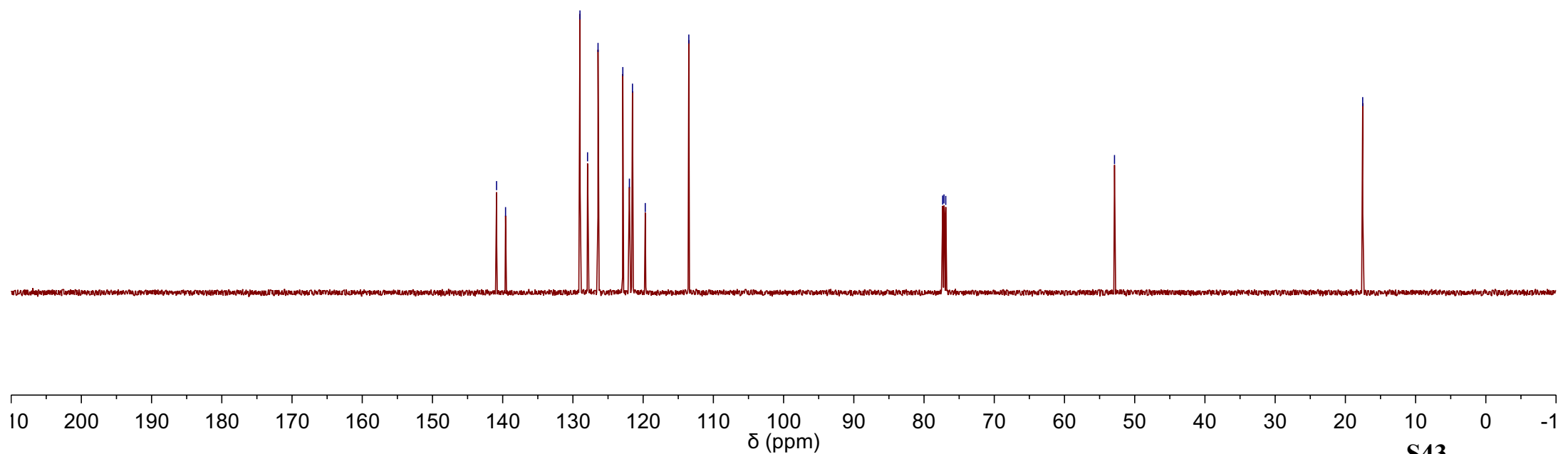
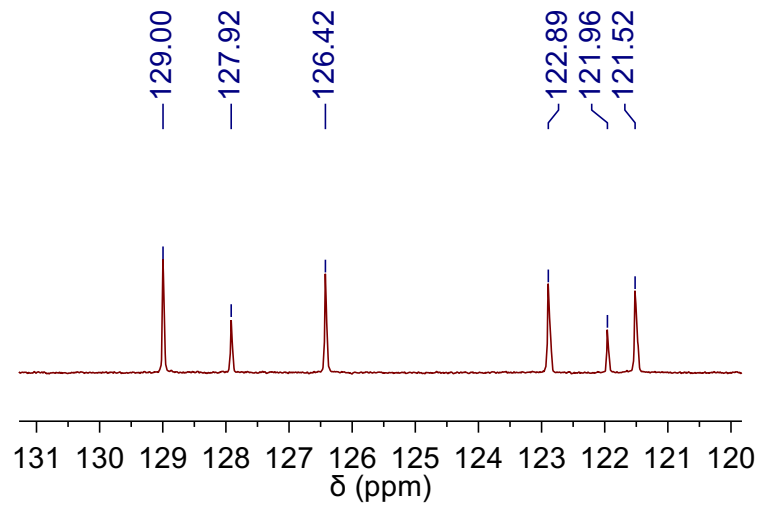
127.92

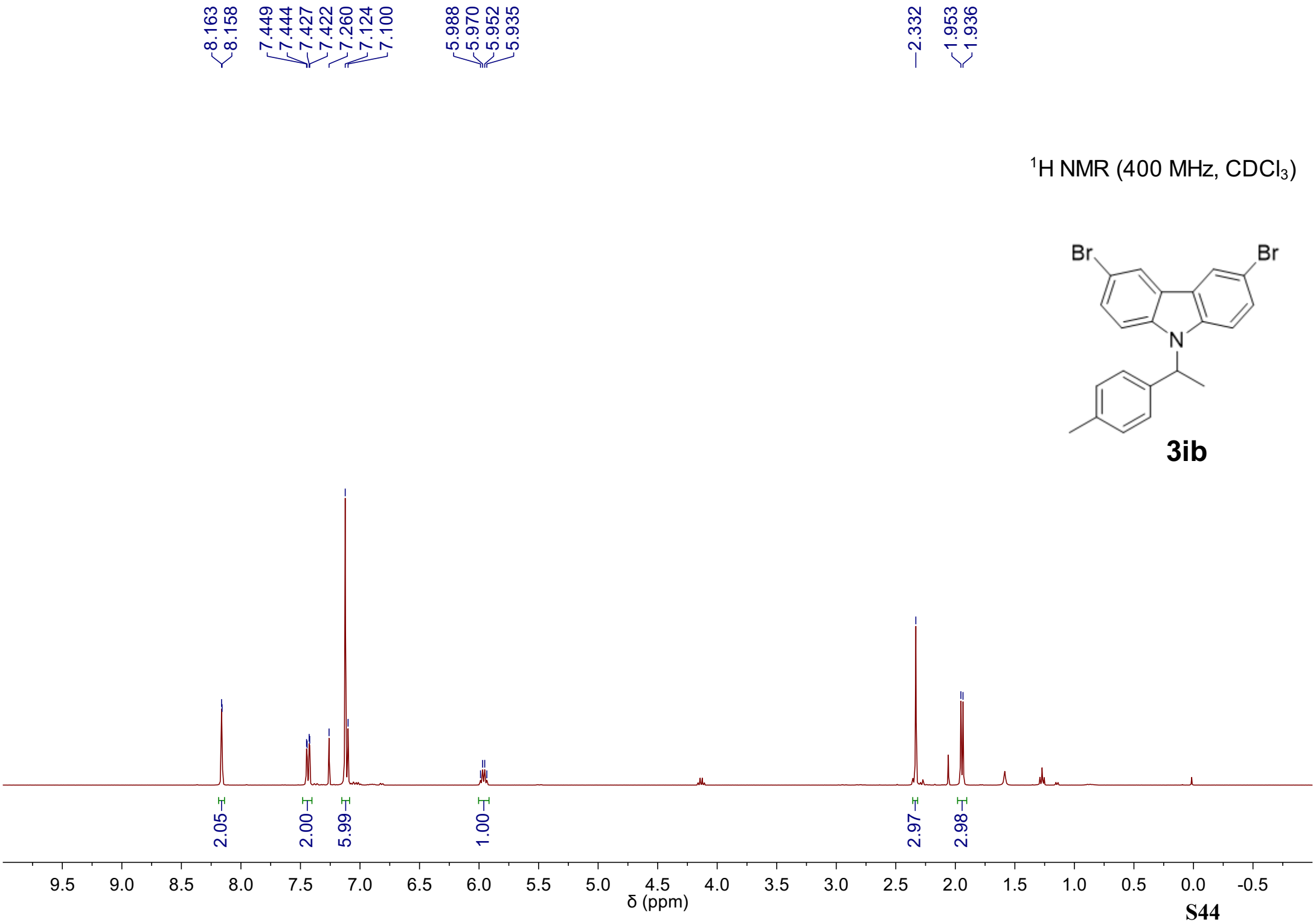
126.42

122.89

121.96

121.52





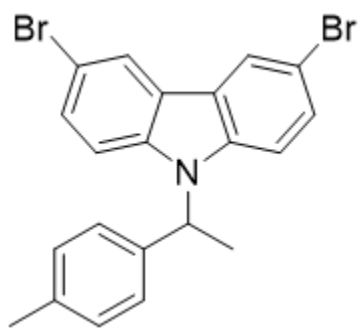
138.89  
137.56  
136.88  
129.62  
129.01  
126.39  
124.19  
123.33  
112.33  
111.93

77.41  
77.16  
76.91

52.61

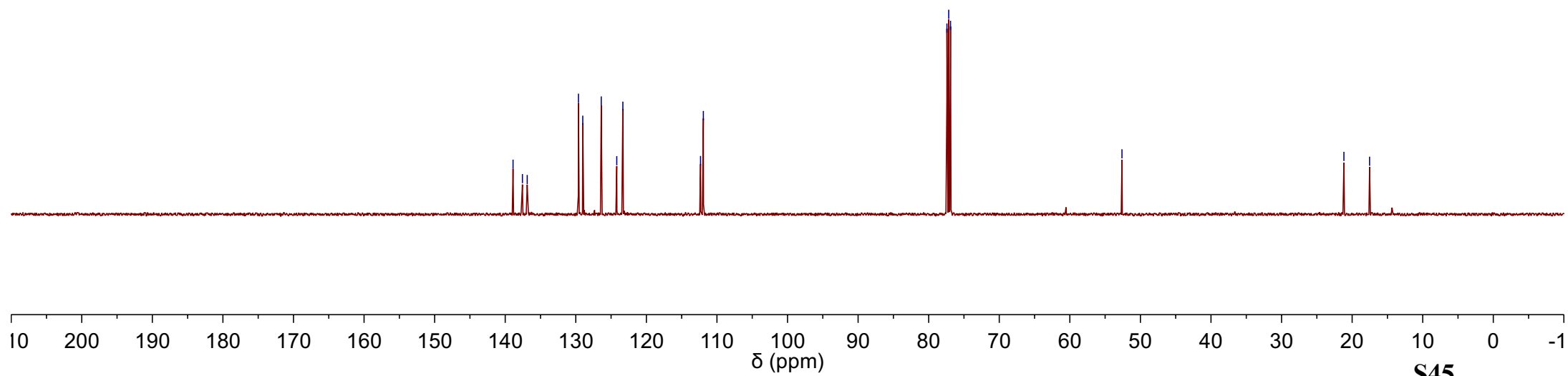
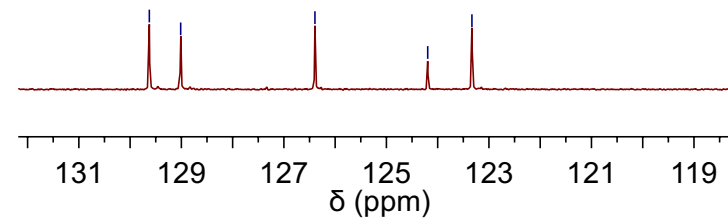
21.17  
17.53

<sup>13</sup>C NMR (126 MHz, CDCl<sub>3</sub>)



**3ib**

129.62  
129.01  
126.39  
124.19  
123.33

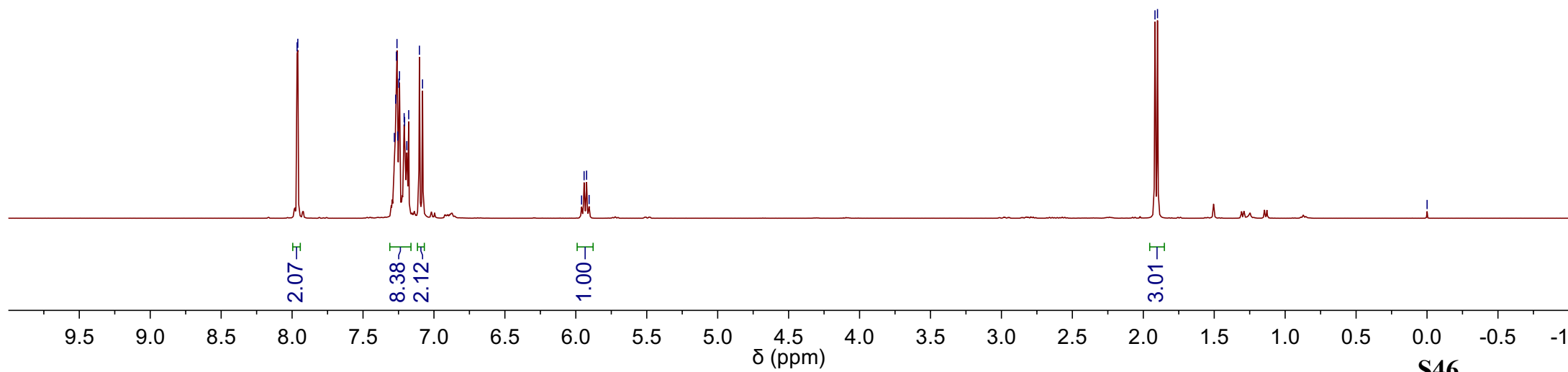
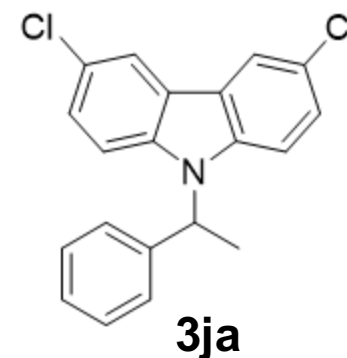


7.965  
7.960  
7.279  
7.270  
7.264  
7.261  
7.255  
7.248  
7.243  
7.210  
7.207  
7.191  
7.178  
7.102  
7.080  
5.959  
5.942  
5.924  
5.906

1.918  
1.900

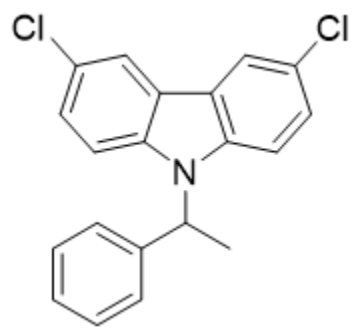
0.000

<sup>1</sup>H NMR (400 MHz, CDCl<sub>3</sub>)



S46

$^{13}\text{C}$  NMR (126 MHz,  $\text{CDCl}_3$ )



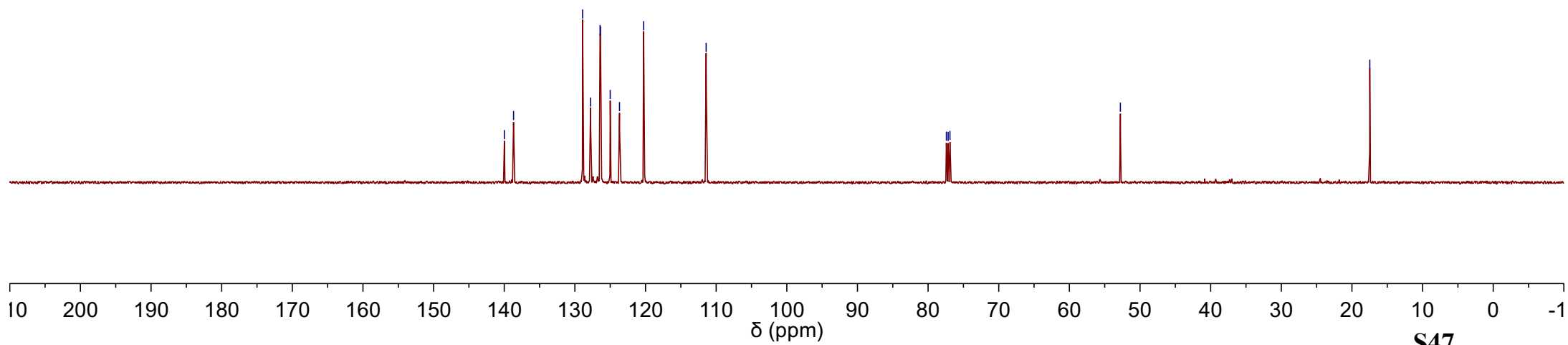
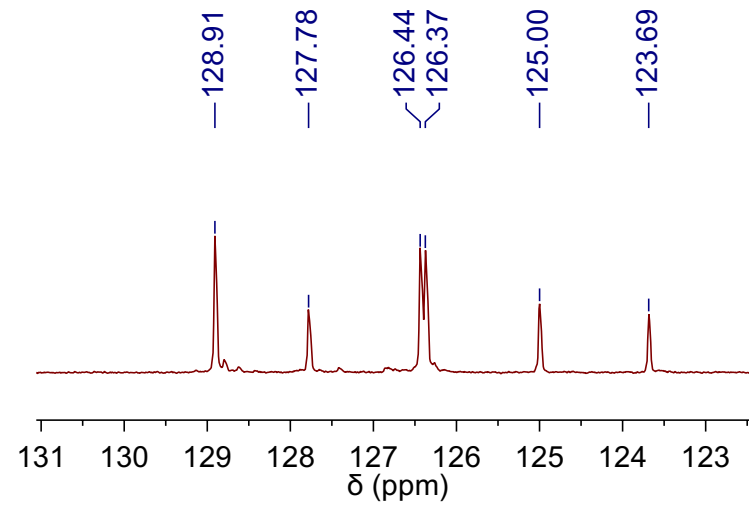
**3ja**

139.98  
138.68  
128.91  
127.78  
126.44  
126.37  
125.00  
123.69  
120.27  
—111.42

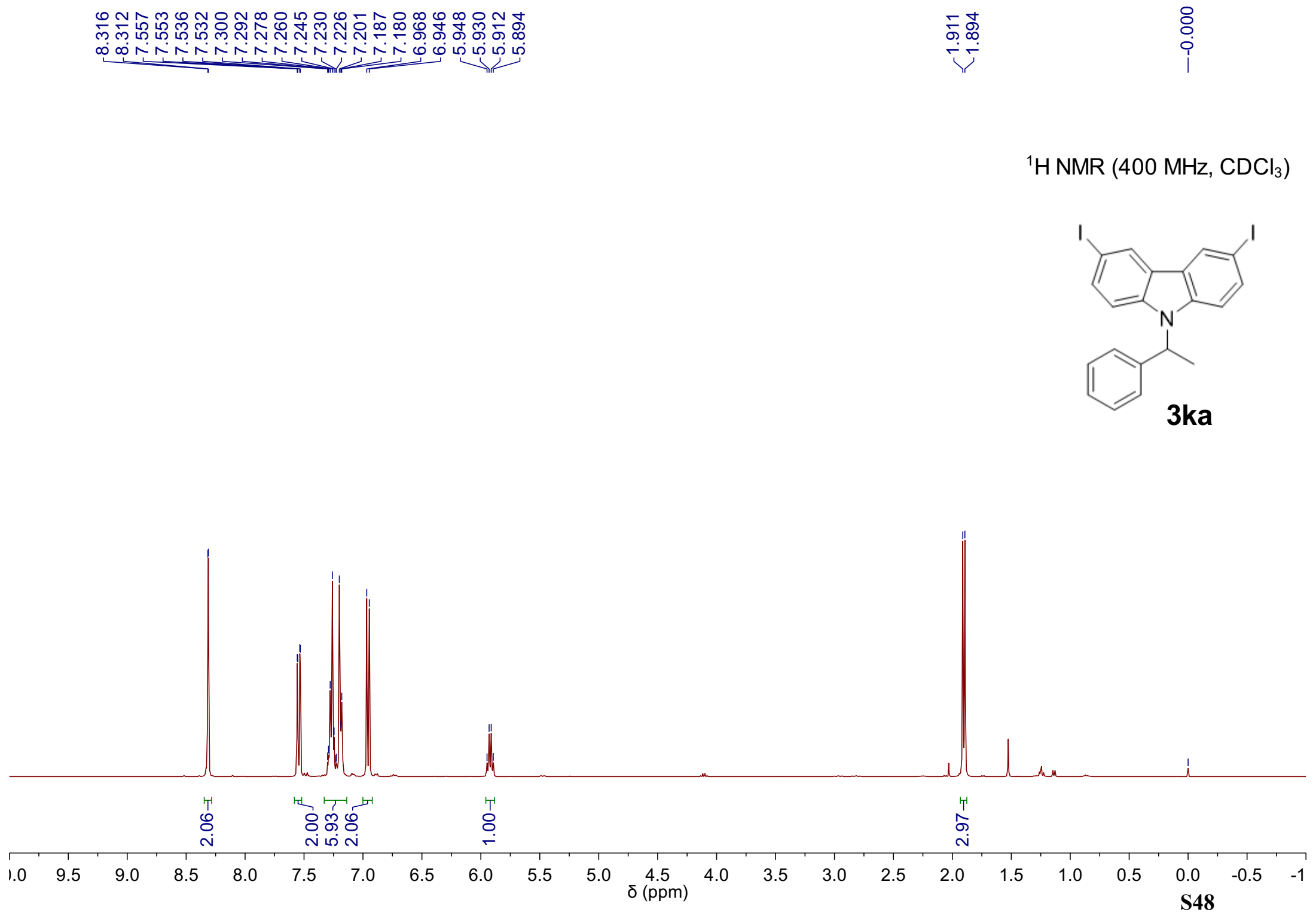
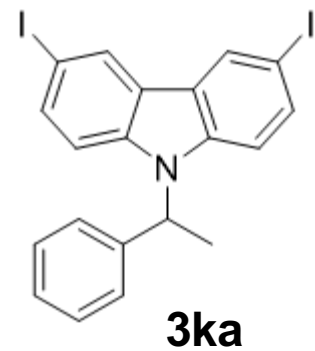
77.41  
77.16  
76.91

—52.78

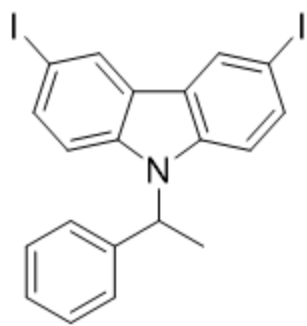
—17.47



<sup>1</sup>H NMR (400 MHz, CDCl<sub>3</sub>)



$^{13}\text{C}$  NMR (126 MHz,  $\text{CDCl}_3$ )



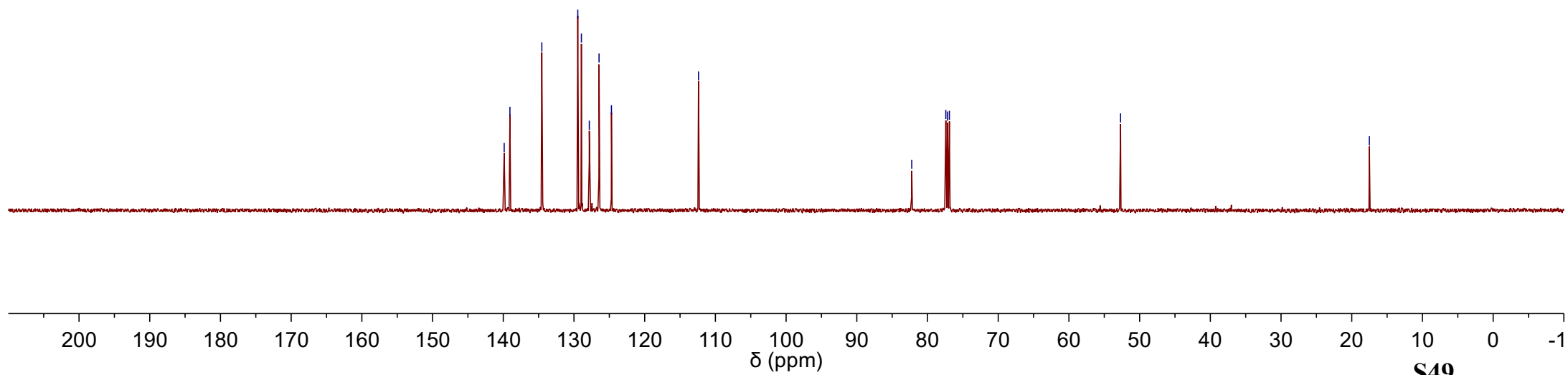
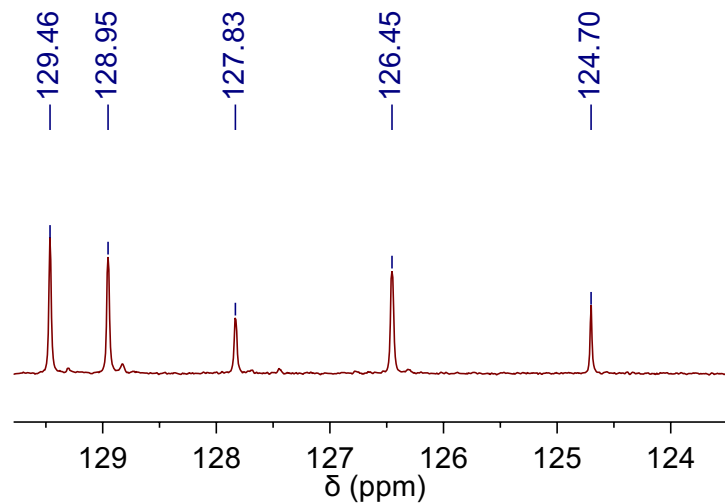
**3ka**

139.87  
139.06  
134.55  
129.46  
128.95  
127.83  
126.45  
124.70  
—112.38

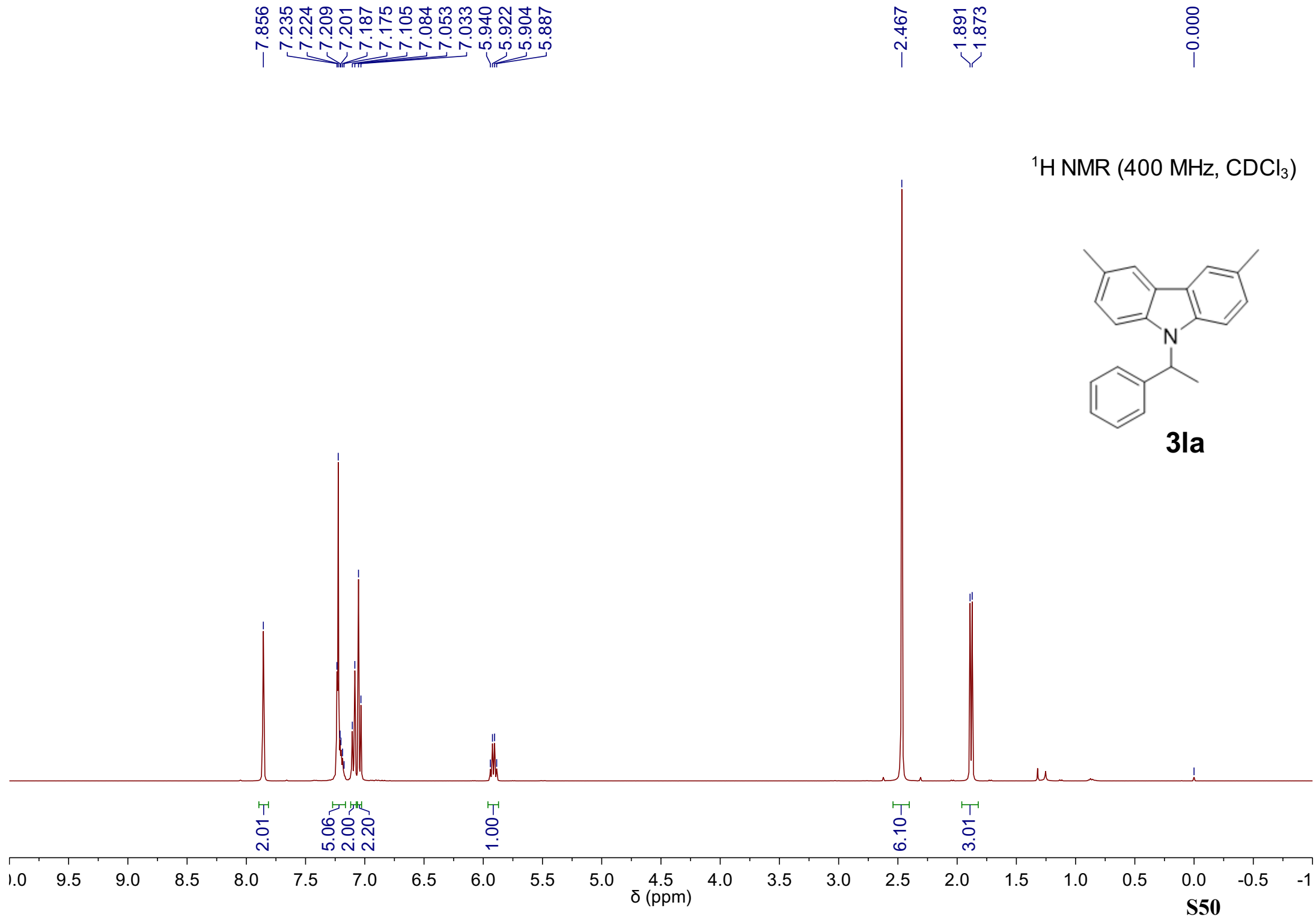
82.23  
77.41  
77.16  
76.91

—52.70

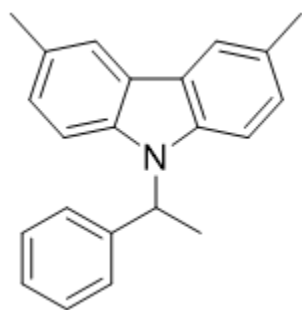
—17.51







$^{13}\text{C}$  NMR (126 MHz,  $\text{CDCl}_3$ )



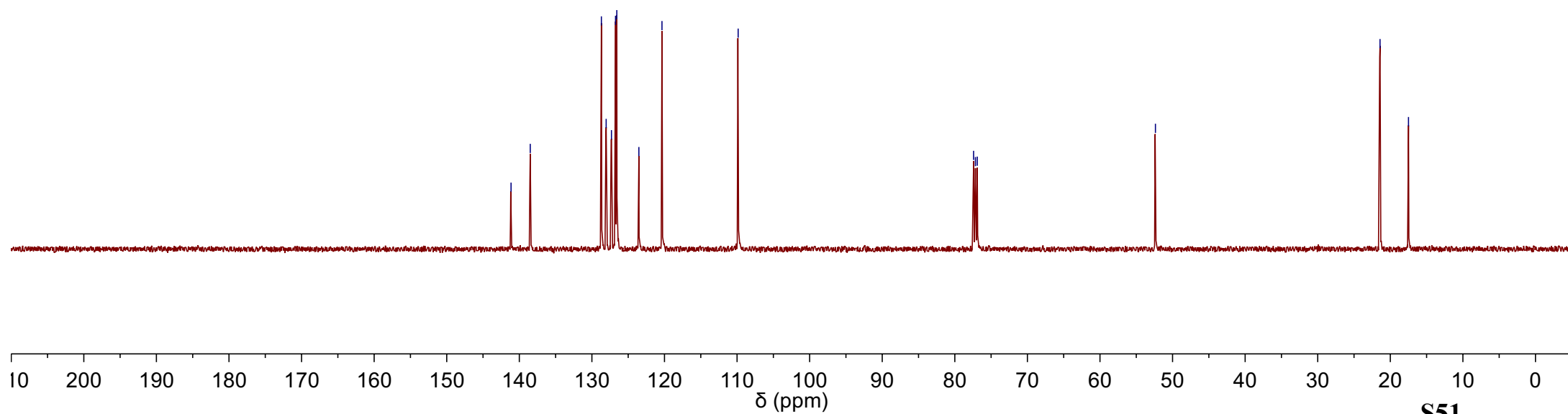
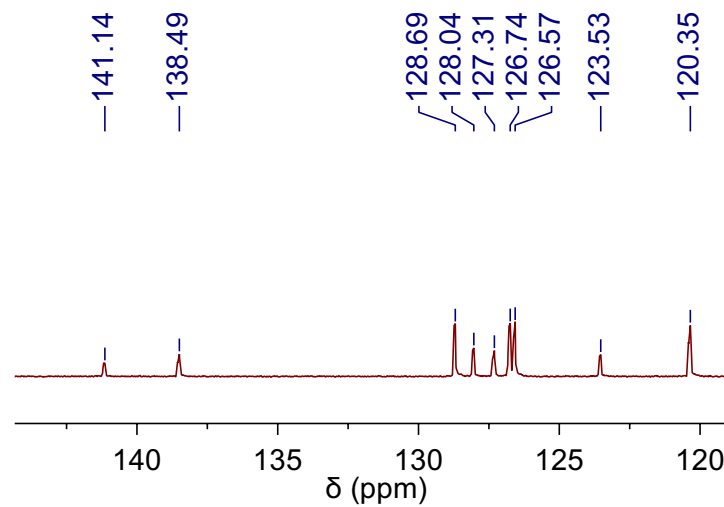
**3la**

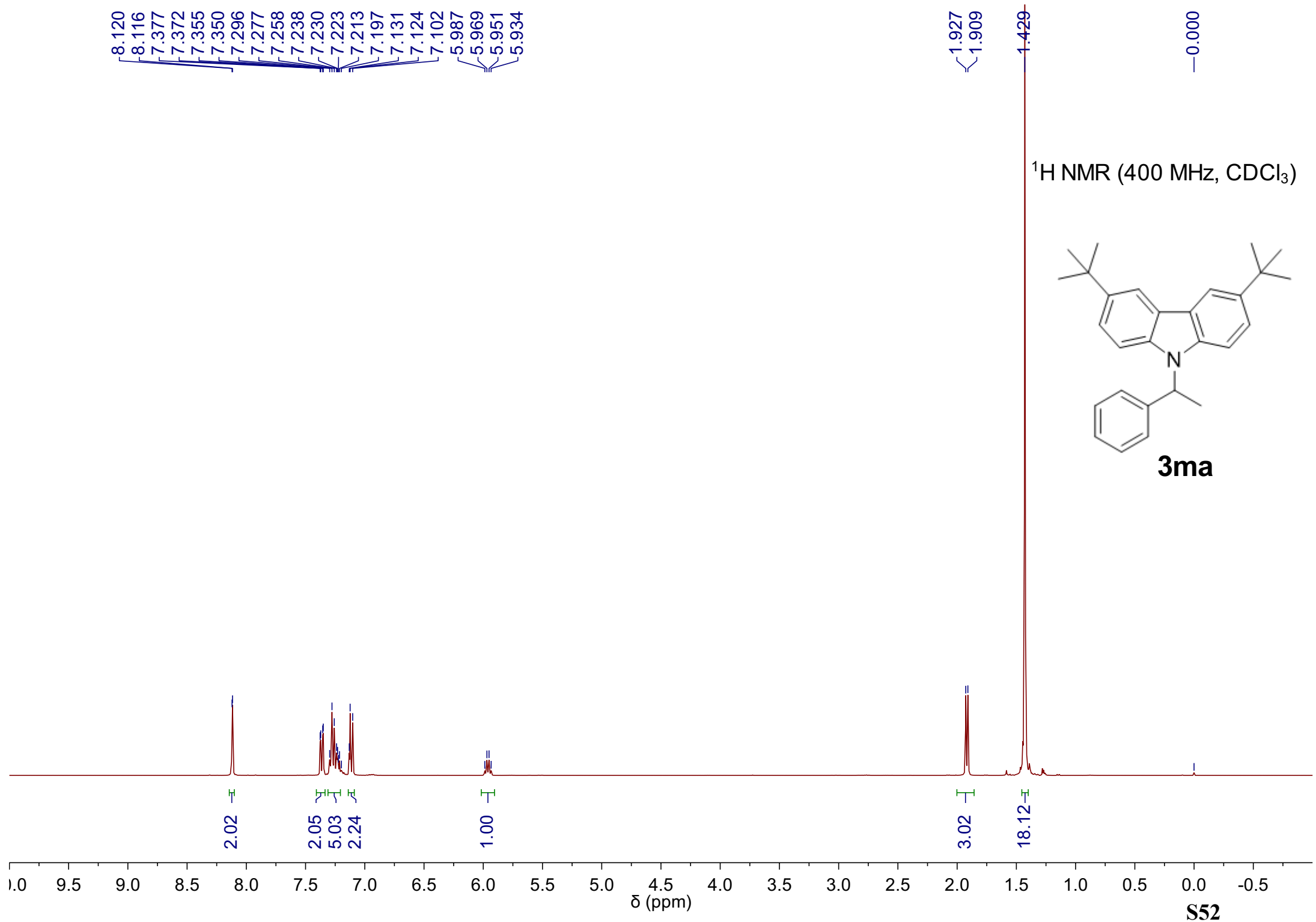
—141.14  
—138.49  
—128.69  
—128.04  
—127.31  
—126.74  
—126.57  
—123.53  
—120.35  
—109.85

—77.41  
—77.16  
—76.91

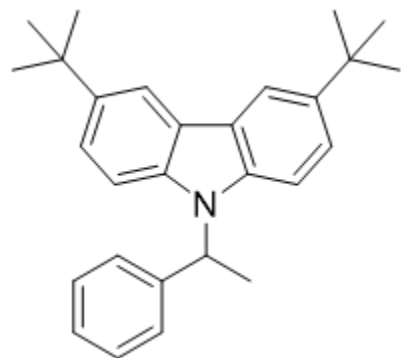
—52.36

—21.42  
—17.49





$^{13}\text{C}$  NMR (126 MHz,  $\text{CDCl}_3$ )



**3ma**

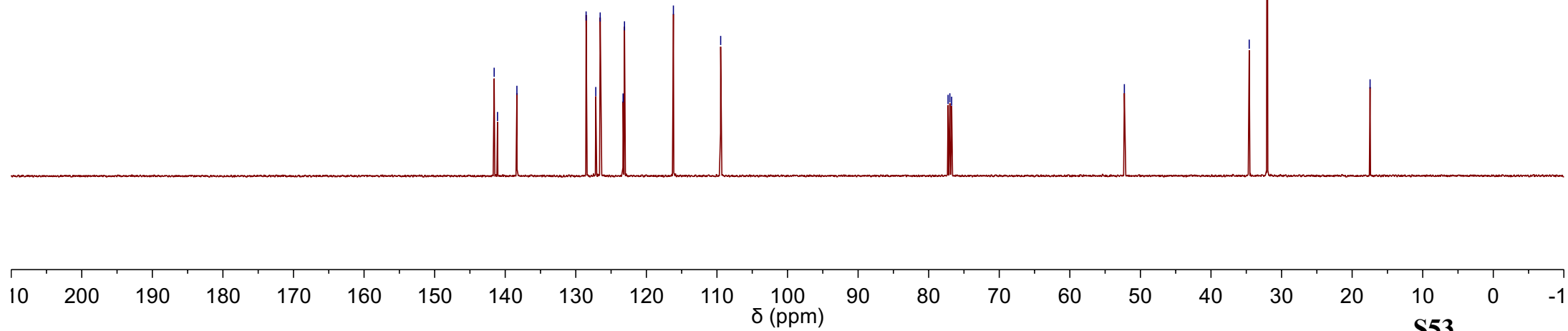
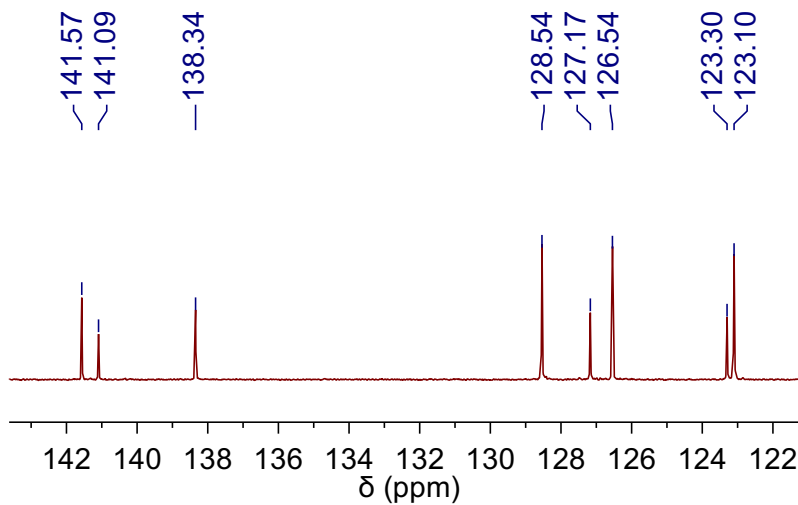
141.57  
141.09  
138.34  
128.54  
127.17  
126.54  
123.30  
123.10  
116.17  
109.47

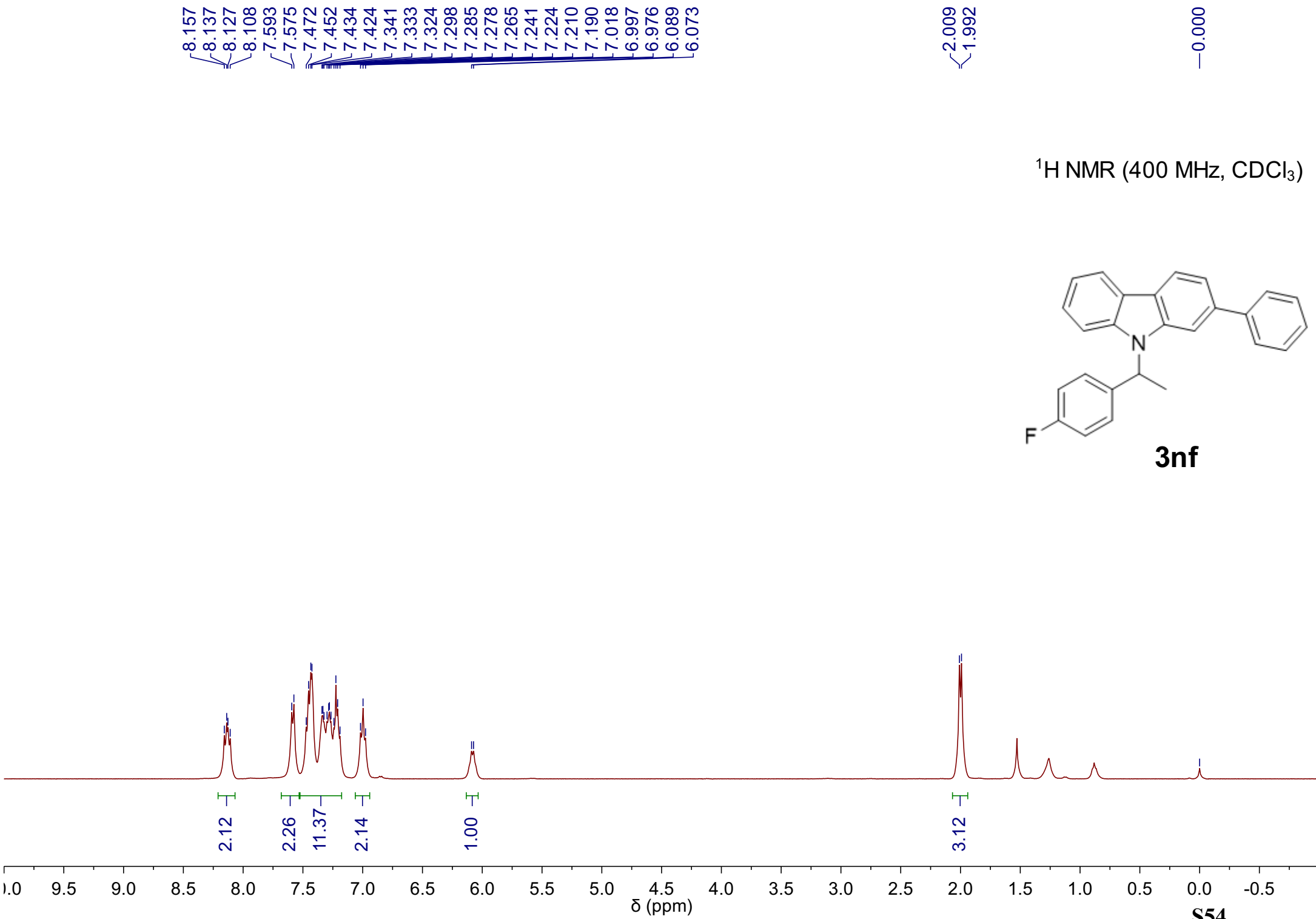
77.25  
77.00  
76.75

52.28

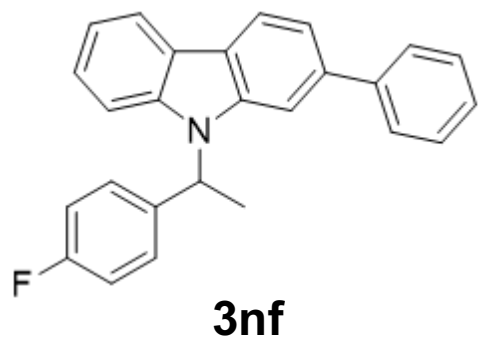
34.58  
32.02

17.46





<sup>13</sup>C NMR (126 MHz, CDCl<sub>3</sub>)

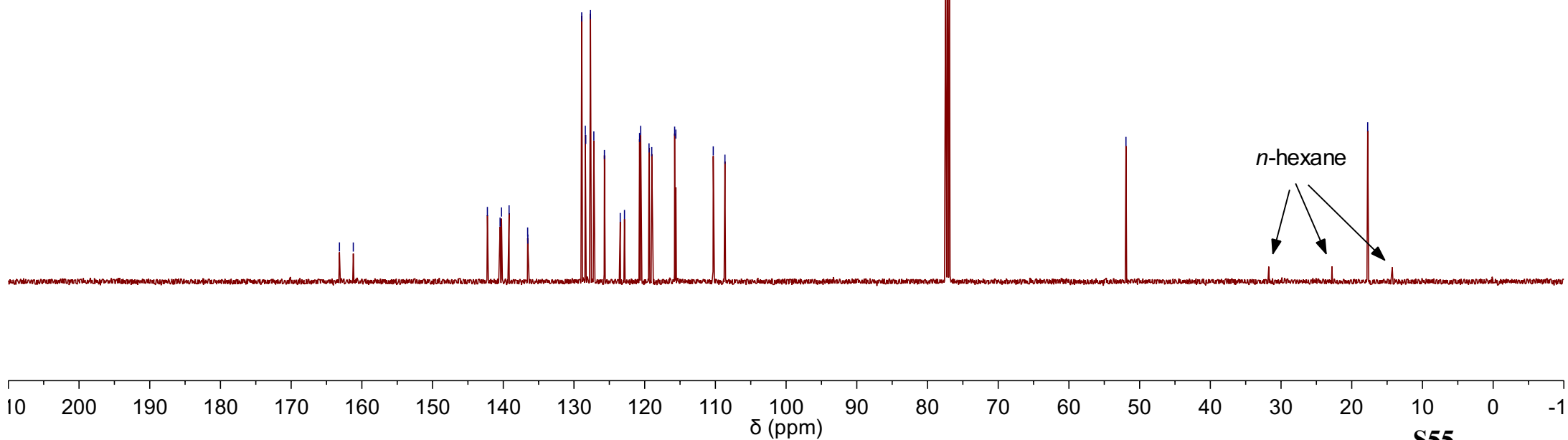
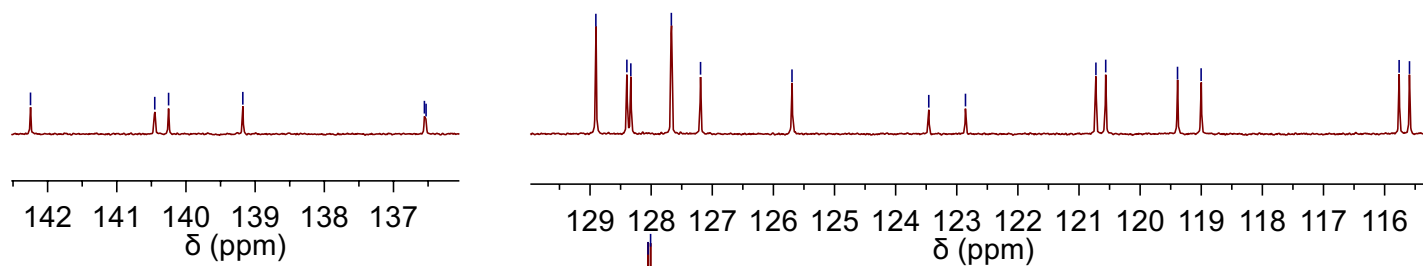


163.17  
161.21  
142.25  
140.45  
140.25  
139.18  
136.55  
136.53  
128.90  
128.40  
128.33  
127.67  
127.19  
125.70  
123.46  
122.86  
120.72  
120.56  
119.39  
119.00  
115.76  
115.59  
110.30  
108.65  
77.41  
77.16  
76.91

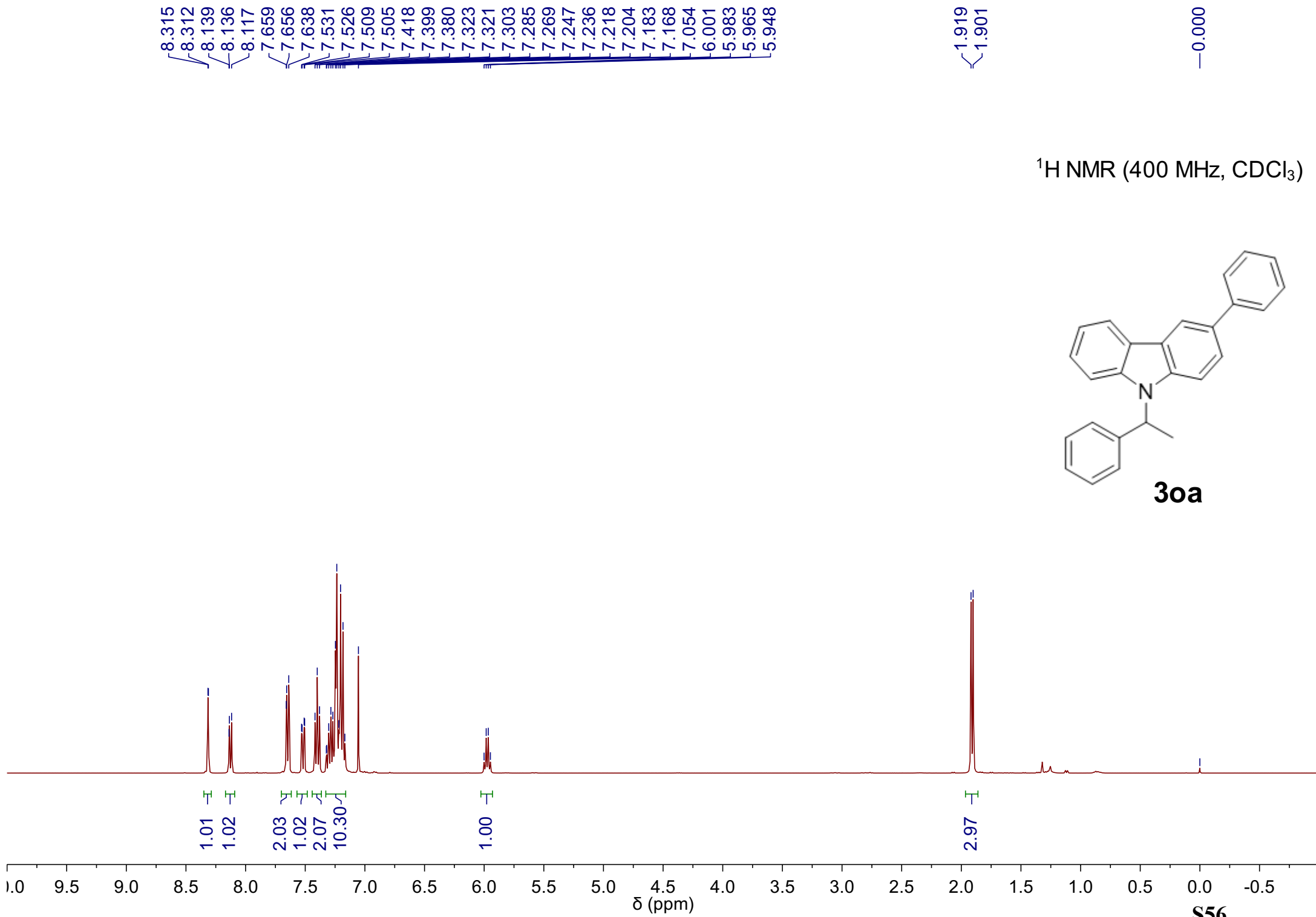
51.93

17.75

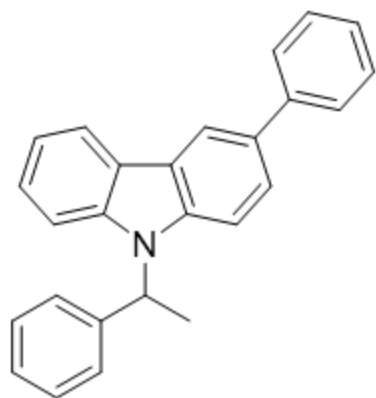
142.25  
140.45  
140.25  
139.18  
136.55  
136.53  
128.90  
128.40  
128.33  
127.67  
127.19  
125.70  
123.46  
122.86  
120.72  
120.56  
119.39  
119.00  
115.76  
115.59



*n*-hexane



<sup>13</sup>C NMR (126 MHz, CDCl<sub>3</sub>)



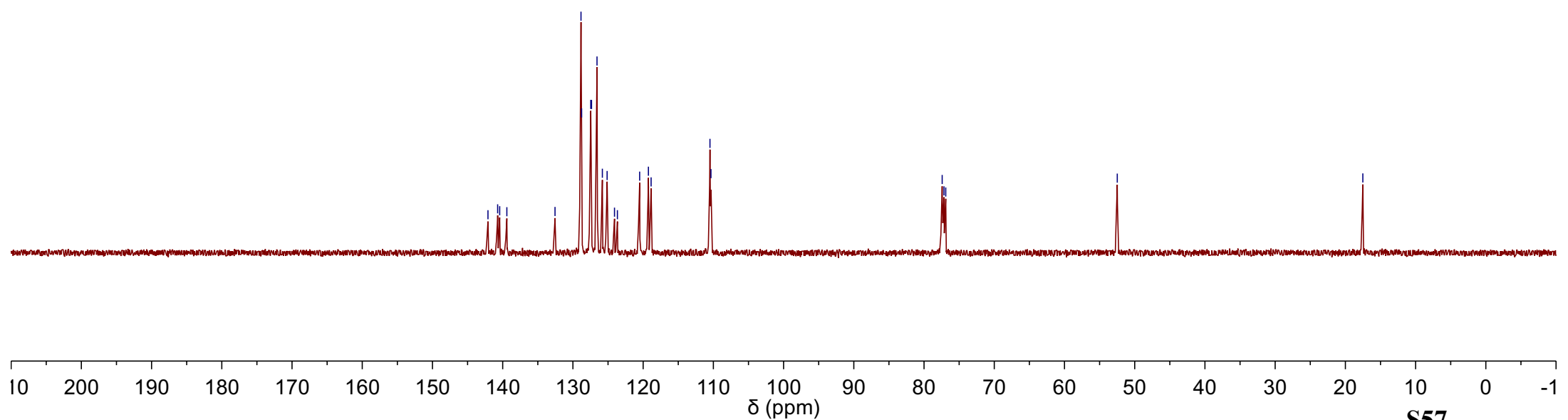
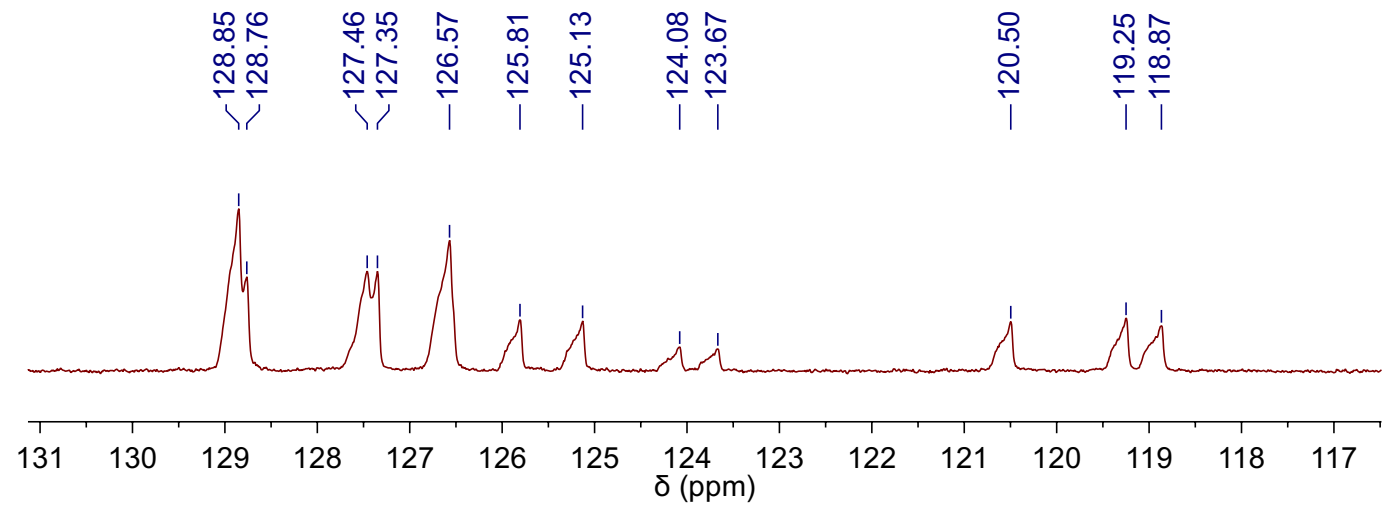
**30a**

142.10  
140.72  
140.43  
139.41  
132.55  
128.85  
128.76  
127.46  
127.35  
126.57  
125.81  
125.13  
124.08  
123.67  
120.50  
119.25  
118.87  
110.48  
110.34

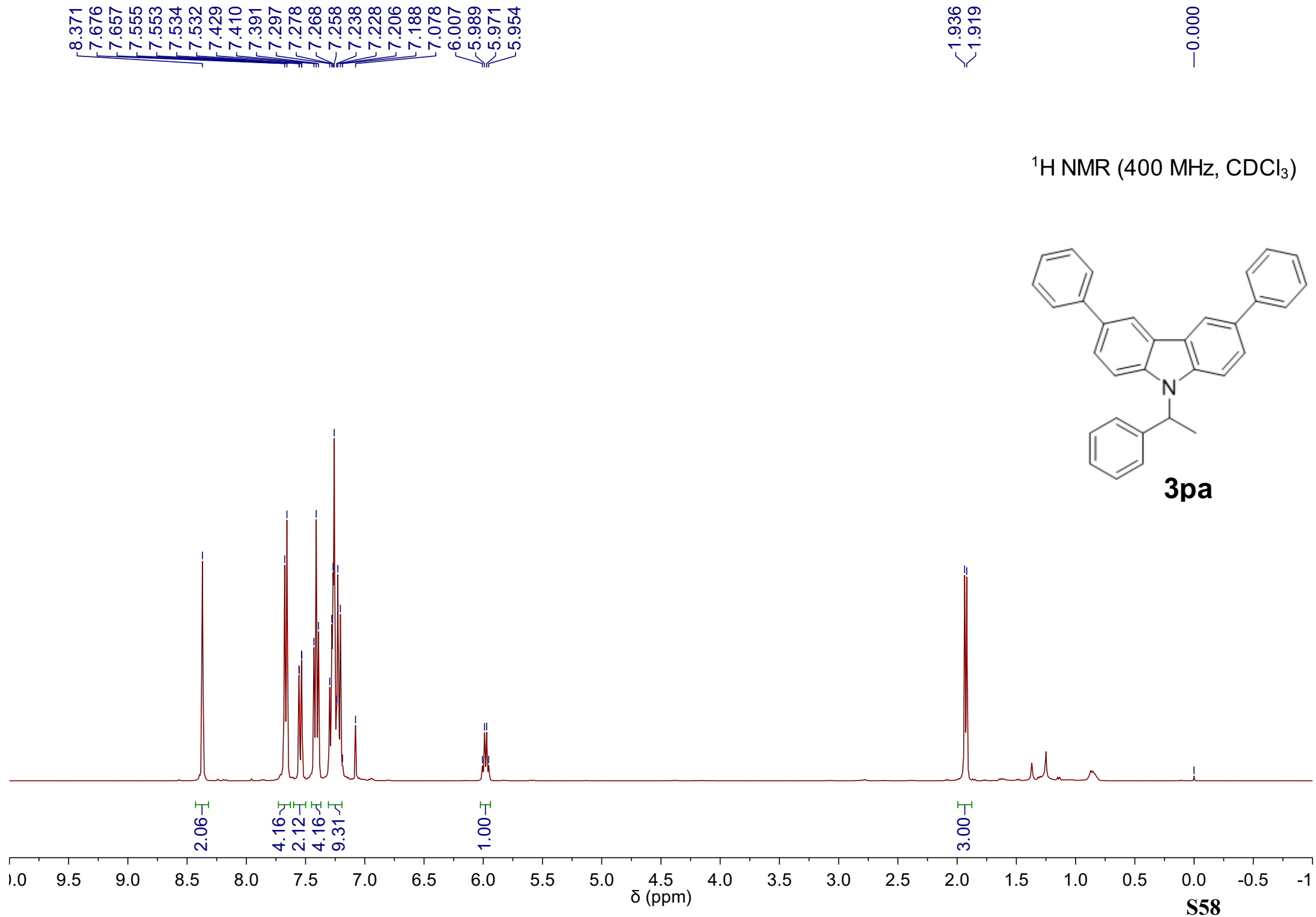
77.42  
77.16  
76.91

52.48

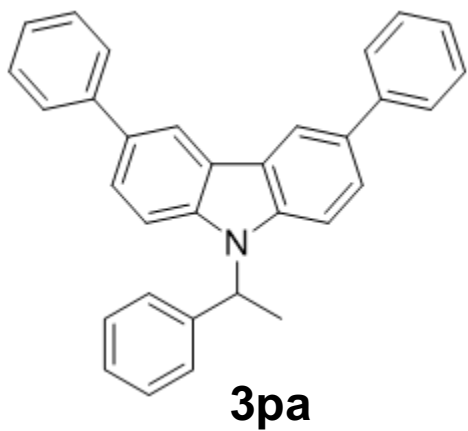
17.51







<sup>13</sup>C NMR (126 MHz, CDCl<sub>3</sub>)

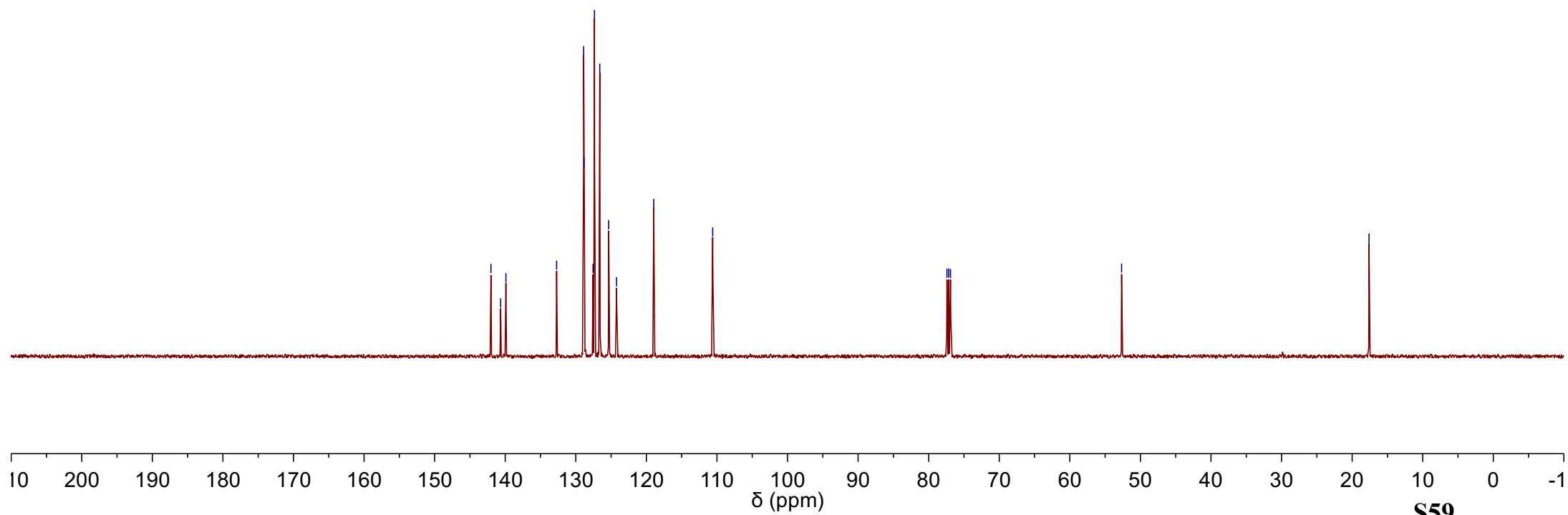
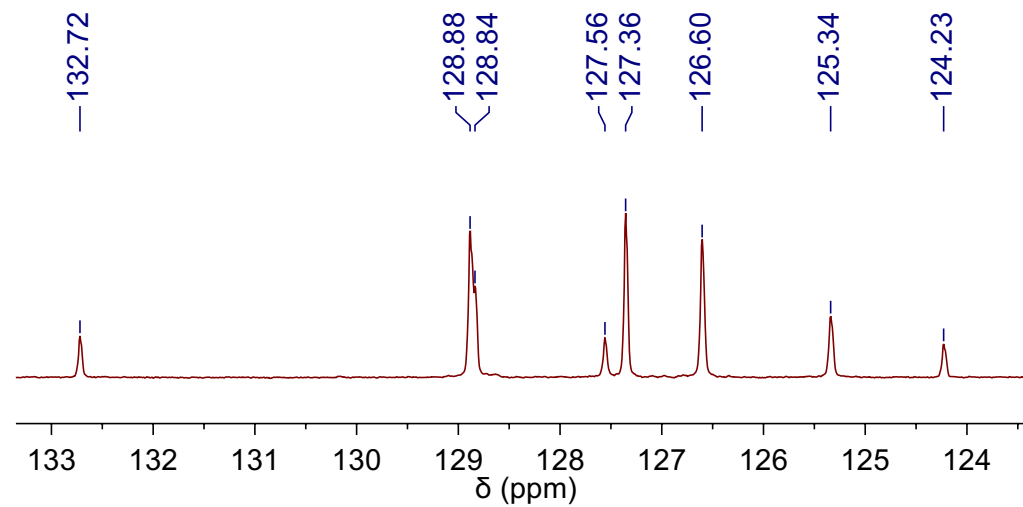


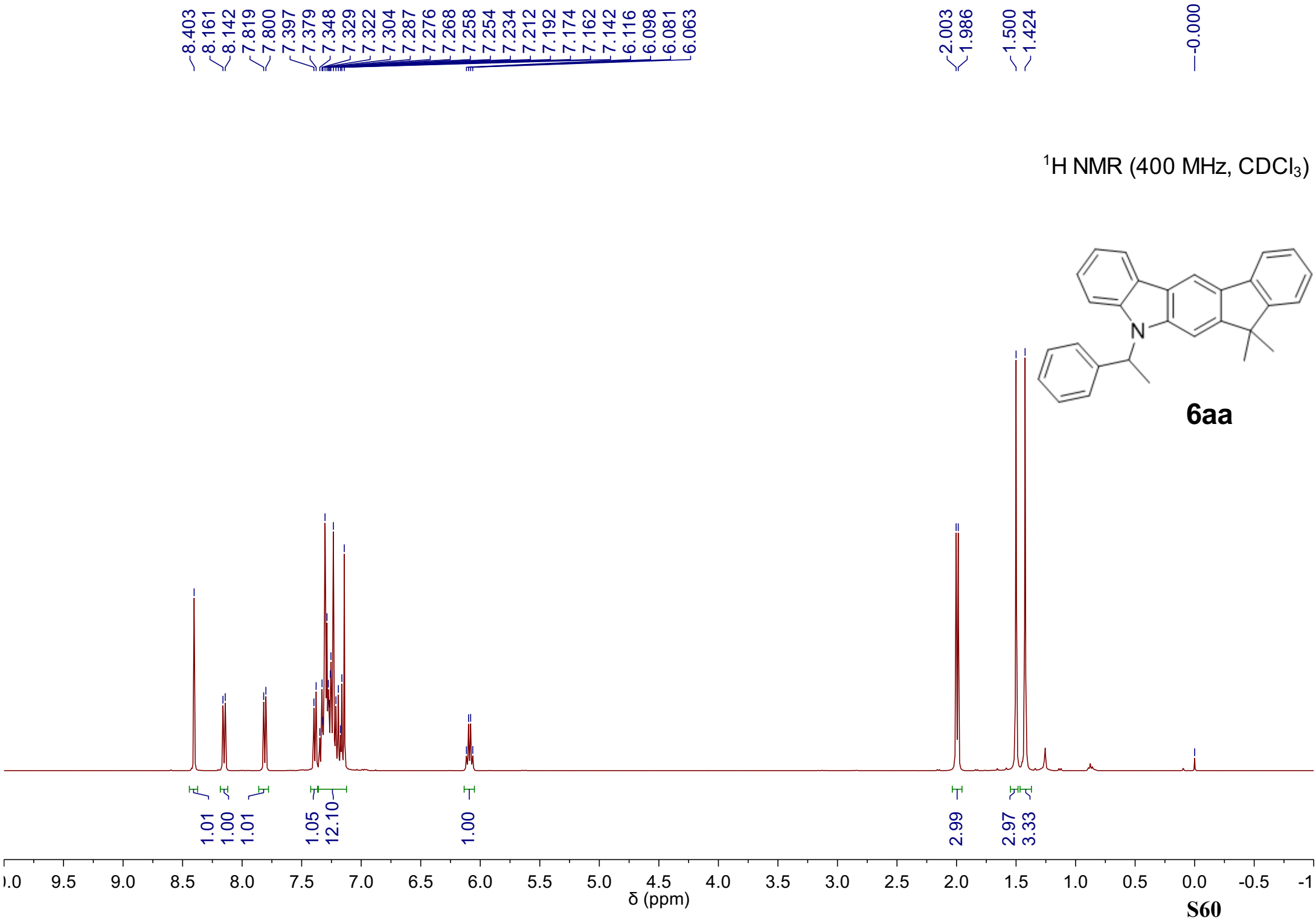
142.02  
140.65  
139.90  
132.72  
128.88  
128.84  
127.56  
127.36  
126.60  
125.34  
124.23  
118.96  
—110.60

77.41  
77.16  
76.91

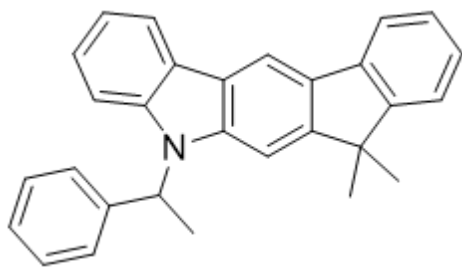
—52.67

—17.61



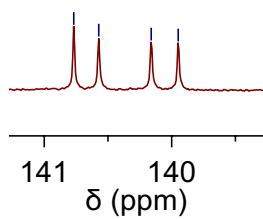


<sup>13</sup>C NMR (126 MHz, CDCl<sub>3</sub>)



**6aa**

140.77  
140.57  
140.16  
139.95



153.32  
152.73  
140.77  
140.57  
140.16  
139.95  
131.52  
128.73  
127.43  
127.14  
126.66  
126.22  
125.22  
123.90  
123.05  
122.59  
120.27  
119.38  
119.10  
111.42  
110.60  
104.14  
77.41  
77.16  
76.91

52.49  
46.74

28.18  
28.10

17.52

131.52

128.73

127.43

127.14

126.66

126.22

125.22

123.90

123.05

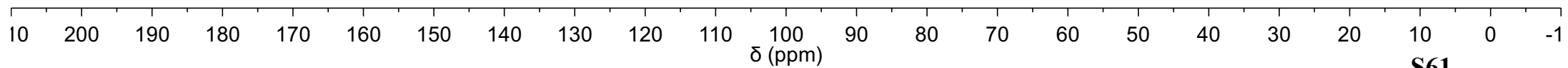
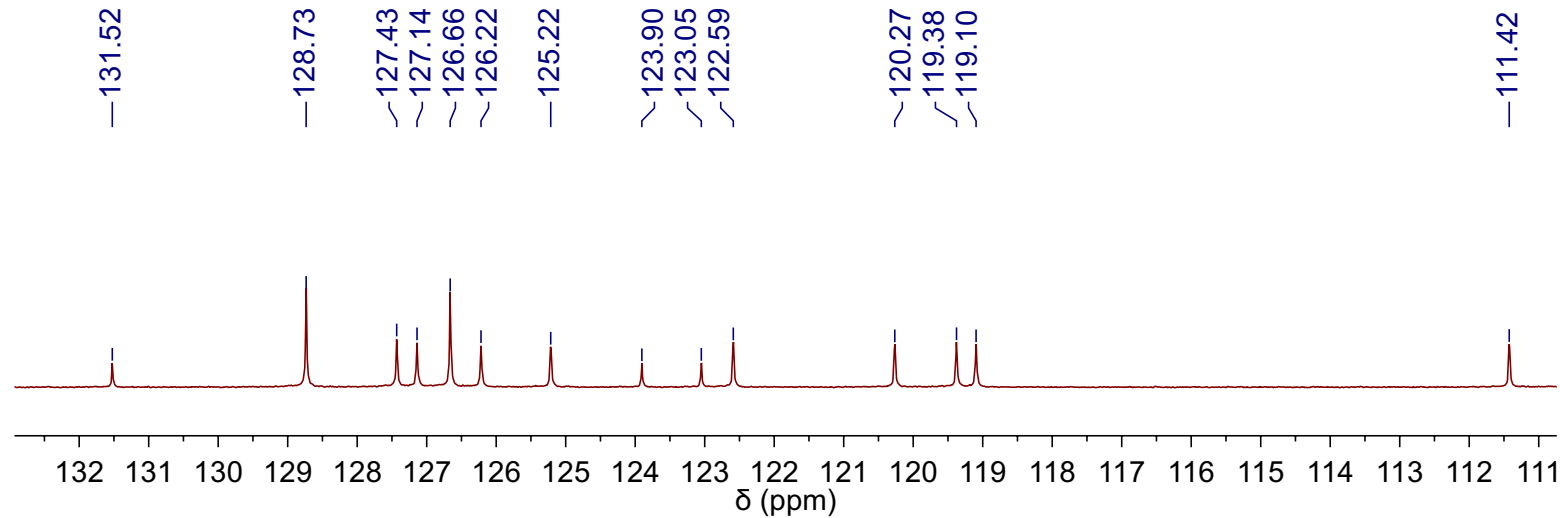
122.59

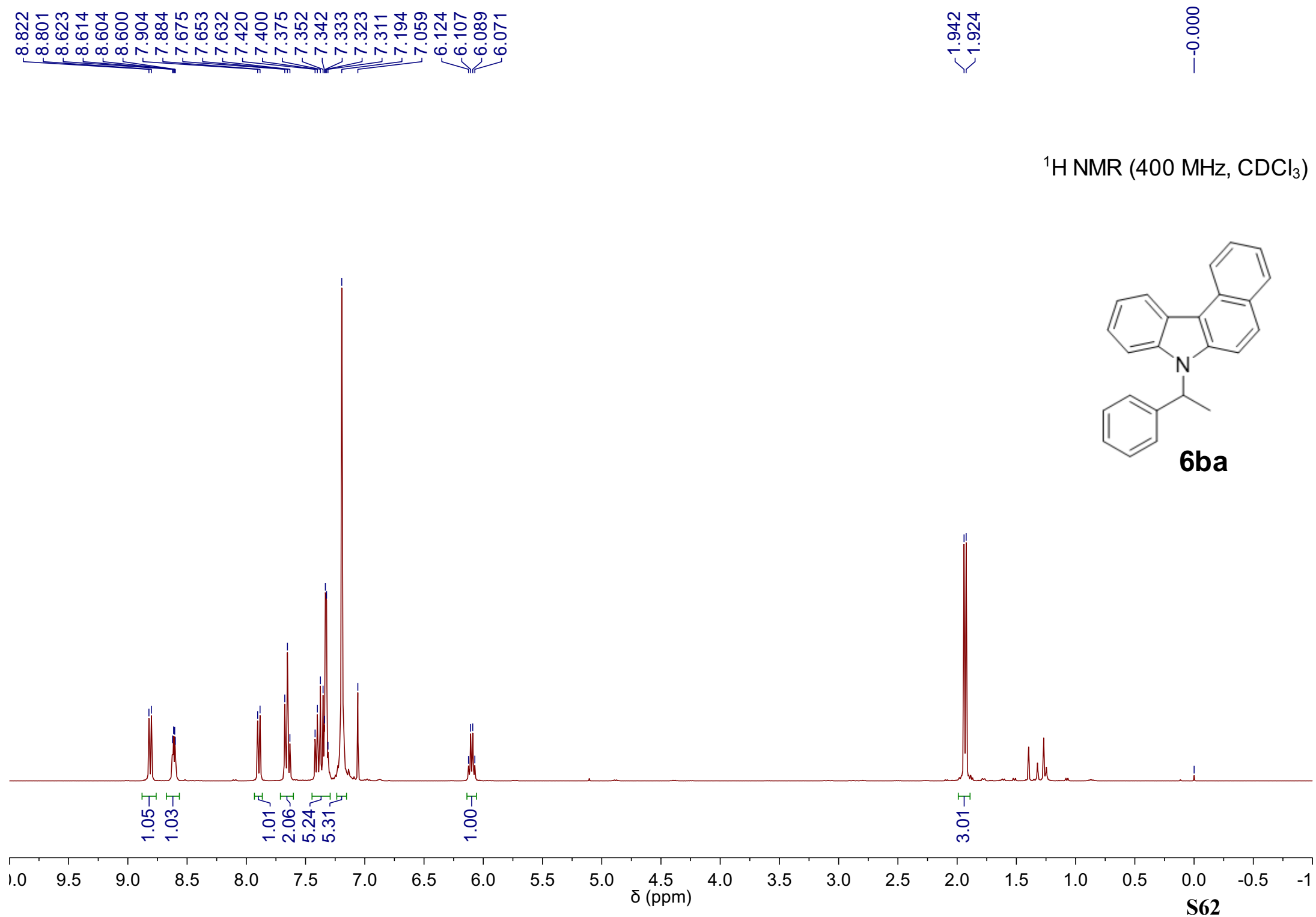
120.27

119.38

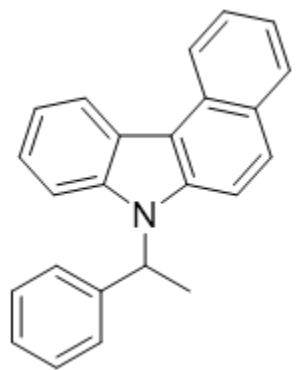
119.10

111.42

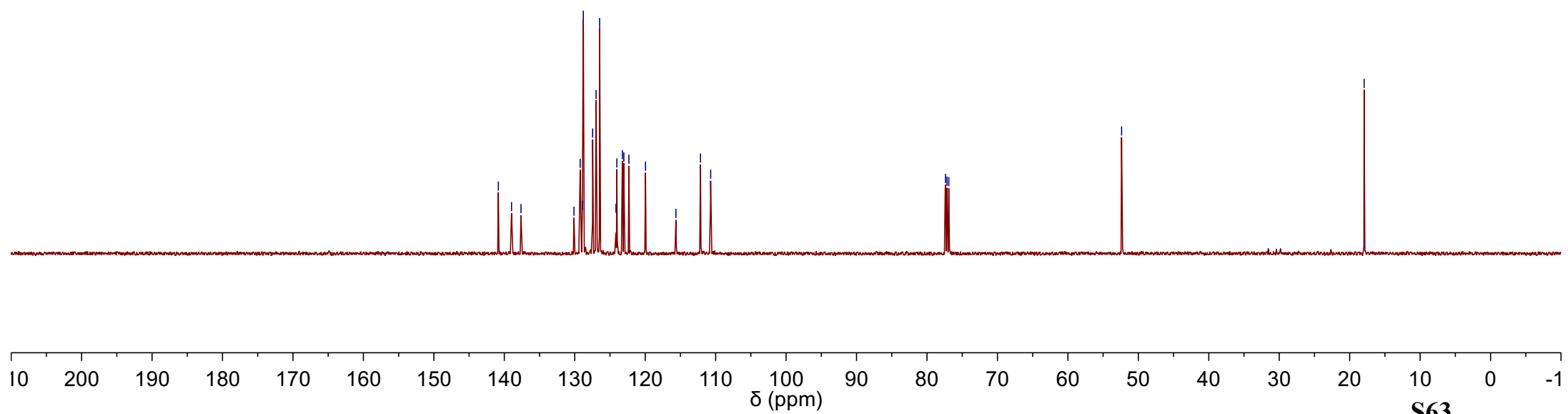
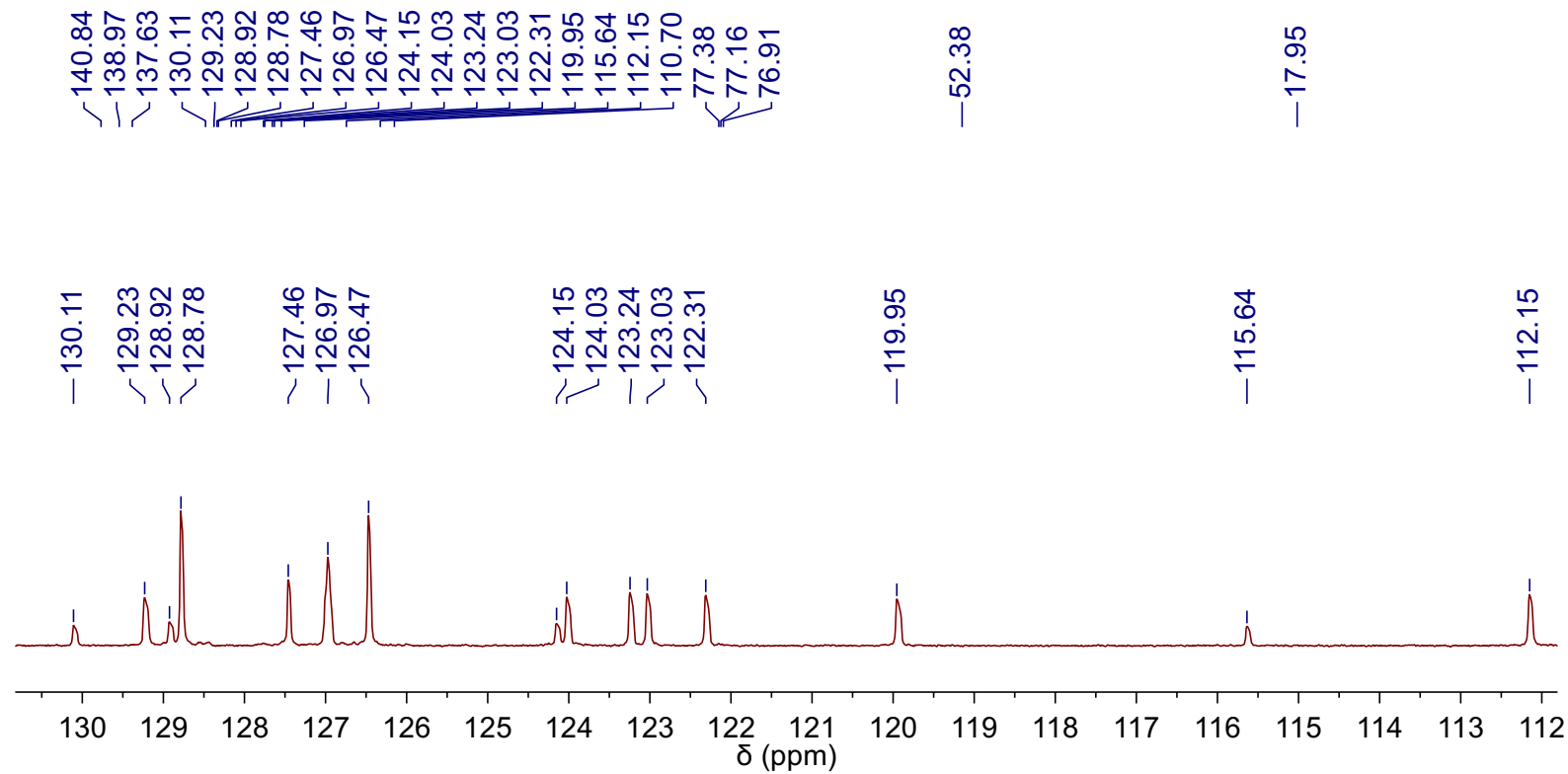


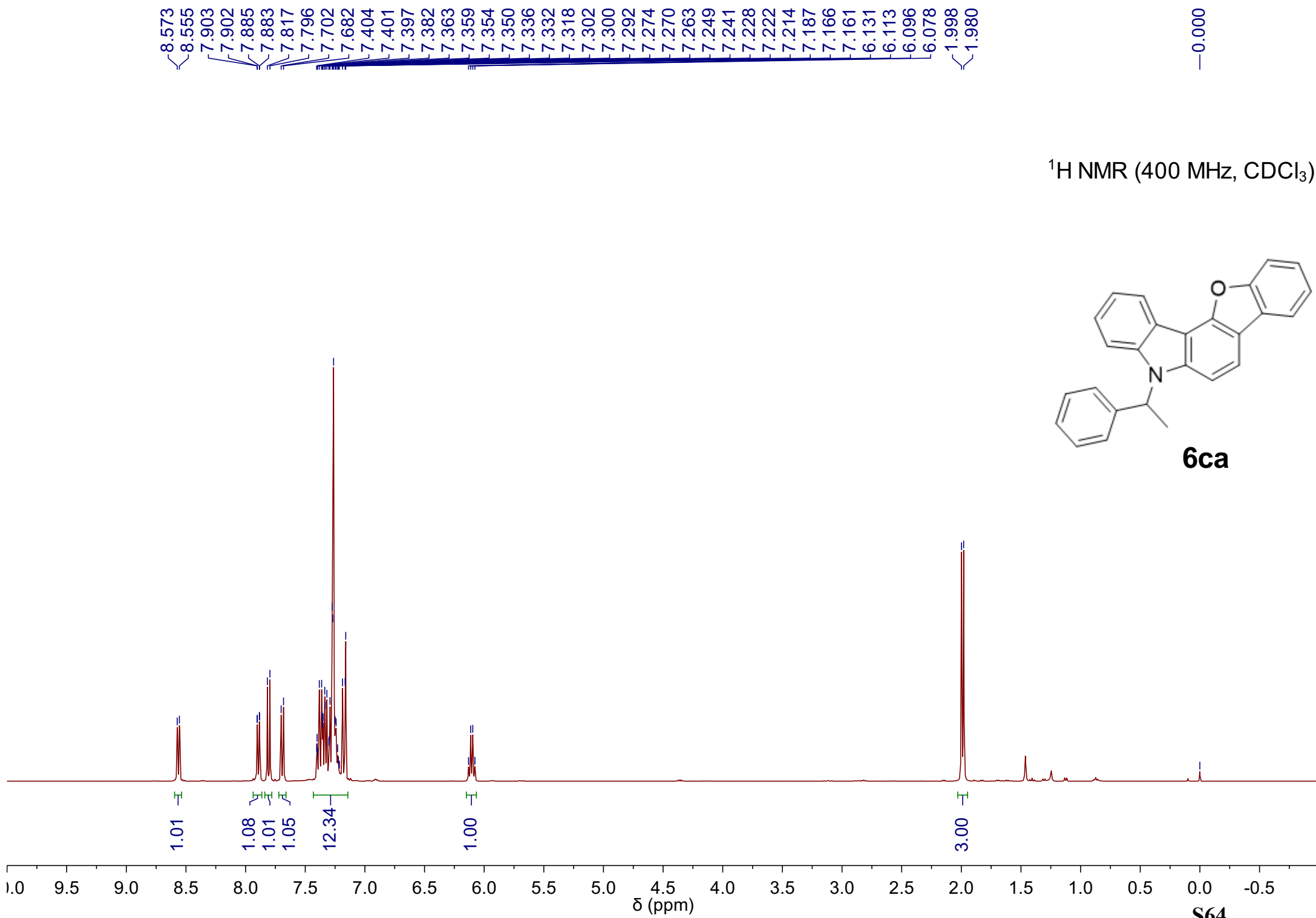


<sup>13</sup>C NMR (126 MHz, CDCl<sub>3</sub>)

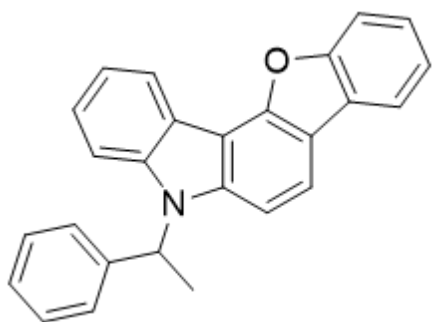


**6ba**

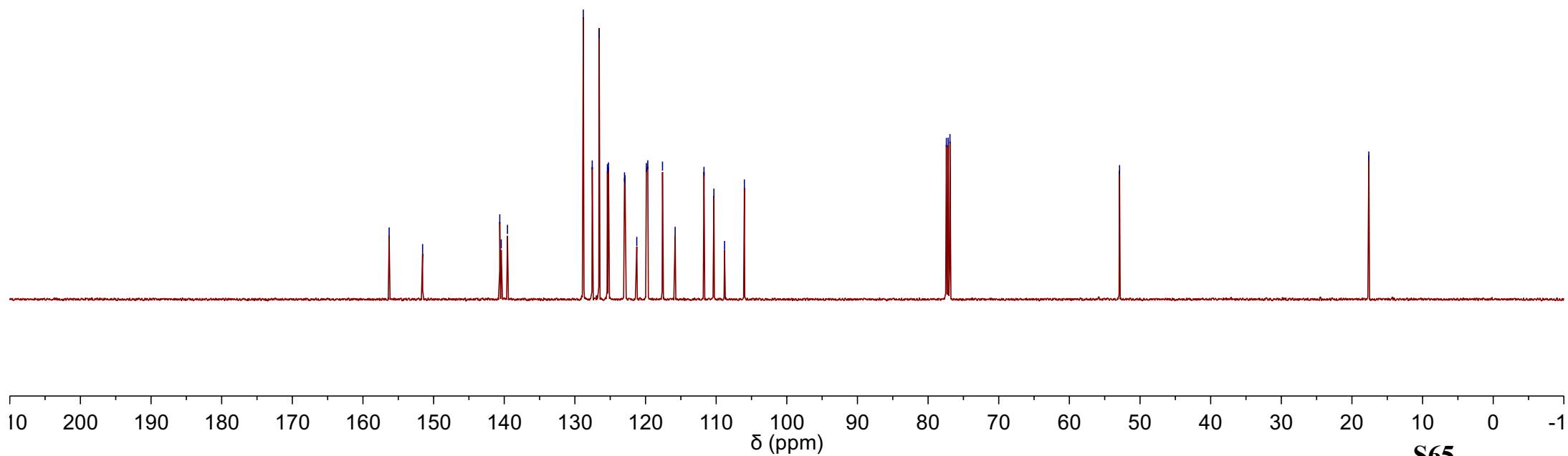
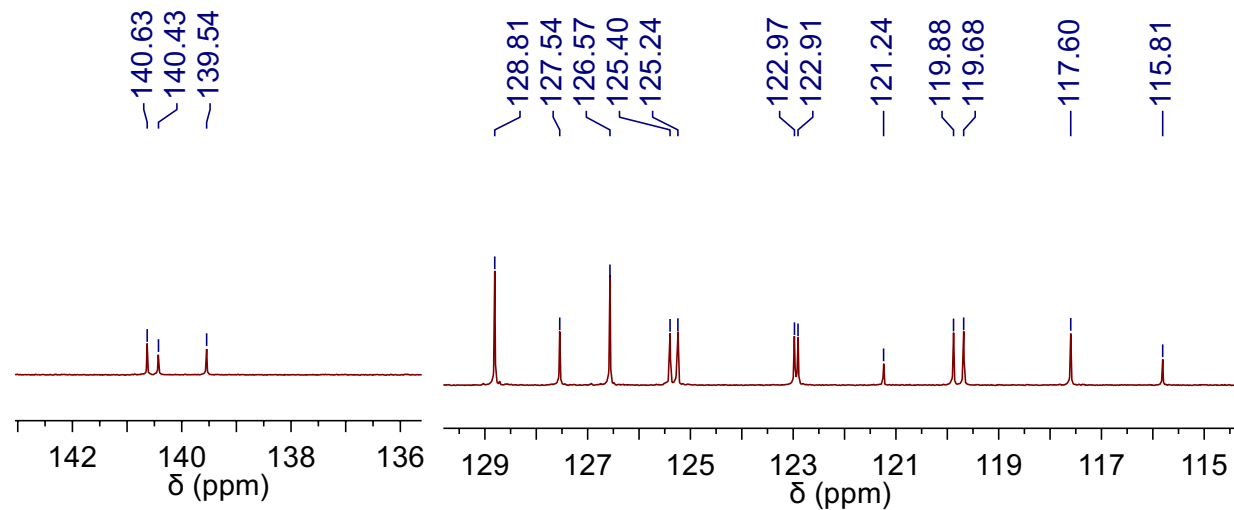
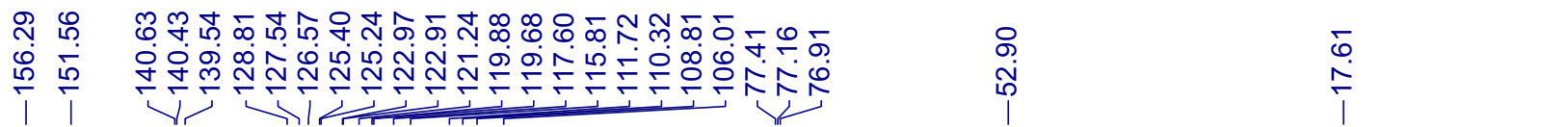




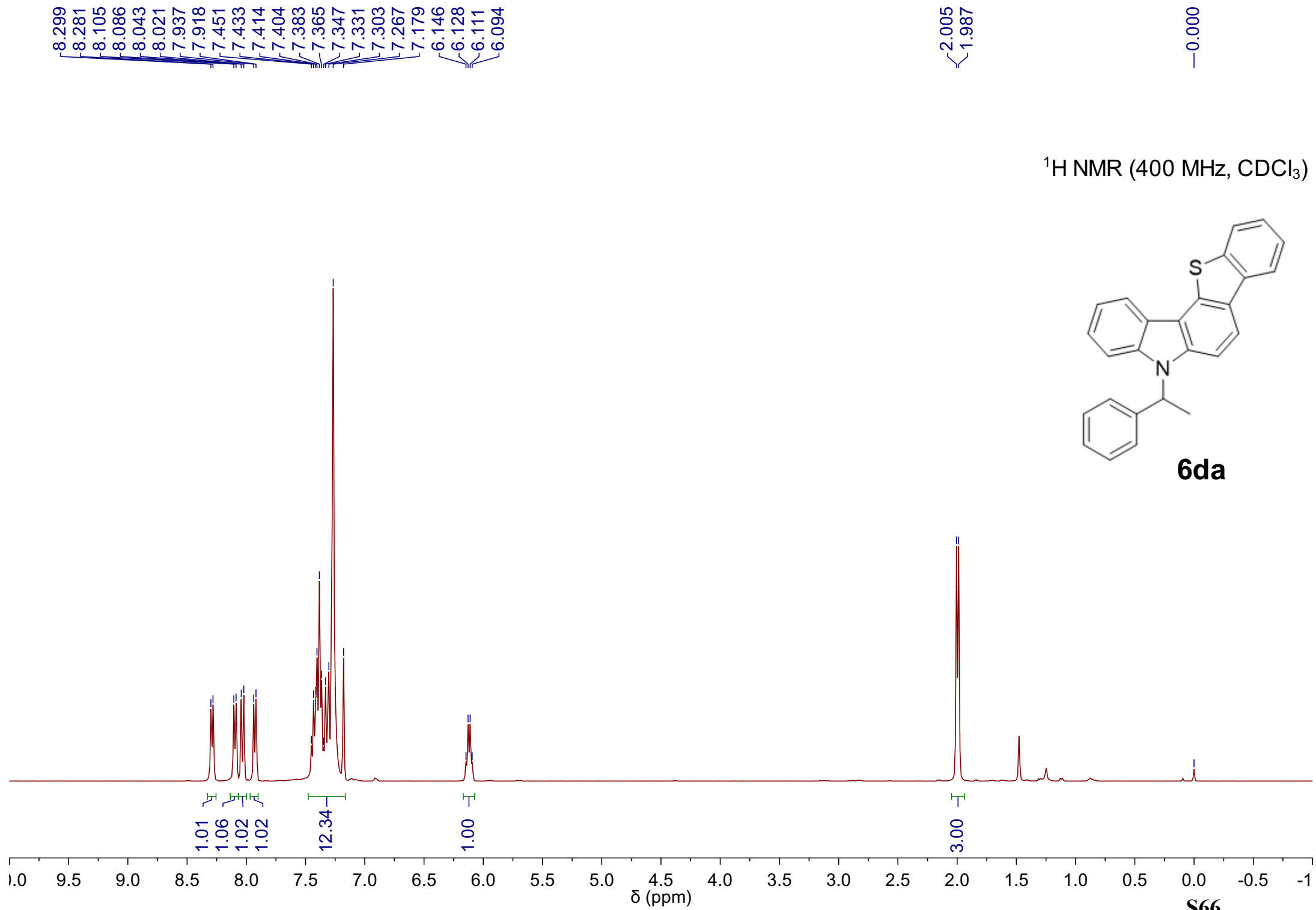
<sup>13</sup>C NMR (126 MHz, CDCl<sub>3</sub>)



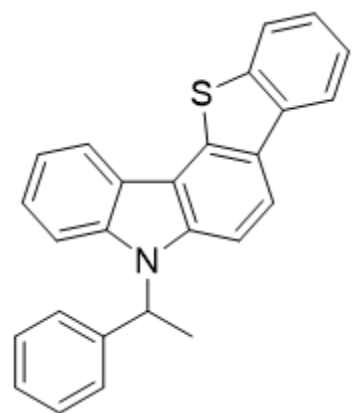
**6ca**







<sup>13</sup>C NMR (126 MHz, CDCl<sub>3</sub>)



**6da**

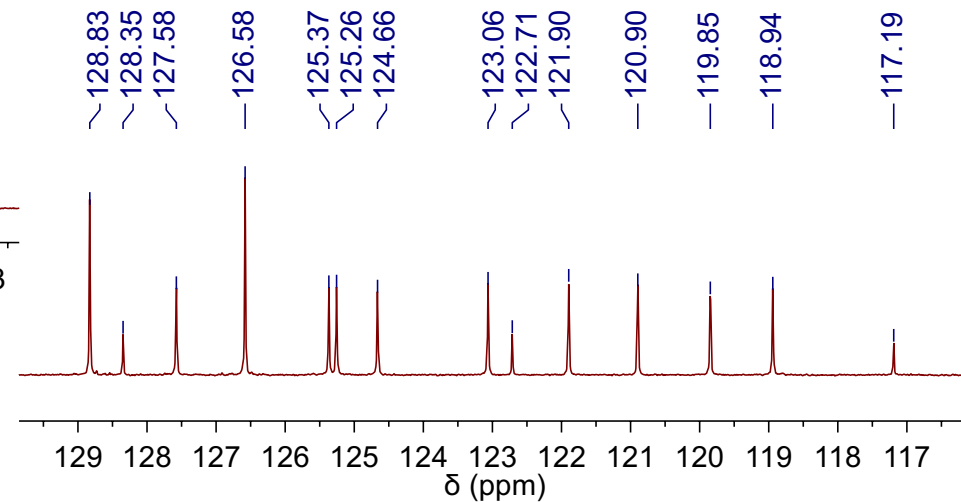
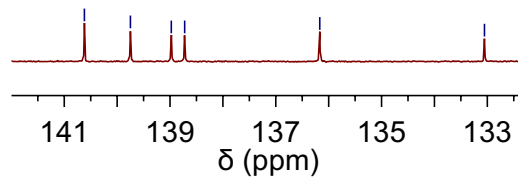
140.62  
139.75  
138.98  
138.72  
136.17  
133.05  
128.83  
128.35  
127.58  
126.58  
125.37  
125.26  
124.66  
123.06  
122.71  
121.90  
120.90  
119.85  
118.94  
117.19  
110.41  
108.09

140.62  
139.75  
138.98  
138.72  
136.17  
133.05

77.41  
77.16  
76.91

52.82

17.72



200 190 180 170 160 150 140 130 120 110 100 90 80 70 60 50 40 30 20 10 0 -1  
δ (ppm)